

**The Role of Static and Dynamic
Frontal Plane and Rotational Alignment, Quadriceps,
and Lower Limb Kinematics as Key Factors
in Patello-femoral Instability**

vorgelegt von
Diplom-Ingenieur, Master of Science
Evgenios I. Kornaropoulos
aus Griechenland

Von der Fakultät V – Verkehrs- und Maschinensysteme
der Technischen Universität Berlin
zur Erlangung des akademischen Grades

Doktor der Ingenieurwissenschaften
– Dr.-Ing. –

genehmigte Dissertation

Promotionsausschuss:

Vorsitzender: Prof. Dr.-Ing. Henning J. Meyer
Berichter: Prof. Dr.-Ing. Georg N. Duda
Berichter: Prof. Dr.-Ing. Marc Kraft

Tag der wissenschaftlichen Aussprache: 03. May 2011

Berlin 2011
D83

**The role of static and dynamic frontal plane and
rotational alignment, quadriceps muscles,
and lower limb kinematics as key factors
in patello-femoral instability**

Evgenios I. Kornaropoulos

Supervisor 1: Prof. Dr. Ing Marc Kraft

Supervisor 2: Univ.-Prof. Dr. Ing. Georg Duda

Mentor: Dr. Ing. William Taylor

February 2011

Evgenios Kornaropoulos

Matrikel-Nr: 0330993

Eigenständigkeitserklärung

Ich versichere, dass ich die vorgelegte Promotionsarbeit mit Titel „The role of static and dynamic frontal plane and rotational alignment, quadriceps muscles, and lower limb kinematics as key factors in patello-femoral instability“ eigenständig und ohne fremde Hilfe verfasst, keine andere als die angegebenen Quellen verwendet und die benutzten Quellen entnommenen Passagen als solche kenntlich gemacht habe.

Die Promotionsarbeit ist in dieser oder ähnlicher Form in keiner anderen Universität vorgelegt worden.

Ort, Datum

Unterschrift

Acknowledgements

I wish to take the opportunity and use this space to give special thanks to all the people who helped me accomplish the scientific work included in this manuscript. I want to firstly and primarily acknowledge the guidance offered by the two Professors supervising this PhD project, Univ-Prof. Dr.Ing Georg N. Duda, and Univ-Prof. Dr. Ing Marc Kraft. I wish to thank them for providing their solid research experience in focusing my work, and always keeping a critical eye, ready to question results presented to them, shaping gradually my work into a PhD project.

My time in Berlin and my work in the Julius Wolff Institut (2007-2010) were not easy, but were made simpler by the two team leaders of the Group of Musculoskeletal Biomechanics (MSBiomech), Dr. William R. Taylor, and Dr. Markus O. Heller. The everyday interaction with both of them built the foundation of the work presented in this manuscript. Their scientific comments, novel ideas, and extensive knowledge of the field were a constant force driving my work forward. At the same time, their efforts in organizing this group kept everyone else focused on only the relevant scientific questions without ever having to worry about anything else. Additionally, I would like to thank fellow colleagues in MSBiomech, for providing help and ideas whenever needed, especially Adam Trepczynski and Stefan Kratzenstein. Research cannot be performed without financial support, so I wish to acknowledge the various institutions that have supported different parts of this project. Mainly the European Committee (FP6: Dessos project; FP7: VPHOP project; FP7: MXL project), the German Research Foundation (SFB360), and the German speaking Arthroscopy Association.

Finally I would like to give my special thanks to the people that privately supported me and encouraged me to complete my doctorate studies in Berlin. I want to thank my parents, Yannis and Charoula, for supporting me throughout my studies, and always providing me with the best possible example. Finally, and most importantly, I want to give my special thanks to my fiancée Mary, for being a constant source of support, understanding and inspiration, and most importantly, being always there, making life in charming but grey Berlin much easier.

Abstract

The Q-angle, describes the angle with which the quadriceps force vector is applied on the patella. Hence, it influences the biomechanical environment of the patello-femoral joint by lateralizing the resultant quadriceps force vector. The latter increases the risk for lateral patellar dislocation and overload of the lateral part of both the tibio-femoral and patello-femoral joint. The Q-angle is influenced by static anatomical parameters such as the frontal plane and rotational alignment, active soft tissues (quadriceps muscle), and knee kinematics, especially the dynamic rotation and abduction of the knee. In this study major goal was to explore the role of frontal plane and rotational malalignment both anatomically but also dynamically in patients with patello-femoral instability.

An MRI protocol has been developed to reliably and non-invasively analyze the 3D geometry of the lower extremity. Goal was to quantify parameters such as the mechanical femoral-tibial angle and the knee version, thereby characterizing the static frontal plane and rotational alignment of the knee joint. For the reliable analysis of the lower limb function, a functional approach for assessing the kinematics of the lower extremity based on motion-capture data was developed, tested, and established. This approach was shown to be repeatable and reproducible, as well as accurate when assessing the dynamic motion of the lower limb joints. By measuring patients in the gait lab, through this approach it was possible to reliably quantify the knee dynamic internal-external rotation and ab-adduction during activities of the daily living.

The results of the MRI analysis of fifteen patients with patello-femoral instability, suggested that they had a significantly increased knee valgus, and significantly increased knee version when compared with fifteen healthy adults. The increased knee version has been additionally linked to femoral deformities. Furthermore, evidence was found that the vastus lateralis is stronger than the vastus medialis, further increasing the lateral force applied on the patella. Additionally, the functional analysis of thirteen patients suggested that the dynamic internal rotation and functional valgus of the knee are significantly increased in patients with patello-femoral instability when compared to fifteen healthy adults. Additional evidence strongly linked both the aforementioned functional as well as anatomical deficits.

The results presented in this study suggest that the patho-anatomic and dynamic features of the lower limb of patients with patello-femoral instability act to increase the Q-angle increasing the risk for dislocation and long term joint degeneration. When the function of the patients was quantified using a reliable functional approach for the analysis of the lower limb kinematics, it was observed that this problem is only magnified during dynamic activities with the secondary knee motion acting to dynamically increase the functional Q-angle. Treatment for patients with patello-femoral instability should therefore focus not only on correcting these patho-anatomic characteristics, but also re-instating normal lower limb kinematics. Whether the latter can be achieved by applying specific rehabilitation protocols, gait retraining, use of knee braces that act as constraints for the knee, or even further surgical intervention remains to be investigated. A combination of these treatments, together with other more traditional therapeutic interventions, might not only increase the success rates of the direct surgical treatment of patello-femoral instability, but also reduce the long term effects such as OA and pain observed in patients with patello-femoral instability, which can severely affect the patient future quality of living.

Zusammenfassung

Der Q-Winkel beschreibt die Kraftwirkungsrichtung des Quadrizepts, mit welcher der Muskel an der Patella angreift. Dieser beeinflusst die Biomechanik des patello-femorale Gelenks durch eine Lateralisierung des Kraftvektors und erhöht somit das Risiko einer Patella Luxation und einer Überlastung der lateralen Kontaktfläche des tibio-femorale, als auch des patello-femorale Gelenks. Der Q-Winkel wird beeinflusst durch statisch anatomische Parameter, wie z.B. der Ausrichtung der Frontal Ebene und der Rotationsachse, durch Muskelaktivität und der Kinematik der Gelenke, wie z.B. das dynamische Rotationsverhalten und die Abduktion des Kniegelenks. Das übergeordnete Ziel dieser Studie war die Untersuchung der Rolle von pathologischer Ausrichtung (anatomisch sowie dynamisch) der Frontalebene, sowie der Rotationsachse in Patienten mit patello-femorale Instabilität.

Ein MRT Protokoll wurde entwickelt, um die 3D Geometrie der unteren Extremitäten zuverlässig und nicht-invasiv zu erfassen und den Winkel zwischen Femur und Tibia, sowie die Neigung (Knieversion) des Kniegelenkes zu quantifizieren, um die statische Ausrichtung der Frontalebene, sowie der Rotationsachse zu charakterisieren. Zur verlässlichen Analyse des funktionellen Status der Gliedmaßen wurde ein funktioneller Ansatz zur kinematischen Beurteilung der unteren Extremitäten entwickelt. Dieser Ansatz, der auf der Erfassung von Bewegungsdaten beruht, wurde in dieser Arbeit verifiziert und etabliert. Die Gütekriterien dieser Methoden erwiesen sich im Verlaufe der Arbeit bestehender Methoden deutlich überlegen. Durch die Anwendung dieses Verfahrens konnte im Rahmen einer Bewegungsanalyse an Patienten die dynamische interne/externe Rotation und die Ab- bzw Adduktion des Kniegelenks während alltäglicher Bewegungen quantifiziert werden.

Das Ergebnis der Analyse von 15 Patienten mit patello-femorale Instabilität ergab, dass die Patienten, im Vergleich zu 15 gesunden Probanden, eine signifikante valgus Deformation und eine signifikante Erhöhung der Knieeigung hatten. Die erhöhte Neigung des Knies war auf die femorale Deformation zurückzuführen. Weiterhin konnte nachgewiesen werden, dass der Vastus Lateralis deutlich kräftiger war als der Vastus Medialis, was zu einer weiteren Lateralisierung der Kraftwirkungsrichtung auf die Patella führte. Die dynamische Untersuchung von 13 Patienten mit patello-femorale Instabilität ergab, dass die interne Rotation, sowie der dynamische Valguswinkel des Knies deutlich höher in Patienten war, als bei vergleichsweise gesunden Probanden. Zudem konnten weitere Erkenntnis erlangt werden, die in deutlicher Beziehung zu den zuvor genannten funktionellen und anatomischen Defiziten stehen.

Die Ergebnisse der anatomischen Analyse zeigten, dass die pathologischen und dynamischen Erscheinungen an den unteren Extremitäten der Patienten mit patello-femorale Instabilität zu einer Erhöhung des statischen Q-Winkels führen und somit das Risiko einer Luxation und die langfristige Degeneration des Gelenks erhöhen. Die Quantifizierung der Funktion des Kniegelenks, mittels des eigens entwickelten funktionellen Ansatzes ergab, dass das oben genannte Problem nur während der sekundären Bewegung des Knies zur Geltung kommt und damit zu einer dynamischen Erhöhung des Q-Winkels führt. Die Behandlung von Patienten mit patello-femorale Instabilität sollte somit auf die Korrektur der patello-femorale Defizite ausgerichtet werden und außerdem die Festigung physiologischer Kinematik durch die Anwendung spezieller Rehabilitationsverfahren, Bewegungstraining oder die Anwendung von Knieorthesen zur Führung der Kniebewegung beinhalten. Die Kombination dieser Behandlungsverfahren, zusammen mit traditionellen, therapeutischen Strategien, würde nicht nur zu einer erfolgreichen Behandlung patello-femorale Instabilität führen, sondern auch langfristige Schädigungen, wie z.B. OA und Gelenksschmerz bei Patienten mit patello-femorale Instabilität mindern. Dies sind Erfolge, die direkt mit einer erhöhten Lebensqualität des Patienten assoziiert werden können.

Table of contents

1	Introduction: Patello-femoral instability	18
1.1	Anatomy of the patello-femoral joint.....	19
1.2	Patello-femoral instability: clinical impact	20
1.3	Anatomical deficits leading to patello-femoral instability	21
1.3.1	<i>Trochlea Dysplasia</i>	21
1.3.2	<i>Lower limb alignment</i>	22
1.3.3	<i>Passive soft tissue deficits</i>	24
1.3.4	<i>Active soft tissue deficits</i>	25
1.4	Treatment of patello-femoral instability.....	25
1.5	Biomechanics of the patello-femoral joint	26
2	Aims and goals	31
3	Development and characterization of a reliable functional approach to assess the kinematics of the lower limb.....	35
3.1	Gait Analysis	36
3.2	Functional methods to identify joint centres and axes of rotation.....	38
3.2.1	<i>SCoRE</i>	38
3.2.2	<i>The SCoRE residual</i>	39
3.2.3	<i>SARA</i>	40
3.3	Soft tissue artefacts.....	40
3.3.1	<i>OCST</i>	41
3.3.2	<i>wOCST</i>	41
3.4	OSSCA, a functional approach to analyze the kinematics of the lower extremity....	42
3.4.1	<i>Materials and methods</i>	42
3.4.2	<i>Results</i>	45
3.4.3	<i>Discussion</i>	48
3.4.4	<i>Conclusions</i>	51
3.5	Use of OSSCA to non-invasively quantify the mechanical femoral-tibial angle.....	51
3.5.1	<i>Materials and methods</i>	53
3.5.2	<i>Results</i>	57
3.5.3	<i>Discussion</i>	60

3.5.4	<i>Conclusions</i>	63
4	Analysis of the patho-anatomy in patients with patello-femoral instability	64
4.1	Magnetic Resonance Imaging for assessing lower limb anatomy.....	65
4.2	Characterization of a dedicated MRI protocol to capture the entire lower limb 3D alignment.....	66
4.2.1	<i>Methods</i>	66
4.2.2	<i>Results</i>	69
4.2.3	<i>Discussion</i>	71
4.3	Frontal and rotational malalignment of the femur: key factors of the patho-anatomy in patellofemoral instability	74
4.3.1	<i>Methods</i>	75
4.3.2	<i>Results</i>	76
4.3.3	<i>Discussion</i>	79
4.4	Effect of patello-femoral instability on the quadriceps anatomy	80
4.4.1	<i>Methods</i>	81
4.4.2	<i>Results</i>	83
4.4.3	<i>Discussion</i>	87
4.4.4	<i>Conclusion</i>	89
5	The influence of patello-femoral instability on lower limb function	91
5.1	wOSSCA and registration of identified joint centres and axes with ordinary procrustes analysis.....	92
5.2	Analysis of lower limb function in patients with patella-femoral instability	93
5.2.1	<i>Methods</i>	95
5.2.2	<i>Results</i>	98
5.2.3	<i>Discussion</i>	103
5.2.4	<i>Conclusion</i>	107
6	Conclusions - Future work.....	108
6.1	Clinical context.....	109
6.2	Major findings	110
6.3	Impact and future work	111

6.4	Epilogue	113
7	References	114

Figure Index

<i>Figure 1-1: Q-angle is the angle between the quadriceps force vector and the patellar tendon. The bigger this angle becomes, the greater the lateral part of the force vector acting on the patella, thereby increasing the risk of dislocation, and the lateral patello-femoral pressure.....</i>	<i>19</i>
<i>Figure 1-2: Image of a dislocated patella in a patient suffering from patello-femoral instability.</i>	<i>20</i>
<i>Figure 1-3: MRI image of a dislocated patella. In such a case, the medial patello-femoral ligament is torn..</i>	<i>21</i>
<i>Figure 1-4: Typical radiographic finding of subjects with trochlea dysplasia (Diederichs, Issever et al.).Figures a, b, c, d follow the classification of Dejour (Dejour H 1994). Patients with Type A, and B, usually are not for surgical correction of the dysplasia....</i>	<i>22</i>
<i>Figure 1-5: Femoral torsion is considered to be a risk factor for patello-femoral instability by increasing the Q-angle and the lateral pressure on the patella(Diederichs, Issever et al.)</i>	<i>23</i>
<i>Figure 1-6: Dynamic valgus is defined as the position or motion where the distal femur moves toward the midline and the distal tibia away from the midline of the body, thereby further increasing torque moments acting on the knee (Hewett, Myer et al. 2005).....</i>	<i>24</i>
<i>Figure 1-7: Schematic of the MPFL rupturing during an initial complete patellar dislocation with the inferomedial patellar touching the lateral trochlea facet(Diederichs, Issever et al.).</i>	<i>25</i>
<i>Figure 1-8: Patello-femoral and tibio-femoral joint models used to track patello-femoral movement during MR imaging. Consecutive positions of the moving tibia and patella in respect to a stationary femur are visible through changes of grey and white color (Yamada, Toritsuka et al. 2007).</i>	<i>27</i>
<i>Figure 1-9: Experimental setup to measure patello-femoral contact mechanics during cadaveric experiment simulating activities of daily living (Goudakos, Konig et al. 2009). Patello-femoral and tibio-femoral kinematics are captured through an optical system (Vicon, Oxford, UK), while PF contact mechanics assessed via an electronic pressure measuring sensor (K-Scan #4000, TekScan Inc., South Boston, MA, USA).</i>	<i>27</i>
<i>Figure 1-10: Tibio-femoral (left) and patello-femoral (right) peak contact forces as calculated by a validated MS model during multiple repetitions of four different activities, and 2 subjects in body weight (BW). Patello-femoral forces, in contrast to the tibio-femoral, are significantly dependent upon the activity (one-way Anova, $p<0.001$),</i>	

<i>surpassing the tibio-femoral contact forces for deep knee flexion activities (Trepczynski, Kutzner et al. 2010).....</i>	<i>28</i>
<i>Figure 1-11: Sample of patients included in the only in vivo study examining gait patterns in patients with PF instability. Control group in this study was the contra-lateral limb, which in this case is the right leg, clearly with a pathologic rotational mal-alignment (Paulos, Swanson et al. 2009).....</i>	<i>30</i>
<i>Figure 3-1: Vicon (Oxford, UK) infa-red camera, and reflective markers used for traditional gait analysis.</i>	<i>36</i>
<i>Figure 3-2: Person performing gait analysis in our local gait laboratory. Infa-red cameras are shown in a frame, while the reflective markers shine.</i>	<i>37</i>
<i>Figure 3-3: As a symmetrical functional approach, the joint centre is expressed into the local coordinates of each segment. If the joint motion though is imperfect, the two segmental joint centers, if transformed in the global space will not coincide.</i>	<i>39</i>
<i>Figure 3-4: Results of computer simulations demonstrating that the global error in the identification of a joint CoR with SCoRE is approximately half of the SCoRE's residual (Kratzenstein, Heller et al. 2010).</i>	<i>40</i>
<i>Figure 3-5: Efficacy of wOCST in minimizing the SCoRE residual benchmarked against the normal OCST in 17 subjects (BMI=28.5±2.1) while performing a StarArc activity (Kratzenstein, Heller et al. 2010).</i>	<i>41</i>
<i>Figure 3-6: General marker placement (from back, side, and front) used for functional determination of skeletal motion. The largest markers (shown in black) represent palpated bony landmarks, while the smaller markers (grey) are placed on the soft tissues of the respective segment. Although the soft tissue markers can be prone to inter- and intra-subject positional variation, the high reproducibility of locating the joint centres using OSSCA demonstrates the robust nature of this functional approach to motion analysis.</i>	<i>43</i>
<i>Figure 3-7: SCoRE hip joint centre residual (mm) determined (upper) at different time points and (lower) by different observers. No significant inter-day or inter-observer variation of the residual was determined, demonstrating the repeatable and reproducible identification of the hip joint centre. This was confirmed by a mean SCoRE residual value of 7.1mm ± 1.2mm, indicating a mean error of the hip joint centre of approximately 3.55mm.....</i>	<i>46</i>
<i>Figure 3-8: Femur and tibia lengths (mm) using the OSSCA and the regression approach, determined (upper) on different days and (lower) by different observers. While OSSCA displayed no significant differences (p>0.05) between days or different observers, the</i>	

regression approach appears to be heavily influenced by the observer ($p < 0.01$ shown as *), and subsequently by the individual marker placement.48

Figure 3-9: Scatter plot depicting the correlation between the mechanical Femoral Tibial Angle (mFTA) measured either functionally (Functional-mFTA), or based on the identification of landmarks and regression analysis (Regression-mFTA), against CT measurements (CT-mFTA). While both the Functional-mFTA ($R=0.91$; $p < 0.0001$) and the Regression-mFTA ($R=0.76$; $p < 0.001$) correlate significantly with the CT-mFTA, the graph illustrates that the Functional-mFTA adheres to the parity line (dashed) to a much greater degree, suggesting a large bias in the Regression-mFTA results.57

Figure 3-10: Bland and Altman plots of the (upper) Functional-mFTA and (lower) Regression-mFTA against the CT-mFTA. The Functional-mFTA has a small bias (deviation of mean value from zero) and exhibits good agreement (low standard deviations (SD)) with the CT-mFTA. In contrast, a considerable bias is present for the Regression-mFTA, which also shows relatively poor agreement with the CT-mFTA.58

Figure 3-11: Box plots of the differences between CT-mFTA, and the Functional-mFTA and the Regression-mFTA as determined in 15 limbs. The CT-mFTA - Functional-mFTA data, indicates a much better prediction of the mFTA from the functional method if compared to the reference method (CT) ($p=0.27$, than the regression approach, which showed significant ($p=0.006$) errors when compared to the CT-mFTA.59

Figure 4-1: Example of landmarks defined on posterior femoral condyles (up) and posterior tibial condyles (down) for a healthy adult (left) with almost no relative rotation of the femur and the tibia, and a patient with PF instability (right) with a relative internal rotation of the femur.76

Figure 4-2: Rotational and frontal plane alignment differences between healthy ($n=15$) adults, and patients ($n=15$) with patello-femoral instability. Significant differences ($p < 0.01$) are indicated with a *. Negative knee version means either internal rotation of the distal femur or external rotation of the proximal tibia. Negative values for the mFTA indicate genu valgum.77

Figure 4-3: Relationship between knee version and femoral torsion (up) and knee version and tibial torsion (down). There is a mild, significant correlation between femoral torsion and knee version ($R=-0.555$), and no correlation between tibial torsion and knee version. This indicates that the torsional deformity local to the knee, is more likely to originate from a femoral deformity than from a tibial deformity.78

Figure 4-4: Example of segmentation and extraction of the quadriceps muscles from an MRI scan of the femur, using Amira(Visage Imaging GmbH, Berlin, Germany).82

<i>Figure 4-5 Differences between right and left leg of 15 healthy adults in distribution of the quadriceps muscles (VM, VL, VI, RF) and the total quadriceps area in the 50% distance between hip centre and knee centre (* $p<0.05$).</i>	84
<i>Figure 4-6: Differences between injured and contralateral limb of 13 subjects PF instability in distribution of the quadriceps muscles (VM, VL, VI, RF) and the total quadriceps area in the 50% distance between hip centre and knee centre (* $p<0.05$).</i>	85
<i>Figure 4-7: Differences in the ratios of the four muscles of the quadriceps group over the entire quadriceps area between healthy adults, and the injured and contralateral limb of patients with PF instability (* $p<0.05$).</i>	86
<i>Figure 4-8: Ratios of the VL over VM in the injured and contralateral limb of patients with patello-femoral instability, as well as control of healthy adults. Whilst no significant differences were found between the different groups, a very clear trend approaching significance ($p=0.065$) was observed as a difference between contralateral and healthy, with the VM being less strong than the VL, as well as between injured and contralateral ($p=0.058$).</i>	87
<i>Figure 5-1: wOSSCA using as input both standardized activities which provide greater RoM for the joints of the lower extremity and the targeted for analysis activities.</i>	93
<i>Figure 5-2: Sample of knee joint flexion calculated during a stair ascending activity. The figure shows how the max, min, and RoM values are being identified.</i>	97
<i>Figure 5-3: Knee ab-adduction angles for three different activities in a comparison between healthy controls (blue) and patients with patella-femoral instability (green). The minimum values during an activity cycle are displayed on top, while the maximum are displayed on the lower graph (*: $p<0.01$).</i>	98
<i>Figure 5-4: Knee internal-external rotation angles for three different activities in a comparison between healthy controls (blue) and patients with patella-femoral instability (green). The minimum values during an activity cycle are displayed on top, while the maximum are displayed on the lower graph (*: $p<0.01$).</i>	99
<i>Figure 5-5: RoM in degrees for knee ab-adduction (top) and internal-external rotation (bottom) during three different activities between healthy adults (blue) and patients with patella-femoral instability (green) (*: $p<0.01$).</i>	100
<i>Figure 5-6: RoM in degrees for hip, knee and ankle flexion RoM between healthy adults (blue) and patients with patella-femoral instability (green) during walking, stair ascending and stair descending.</i>	101

<i>Figure 5-7: Secondary motion RoM (rotation and ab-adduction) in degrees for hip and ankle joints between healthy adults (blue) and patients with patella-femoral instability (green) during walking, stair ascending and stair descending.</i>	<i>102</i>
<i>Figure 5-8: Frontal plane mechanical femoral-tibial angle for patients with patello-femoral instability and healthy controls using the Functional-mFTA. Positive values in this figure indicate valgus alignment (*: $p<0.000$).....</i>	<i>103</i>
<i>Figure 5-9: Correlation between frontal plane anatomical alignment (Functional-mFTA) and dynamic valgus alignment in patients with patello-femoral instability.</i>	<i>104</i>
<i>Figure 6-1: How frontal plane and rotational mal-alignment can influence both the stability of the PF joint and future joint degeneration by increasing the Q-angle.</i>	<i>110</i>

Table Index

<i>Table 2-1: Summary of goals aimed to be investigated through this PhD project</i>	<i>33</i>
<i>Table 2-2: Summary of technical-related hypotheses</i>	<i>34</i>
<i>Table 2-3: Summary of clinically related hypotheses concerning patello-femoral instability</i>	<i>34</i>
<i>Table 3-1: Intra-class correlation (ICC (3,4)) showing repeatability between days (inter-day reliability) and reproducibility between different observers (inter-observer reliability) as well as the upper and lower bounds for the 95% confidence interval (CI).</i>	<i>47</i>
<i>Table 3-2: A considerable variation in patients' characteristics was deliberately selected in this study cohort, including BMI and joint status (native vs. replaced) to demonstrate applicability of the functional methods in clinically relevant situations.</i>	<i>54</i>
<i>Table 3-3 Lower limb alignment as defined by the mechanical femoral tibial angle (mFTA) determined by the CT-mFTA, the Functional-mFTA, or the Regression-mFTA. Positive mFTAs correspond to varus and negative to valgus knee alignment. Values are reported as mean \pm standard deviation (min, max). For the Functional-mFTA and the Regression-mFTA, the 95% confidence interval of the difference to CT-mFTA [margin of error] is additionally shown. Lower limb alignment as defined by the mechanical femoral tibial angle (mFTA) determined by the CT-mFTA, the Functional-mFTA, or the Regression-mFTA. Positive mFTAs correspond to varus and negative to valgus knee alignment. Values are reported as mean \pm standard deviation (min, max). For the Functional-mFTA and the Regression-mFTA, the 95% confidence interval of the difference to CT-mFTA [margin of error] is additionally shown.</i>	<i>60</i>
<i>Table 4-1: MRI protocol for the assessment of the 3D skeletal anatomy of the lower limb. ...</i>	<i>67</i>
<i>Table 4-2: Definition of the parameters (lengths, frontal plane, and rotational alignment) characterizing 3D skeletal anatomy of the lower extremity. FHC, KC, and AC represent the hip, knee, and ankle centre respectively. FNA is the femoral neck axis. DTFC and DTTC are the dorsal tangents of the femoral and tibial condyles respectively, while MA represents the torsional malleoli axis.</i>	<i>69</i>
<i>Table 4-3: Intra-class correlation coefficients (ICC (3,4)) including the upper and lower bounds for the ICCs 95% confidence interval (CI) showing repeatability at different time points (inter-day reliability). In addition, the mean differences (MD) between the two measurements are provided (and standard deviation (SD)), with the AD indicating a possible bias in the measurements.</i>	<i>70</i>
<i>Table 4-4: Intra-class correlation coefficients (ICC (3,4)) including the upper and lower bounds for the ICCs 95% confidence interval (CI) showing reproducibility between different evaluators (inter-observer reliability). In addition, the mean differences (MD)</i>	

between the two measurements are provided (and standard deviation (SD)), with the AD indicating a possible bias in the measurements.	70
Table 4-5: Table 5: Intra-class correlation coefficients (ICC (3,4)) including the upper and lower bounds for the ICCs 95% confidence interval (CI) showing reproducibility between different measurements by the same evaluator (intra-observer reliability).	71
Table 4-6: The mean differences (MD) between the two measurements of the quadriceps of 15 healthy adults are provided (and standard deviation (SD)), with the AD indicating a possible bias in the measurements. As a measure of comparison, the mean values of each measurement (MV) are presented, as well as the % error of the MD as a percent of the MV. All area values are in mm ²	71
Table 4-7: Mean and standard deviation of rotational and frontal (mFTA) alignment parameters in both healthy subjects (n=15) and patients with PF instability (n=15). P-values are presented in bold for parameters when significant differences are observed.	77
Table 4-8: Average area of the four quadriceps muscle groups (VM at 30%, the rest at 50% of the distance between hip and knee joint centre) for 15 healthy adults. P-values of the differences are also indicated (* $p < 0.05$), as well as the correlation coefficients between the absolute values.	83
Table 4-9: Average area of the four quadriceps muscle groups (VM at 30%, the rest at 50% of the distance between hip and knee joint centre) for 13 subjects with PF instability. P-values of the differences are indicated ($p < 0.05$), as well as the correlation coefficients between the absolute values.	84
Table 5-1: Demographic characteristics of healthy controls and patients with patello-femoral instability.	95
Table 5-2: Summary of all measured values for the RoM of flexion, ab-adduction, and internal-external rotation, for the three lower limb joints (hip, knee and ankle), and during three different activities (walking, stair ascending, stair descending). Significance of the differences is also provided, with the significance levels being set on $p < 0.05$	1

1

Introduction: Patello-femoral instability

This chapter will deal with describing the clinical problem and the biomechanics of patello-femoral instability. It is going to be clear why patello-femoral instability is a significant source of patient discomfort, what the main accepted risk factors are and which the proposed treatment recommendations are. Furthermore, it is going to be clear throughout, what the gaps in the existing clinical and biomechanical knowledge are.

1.1 Anatomy of the patello-femoral joint

The patellofemoral joint includes the articulation between the patella and the trochlear groove of the femur. The patella is divided into the medial and lateral facet. On the femoral side, the patellofemoral joint consists of the trochlear groove, formed by the anterior surface of the distal femur (Walsh 2003). When the knee flexion increases, the patella engages the trochlea groove, sliding on its surface (Colvin and West 2008), providing stability for knee flexion angles greater than 30° . An important parameter in characterizing the patellofemoral joint is the quadriceps angle (Q-Angle), defined as the 3D angle between the anterior superior iliac spine (ASIS), the patella, and the tibial tuberosity, describing the direction of the quadriceps force vector relative to the patellar tendon (Fig. 1-1).

The patello-femoral joint is of major importance to the normal function of the lower limb. The knee extensor mechanism uses the patella as the force transducer applying the quadriceps force vector through the patellar tendon on the tibia. If the patello-femoral joint fails to properly operate, then subjects suffer from significant disability and discomfort.

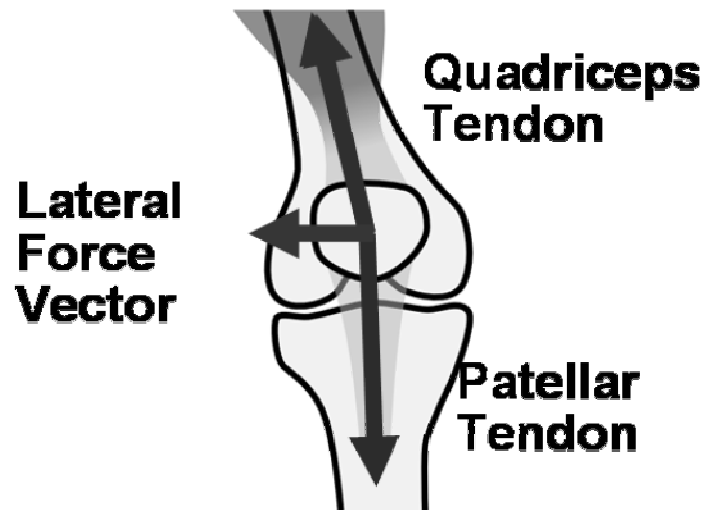


Figure 1-1: Q-angle is the angle between the quadriceps force vector and the patellar tendon. The bigger this angle becomes, the greater the lateral part of the force vector acting on the patella, thereby increasing the risk of dislocation, and the lateral patello-femoral pressure.

1.2 Patello-femoral instability: clinical impact

Patellofemoral instability is defined as a patellar dislocation, which can either be acute as a primary, traumatic event or chronic with recurrent episodes. Patello-femoral instability and subsequent patellar dislocation have an approximate frequency of occurrence in the general population of 5.8 per 100,000 (Fithian, Paxton et al. 2004), with an increased bias towards young females. Recurrence after an acute episode of dislocation, if not treated operatively, happens with a rate of 15-44% (Hawkins RJ 1986). An acute dislocation influences the biomechanical environment of the knee joint with more than half of the patients not able to engage in sports activities. In most cases, dislocation happens laterally (White and Sherman 2009).

The effects observed on patients with patello-femoral instability can be divided into anatomical and functional. On the one hand, patellar dislocations damage the soft tissues surrounding the joint, causing severe pain, and long term effects such as osteoarthritis or patello-femoral pain syndrome. On the other hand, both the physical and the psychological harm from the dislocations have also a dynamic effect leading to multiple functional deficits: loss of normal knee function, fear of re-dislocation, functional adaptation, joint overloading. It is therefore important to examine patello-femoral instability not by just looking on the static, anatomical picture, but considering function as well. However, detail analysis of patient everyday function and lower limb kinematics is not reported as part of the routine examination associated with patello-femoral instability.



Figure 1-2: Image of a dislocated patella in a patient suffering from patello-femoral instability.



Figure 1-3: MRI image of a dislocated patella. In such a case, the medial patello-femoral ligament is torn..

1.3 Anatomical deficits leading to patello-femoral instability

Stability of the patello-femoral joint is perceived as a complex interaction between passive components (bony anatomy, ligaments) and active structures (muscles). Patello-femoral instability has primarily been attributed to a dysplastic trochlea (Fucentese, von Roll et al. 2006; Mulford, Wakeley et al. 2007; Amis, Oguz et al. 2008), but also to confounding factors such as hyper-extension of the knee joint and insufficiency of the medial patello-femoral ligament (Amis, Firer et al. 2003).

1.3.1 Trochlea Dysplasia

Trochlear dysplasia prohibits the early engagement of the patella in the trochlear groove during or near knee joint extension, leading to low levels of physical constraint and therefore possible dynamic instability (Murray TF 1999). According to the literature, more than nine out of every ten patello-femoral instability patients suffer from dysplastic trochlea (Dejour and Le Coultre 2007) (Fig. 1-4).

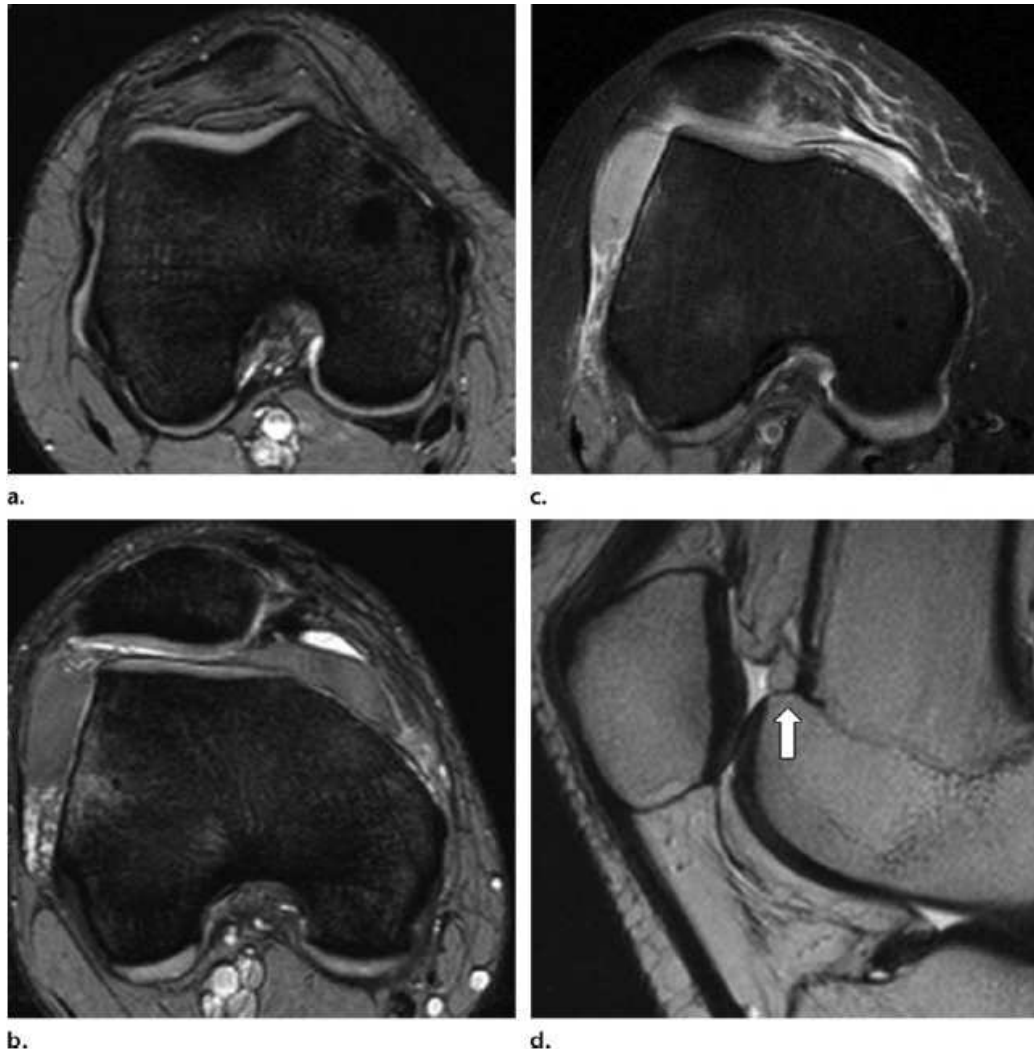


Figure 1-4: Typical radiographic finding of subjects with trochlea dysplasia (Diederichs, Issever et al.). Figures a, b, c, d follow the classification of Dejour (Dejour H 1994). Patients with Type A, and B, usually are not for surgical correction of the dysplasia.

1.3.2 Lower limb alignment

Frontal plane alignment also contributes to patello-femoral instability, particularly in valgus limbs (Fig. 1-6) where the relative attachment sites of the patellar extensor mechanism result in a higher Q-angle (angle between the lines of action of the patellar and quadriceps tendons) (Rünow A 1983), and therefore an increased lateral pressure on the patella. This relationship is possibly associated with the higher propensity towards patella-femoral instability in young females who often have a tendency to genu valgum.

Femoral or tibial rotational deformities (Fig. 1-5) can also influence the Q-angle, as well as the torsional loads acting on the patella (Rünow A 1983). Patella alta has also been associated with recurrent dislocations and higher instability (Insall, Goldberg et al. 1972; Carson, James et al. 1984; Farahmand, Senavongse et al. 1998).

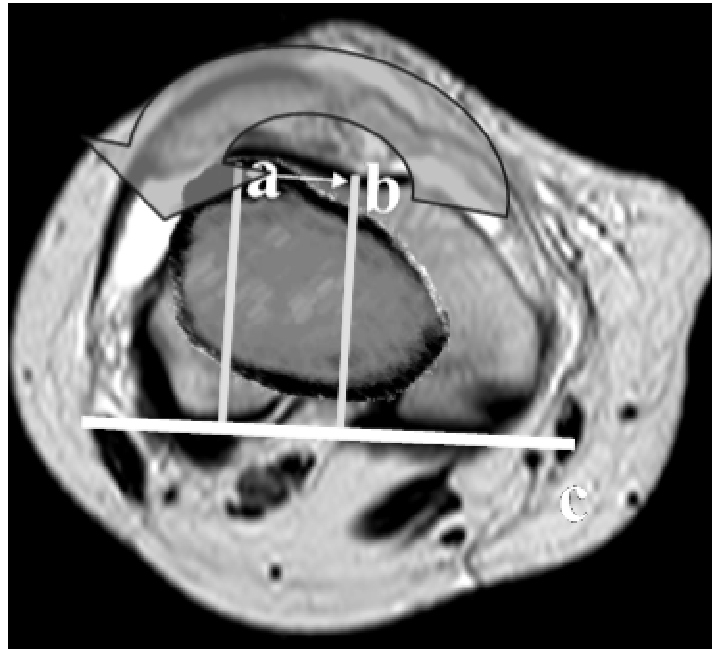


Figure 1-5: Femoral torsion is considered to be a risk factor for patello-femoral instability by increasing the Q-angle and the lateral pressure on the patella(Diederichs, Issever et al.)

Whilst a static mal-alignment of the lower limb has been identified as a possible risk factor for patellar instability, if a valgus knee together with an increased internal rotation of the distant femur is combined, this anatomical configuration often leads to a “functional” valgus, which influences the adduction moments acting on the knee, thereby further increasing the risk for not only patellar dislocation, but also ACL tear or patello-femoral pain syndrome (Amis, Firer et al. 2003).

Even though there is a suggestion in the literature that femoral anteversion and genu valgum biomechanically qualify as risk factors for patello-femoral instability it is unclear in what extent this is true. Furthermore, while it makes sense that an internal rotation of the femur against the tibia will result in a higher risk of patellar dislocation, it remains unclear whether this deficit is femur- or tibia-originated.

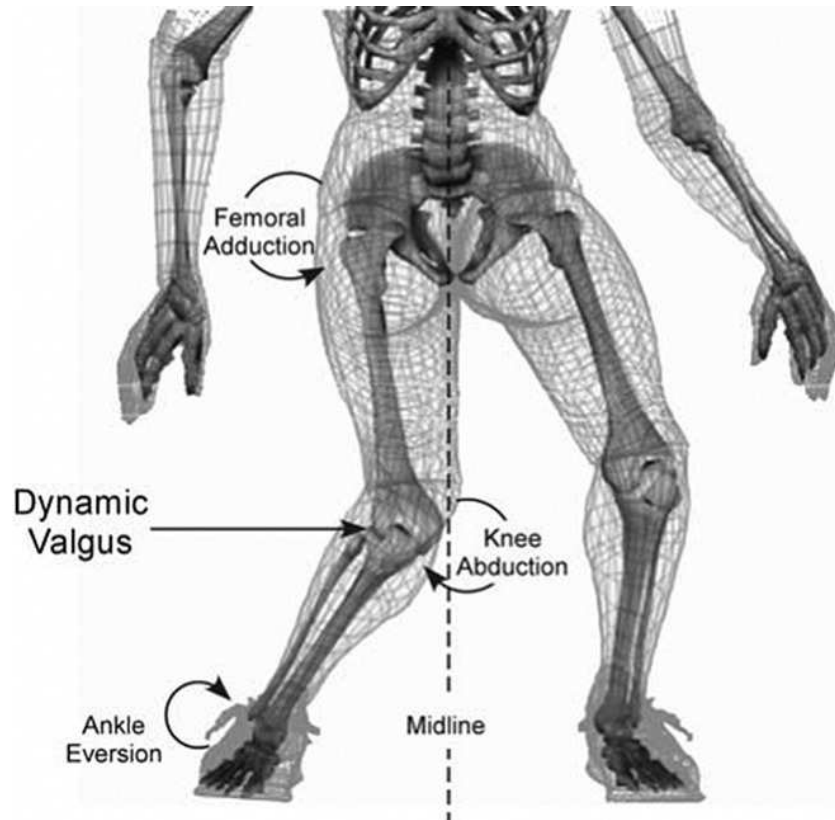


Figure 1-6: Dynamic valgus is defined as the position or motion where the distal femur moves toward the midline and the distal tibia away from the midline of the body, thereby further increasing torque moments acting on the knee (Hewett, Myer et al. 2005).

1.3.3 Passive soft tissue deficits

In addition to the bony constraints, the soft-tissues, particularly the ligaments and active muscle stabilisers provide additional stability to the joint, particularly during dynamic activities. The medial patello-femoral ligament (MPFL) is an important structure inserting medially near the femoral cruciate attachment and laterally to the medial facet of the patella. By constraining lateral motion of the patella, this structure is thought to provide stability to the patello-femoral joint, especially at lower knee flexion angles. Laxity or deficiency of the MPFL is thought to increase the risk of patella dislocation especially in dysplastic knees (Goodfellow, Hungerford et al. 1976), with the resulting damage reducing joint stability and therefore possibly leading to recurrent dislocation problems. It is additionally shown in the literature that in 98.6% of the initial lateral patellar dislocations there is some

sort of lesion occurring to the MPFL, with more than 50% of these cases involving a complete tear (Balcerek, Ammon et al.).

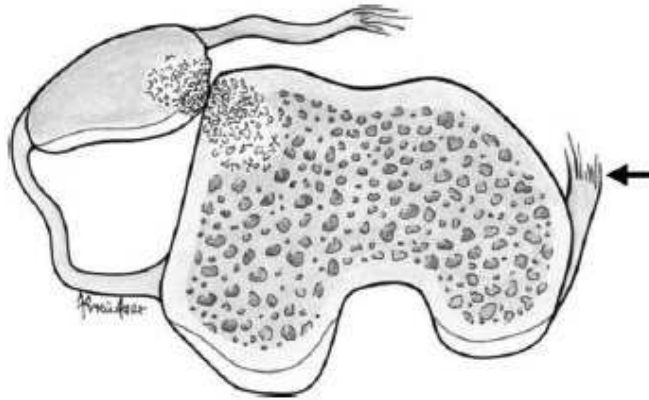


Figure 1-7: Schematic of the MPFL rupturing during an initial complete patellar dislocation with the inferomedial patellar touching the lateral trochlea facet (Diederichs, Issever et al.).

1.3.4 Active soft tissue deficits

Active muscle forces play an important role in the dynamic stabilisation of the joint. The vastus medialis and lateralis provide force vectors that contribute to balancing the medial and lateral loading on the patella, with their combined action normally parallel to the femoral anatomical axis (Wittstein, Bartlett et al. 2006). A force imbalance, in this case due to possible muscular adaptation after prolonged deviation from physiologically normal function, could hinder patients' rehabilitation and return to normal function and physiological loading during activities of daily living. However, clear evidence linking such a muscular deficit to patello-femoral instability cannot be easily found throughout the literature, especially evidence on possible muscular imbalance not only on the affected side, but also on the contra-lateral side of patients with patello-femoral instability. If such evidence is presented, this could potentially explain why there is a high risk of bilateral deficiencies associated with patello-femoral instability.

1.4 Treatment of patello-femoral instability

Instability of the patello-femoral joint is clearly a multi-faceted problem, with various conservative and surgical approaches having been suggested to treat both acute and recurrent instabilities.

Non-operative approaches have been used to cope with either acute or recurrent episodes of patello-femoral instability. Although immobilization has been suggested as a non-invasive approach (Colvin and West 2008), little or no evidence is available that non-operative approaches such as bracing or physiotherapy have a positive effect after acute dislocations. Patients suffering from recurrent episodes, however, can benefit from patellar taping or physical therapy aimed at strengthening targeted muscle groups to enhance patellar stability (Mulford, Wakeley et al. 2007). However, what is not present in the literature, is whether those patients might benefit from equal strengthening of the same muscles of the unaffected side, thereby minimizing the risk for an initial patellar dislocation on the contralateral limb.

Surgical interventions aim to repair the static anatomical deficit. Although traditionally, low-level recommendations for therapy have been followed, more recent approaches have included early MPFL repair (for acute dislocation or MPFL injury) (Schottle, Goudakos et al. 2009), tibial tubercle reconstruction (for chronic instability, patella alta or elevated tibial tubercle to trochlear groove (TTTG) distance), or trochleoplasty for patients with trochlear dysplasia.

Each clinical researcher reporting results concerning an operative technique focus on the immediate outcome on patello-femoral instability. Several of these approaches have therefore been reported to be effective with handling instability. The long term effects of these treatments though are generally unknown. As suggested recently (Paulos, Swanson et al. 2009), patients although do not suffer from instability post-operatively are not always happy. Furthermore, long term effects such as joint degeneration in means of patello-femoral or tibio-femoral osteoarthritis, or patello-femoral pain syndrome are often encountered within these patient groups. It is clear therefore, that current intervention techniques, possibly fail to encompass both the entire complexity of anatomical deficits causing patello-femoral instability (by e.g. ignoring some anatomical deficiencies) and offer treatment which also restores not only the anatomical norm, but also the functional norm to these patients.

1.5 Biomechanics of the patello-femoral joint

Previous studies to understand patello-femoral instability have focused on models of patellar kinematics derived from MRI (Yamada, Toritsuka et al. 2007; Yamada, Toritsuka et al. 2007; Draper, Besier et al. 2009) (Fig. 1-8).



Figure 1-8: Patello-femoral and tibio-femoral joint models used to track patello-femoral movement during MR imaging. Consecutive positions of the moving tibia and patella in respect to a stationary femur are visible through changes of grey and white color (Yamada, Toritsuka et al. 2007).

Within our research group there have been extensive cadaveric studies in-vitro aiming to understand the biomechanics of the patello-femoral joint prior to the commence of this study (Goudakos, Konig et al.; Goudakos, König et al. 2008; Goudakos, Konig et al. 2009). During this project several cadavers were tested under an experimental design which simulates activities of daily living (walking and stair climbing) (Fig. 1-9).

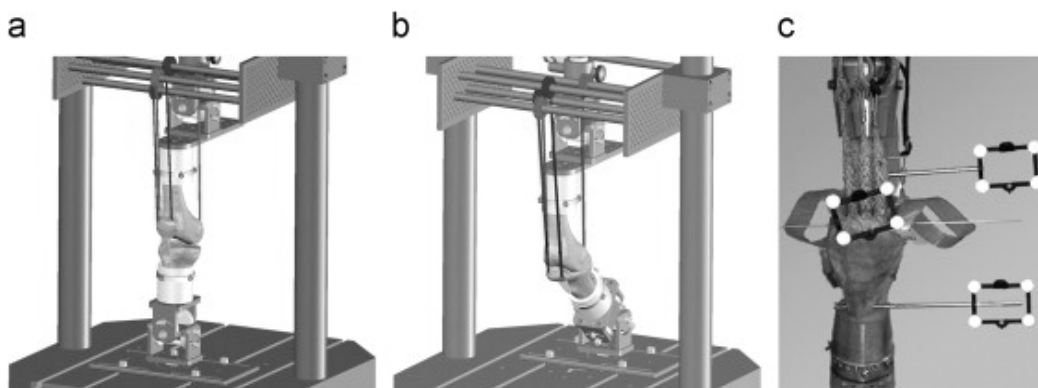


Figure 1-9: Experimental setup to measure patello-femoral contact mechanics during cadaveric experiment simulating activities of daily living (Goudakos, Konig et al. 2009). Patello-femoral and tibio-femoral kinematics are captured through an optical system (Vicon, Oxford, UK), while PF contact mechanics assessed via an electronic pressure measuring sensor (K-Scan #4000, TekScan Inc., South Boston, MA, USA).

According to this study, the stairs ascending when compared to ground walking results into more challenging patellofemoral contact mechanics and kinematics at early knee flexion angles, which are the most critical for patellar instability (Goudakos, Konig et al. 2009). More specifically, it is demonstrated that patellofemoral pressure, lateral force distribution and lateral tilt are activity dependent, which can offer explanation why patellar instability, along other patello-femoral problems (e.g. patello-femoral pain) mostly appear during stairs ascending-descending.

The latter experiments have demonstrated the need for a better understanding of the patello-femoral mechanics *in vivo*. Using patient specific gait analysis, CT-generated musculoskeletal models, and a validated process to access the internal musculoskeletal forces of the lower extremity (Heller, Bergmann et al. 2001), it was possible to assess the patello-femoral contact forces during activities of daily living for two subjects carrying an total knee prosthesis (Trepczynski, Kutzner et al. 2010). In this study, we have shown that whilst patello-femoral contact forces during low flexion activities, are significantly smaller than tibio-femoral, for activities where high flexion angles is achieved, these forces surpass the values of the tibio-femoral forces. The latter finding makes clear, that higher knee flexion angles lead to increased patello-femoral forces (Fig. 1-10). It can be therefore deducted, that possible adaptations of gait characteristics in subjects with patello-femoral instability, which could result in increasing the knee flexion angle to avoid the “instable” situation of full extension, can cause an overload on the patello-femoral joint, which if chronic could lead to joint degeneration and OA.



Figure 1-10: Tibio-femoral (left) and patello-femoral (right) peak contact forces as calculated by a validated MS model during multiple repetitions of four different activities, and 2 subjects in body weight (BW). Patello-femoral forces, in contrast to the tibio-femoral, are significantly dependent upon

the activity (one-way Anova, $p < 0.001$), surpassing the tibio-femoral contact forces for deep knee flexion activities (Trepczynski, Kutzner et al. 2010).

Of course, according to the literature, there is a regulatory mechanism on the biomechanical environment of the patello-femoral joint, protecting the joint from local overloading, when the joint contact force increases. This mechanism involves the increase of the patello-femoral contact area for a smoother distribution of the contact pressure, and is corroborated in computer simulations (Mesfar and Shirazi-Adl 2008; Adouni and Shirazi-Adl 2009). However, in an *in vitro* study within our study group it was shown that this mechanism seems to exhaust efficacy in relatively low patello-femoral contact forces (<500N) (Goudakos, Konig et al.). This fact becomes increasingly important if combined with the findings proposed in Fig. 1-10, with peak patello-femoral forces of 3-4 times bodyweight, or approximately (2500 - 3200 N) for an average adult weighing 80kg. Whether the inefficacy of this regulatory mechanism is linked to further joint degeneration remains unknown.

However, limited knowledge exists regarding this influence of patello-femoral instability on subjects' function, either in terms of kinematic adaptation or in their deviation from normal patterns during loaded dynamic activities *in vivo*. While gait patterns in such patients have been examined post-operatively (Paulos, Swanson et al. 2009), a proper control cohort was not included in that study. More precisely, control cohort was taken as the contra-lateral limb of the patients, which in some cases was as pathological as the examined instable limb (Fig. 1-11). Furthermore, how these functional insufficiencies relate to anatomical deficits remains to be investigated.

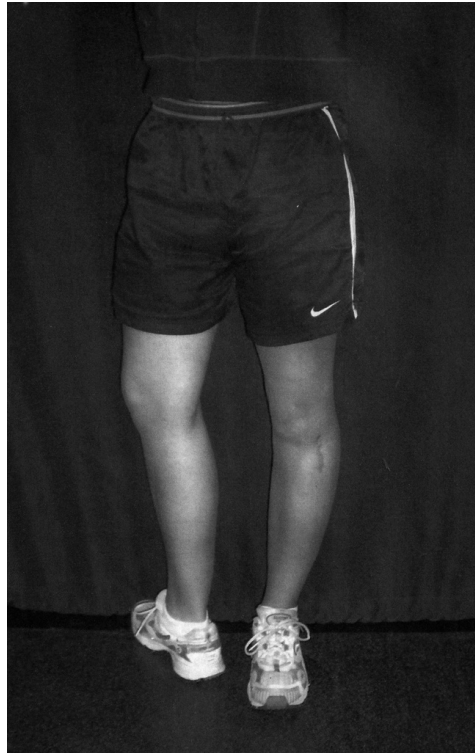


Figure 1-11: Sample of patients included in the only in vivo study examining gait patterns in patients with PF instability. Control group in this study was the contra-lateral limb, which in this case is the right leg, clearly with a pathologic rotational mal-alignment (Paulos, Swanson et al. 2009).

Altered biomechanical (both anatomic, and functional) environments of the patella are known to lead to overloading of both the tibial femoral, but importantly also the patello-femoral joints. Although modern treatments are now able to deal successfully with the joint instability, secondary joint degeneration and arthritis have been observed (von Knoch, Bohm et al. 2006; Paulos, Swanson et al. 2009). An understanding of how static mal-alignment is linked with patellar instability, whether muscle groups such as the quadriceps are different than normal, and whether patients' function post-operatively is returned to normal will offer an insight into the biomechanics of the pathological joint.

2

Aims and goals

This chapter briefly summarizes the findings of the literature review mentioned in the Introduction, and highlights the existing gap in knowledge related to patello-femoral instability that acts as motivation to the present study. The goals and the hypotheses of this study are presented here in detail.

It is clear throughout the literature that patello-femoral instability is a multifactorial problem. It results in severe loss of function, fear of re-dislocation, and pain. There are multiple surgical approaches proposed in the literature to cope with the instability. For a large volume of patients, operative solution involves reconstruction of the medial patello-femoral ligament, hence repairing the primary medio-lateral stabilizer of the patella to refrain the patella from recurrent dislocation, but not actually repairing the underlying anatomical pathology leading to the instability. Hence the underlying risk for a new patellar dislocation often remains. Nevertheless, no consistent treatment recommendation exists in the literature, partially because the patho-anatomy leading to instability and the anatomical risk factors, remain not fully characterized. A proper characterization of e.g. mal-alignment and its role on instability, or the role of quadriceps muscular force imbalance, could potentially refocus intervention techniques by including these factors also in the treatment planning.

An additional problem appears to be that although most operative procedures appear to be successful in reinstating stability on the patello-femoral joint, there is a substantial number of patients who in the long-term develop secondary problems such as patello-femoral or tibio-femoral osteoarthritis, or patello-femoral pain syndrome, all of which affect their quality of living. Functional adaptations, or anatomical deficits that are not surgically corrected, can result in joint overloading and subsequent joint degeneration.

The focus of this study is to address the aforementioned deficits, and create new knowledge in the area of patello-femoral instability. Specifically, this work attempts to understand the role of lower limb frontal plane, and rotational mal-alignment as part of the patho-anatomy leading to patello-femoral instability. Additionally, it will be explored whether a functional adaptation of the quadriceps muscles and the lower limb joint kinematics occurs in patients with patello-femoral instability.

Furthermore, in order to be able to explore the previous target areas, it is planned to develop novel techniques for the accurate and reliable analysis of both the lower limb 3D anatomy, and subjects' lower limb function, in terms of joint kinematics.

The goals and the subsequent patello-femoral instability-related formulated hypothesis are summarized in Tables 2-1 and 2-2 and 2-3 by separating the focus areas in anatomy and function, and methodological vs. clinical-oriented goals:

Table 2-1: Summary of goals aimed to be investigated through this PhD project

Area	Goal
Anatomy	Technology: Develop MRI protocol for the reliable analysis of global lower limb alignment and quadriceps anatomy
	Application: Investigate the role of frontal plane and rotational mal-alignment as key factors of the patho-anatomy in patello-femoral instability
	Application: Investigate whether patello-femoral instability leads to an adaptation of the quadriceps anatomy
Function	Technology: Develop and characterize a reliable and accurate functional approach for the analysis of the kinematics of the lower extremity
	Application: Use this approach to measure lower limb frontal plane alignment functionally and non-invasively
	Application: Investigate whether patello-femoral instability leads to an adaptation of lower limb joint kinematics

Table 2-2: Summary of technical-related hypotheses

Area	Hypothesis
Anatomy	T1. An MRI protocol can be used to provide repeatable and reproducible analysis of the lower limb alignment and quadriceps anatomy
Function	T2. Functional approaches to gait analysis can be used for the repeatable and reproducible determination of lower limb joint kinematics
	T3. Functional approaches to gait analysis can be used to accurately assess the frontal plane mechanical femoral tibial angle non-invasively

Table 2-3: Summary of clinically related hypotheses concerning patello-femoral instability

Area	Hypothesis
Anatomy	C1. Patients with patello-femoral instability have significantly more internally rotated knees and have a significant genu valgum
	C2. The pathologic internal knee version in patients with patello-femoral instability can be explained by femur- and not tibia-based deficits
	C3. Patients with patello-femoral instability have a pathologic distribution of the vastus medialis/lateralis cross sectional area
Function	C4. Patients with patello-femoral instability display an increased functional valgus, and increased functional internal rotation than healthy adults
	C5. Patients with patello-femoral instability have different than normal lower limb joint kinematics during activities of daily living

In the coming chapters, these hypotheses will be methodically tested, with the conclusions of this work used to provide adequate answers for the aims presented here.

3

Development and characterization of a reliable functional approach to assess the kinematics of the lower limb

This chapter deals with the methodological aspect of developing a reliable functional approach for the analysis of human lower limb kinematics, which will be used for the analysis of patients with patello-femoral instability. The basic principles of gait analysis, soft tissue artifacts and functional characterization of joints are presented here. The description and characterization of OSSCA, a functional approach to gait analysis presented in this chapter is published under Taylor, Kornaropoulos et al., Gait Posture 2010, whereas its application to quantify the frontal plane mechanical femoral-tibial angle is also published under Kornaropoulos, Taylor et al., Gait Posture 2010.

3.1 Gait Analysis

The reliable assessment of skeletal motion is important for a wide range of clinical investigations in studies where the correct interpretation of results relies on the ability to detect small differences between cohorts, but also in longitudinal studies when multiple measurements are required, possibly performed by different observers. By providing access to subject specific motion patterns, movement analysis allows quantitative assessment of a range of functional and kinematic parameters and can therefore provide a direct comparison for the efficacy of interventional approaches (Rose, DeLuca et al. 1993; Stout, Gage et al. 2008), or complement imaging and physical examination findings to support clinical decisions. Furthermore, the additional registration of synchronous external kinetic data can provide essential information for the determination of internal loading conditions using e.g. musculoskeletal analyses (Heller, Bergmann et al. 2001; Heller, Taylor et al. 2003; Taylor, Heller et al. 2004).

The non-invasive capture of human motion is generally performed by attaching reflective markers to the subject's skin and has been proven effective in the literature (Andriacchi and Alexander 2000; Ehrig et al. 2006; Ehrig et al. 2007; Leardini et al. 2005; Taylor et al. 2005). Nowadays the use of three-dimensional motion capturing using infrared cameras is the most common method to minimize light artefacts and therefore to lighten the marker capturing.

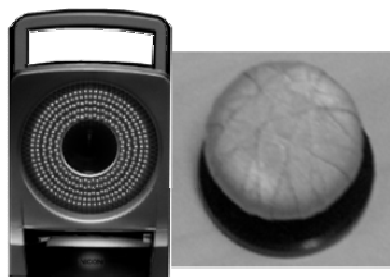


Figure 3-1: Vicon (Oxford, UK) infra-red camera, and reflective markers used for traditional gait analysis.

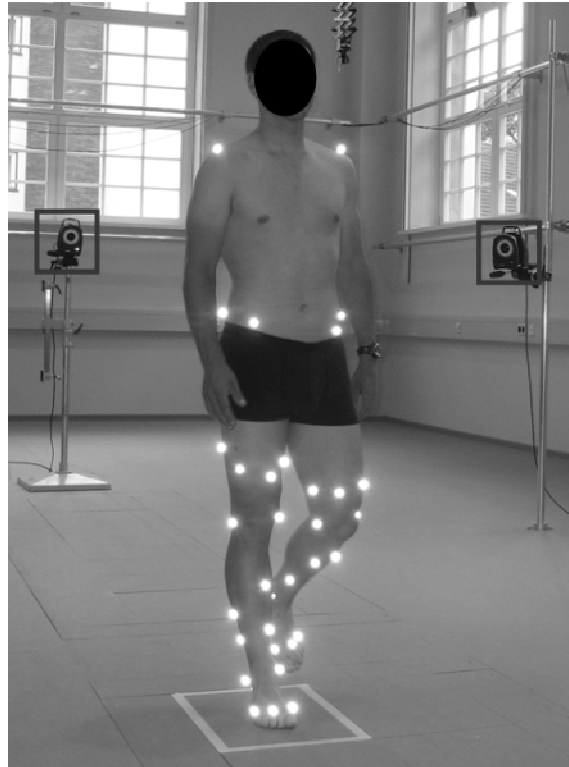


Figure 3-2: Person performing gait analysis in our local gait laboratory. Infra-red cameras are shown in a frame, while the reflective markers shine.

To assess the skeletal motion from these marker positions, a number of techniques have been developed to identify specific bone structures or landmarks. Geometric regression relationships, that are still used in the majority of motion capture systems, describe the location of e.g. the hip joint centre relative to specific skin markers placed over the left or right superior inferior iliac spine and the posterior superior iliac spine (Kadaba, Ramakrishnan et al. 1990; Davis, Ounpuu et al. 1991). Such regression methods, however, are subject to errors (Bell, Pedersen et al. 1990) due to their generic nature, since bony deformities or gender-based skeletal differences (Shultz, Nguyen et al. 2008; Dandachli, Nakhla et al. 2009) are not considered, but also the variation of marker placement. Furthermore, these approaches are subject to soft tissue artefact (STA) (Cappozzo, Catani et al. 1996; Leardini, Chiari et al. 2005; Cereatti, Della Croce et al. 2006), where the attached markers move relative to the underlying skeletal structures, resulting in errors in the

determination of the skeletal motion. The efficacy of these techniques is therefore limited, particularly in subjects with high soft tissue coverage.

Recently, methods to minimise the errors associated with skin marker artefact have been proposed using the Point Cluster Technique (Alexander and Andriacchi 2001) or the Optimal Common Shape Technique (OCST) (Taylor, Ehrig et al. 2005). In the latter, the motion of markers attached to the skin relative to one another is minimised using a so-called Procrustes Analysis (Dryden and Mardia 2002) to generate a rigid configuration of the segment marker set, formed from all time points of the trial. By replacing the original segment marker set with this OCST configuration, the relative motion of markers, and therefore the effects of skin elasticity can be minimized.

Furthermore, rapid (Rozumalski and Schwartz 2008), accurate, and robust methods to functionally determine spherical joint centres, using the Symmetrical Centre of Rotation Estimation (SCoRE) (Ehrig, Taylor et al. 2006) and joint axes, using the Symmetrical Axis of Rotation Approach (SARA) (Ehrig, Taylor et al. 2007), have been developed and verified *in silico*. The combination of these techniques allows the location of joints to be estimated from kinematic data alone, without the assumptions associated with generic anatomical relationships.

3.2 Functional methods to identify joint centres and axes of rotation

The development and *in silico* verification of the aforementioned techniques to functionally identify the joint centres of rotation (SCoRE) (Ehrig, Taylor et al. 2006), and the joint axes of rotation (SARA) (Ehrig, Taylor et al. 2007) has been work of the team supervising this PhD project, and has been completed prior to the commence of this study. However, for completeness, a brief description of these techniques is included in this manuscript.

3.2.1 SCoRE

In clinical gait analysis, in order to access the skeletal kinematics using markers attached on the skin surface, it is important to identify the location of the

joint centres of rotation. In the past this group has introduced the Symmetrical Center of Rotation Estimation (SCoRE) approach. This approach, whilst uses the kinematics of the segment markers to identify the Center of Rotation (COR), it assumes also that the coordinates of the joint centre must only remain constant relative to each segment, thus not requiring the assumption that one segment should remain at rest (Fig. 3-3). The SCoRE approach has been previously shown to be robust and more accurate than any other available technique (Ehrig, Taylor et al. 2006), and was additionally shown to be significantly faster when compared to a mathematically similar functional technique (Rozumalski and Schwartz 2008).

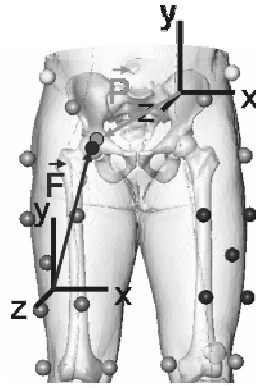


Figure 3-3: As a symmetrical functional approach, the joint centre is expressed into the local coordinates of each segment. If the joint motion though is imperfect, the two segmental joint centers, if transformed in the global space will not coincide.

3.2.2 The SCoRE residual

SCoRE is a symmetrical mathematical approach. This translates into a resulting joint centre as a representation of both joint segments' local coordinate systems. This means, that if transformed in the global space, if the joint motion is imperfect, then the two segmental joint centres $c_{1,i}, c_{2,i}$ will not coincide. The coincidence of the two local centre representations is improved the more perfect the motion of the segments is around a common centre. The SCoRE residual r is then defined as $r = \left\| \sum_{i=1}^n c_{1,i} - c_{2,i} \right\| / \sqrt{n}$ where n is the number of time points (Kratzenstein, Heller et al. 2010). r is mathematically exactly the residual of the underlying linear least squares problem. Using computer simulations it was possible to derive relationships between the residual, r , and the mean error of the estimated joint

position in global coordinates. This relationship indicated that the SCoRE's error err can be approximated as half of the residual r : $err \approx 0.5 \cdot r$ (Fig. 3-4). Hence, the residual of SCoRE offers a quality index for the determination of a CoR from marker data.

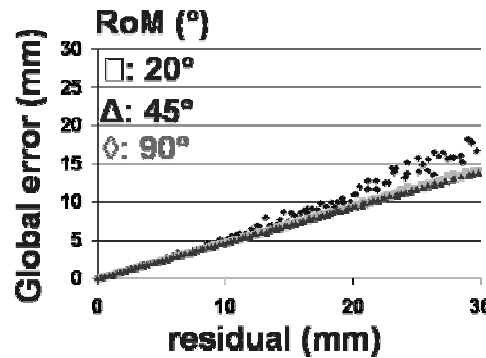


Figure 3-4: Results of computer simulations demonstrating that the global error in the identification of a joint CoR with SCoRE is approximately half of the SCoRE's residual (Kratzenstein, Heller et al. 2010).

3.2.3 SARA

Similarly to SCoRE, this group has previously introduced the Symmetrical Axis of Rotation Approach, SARA, a functional approach to determine the axis of rotation of joints, based on the same principles and mathematical background with SCoRE (Ehrig, Taylor et al. 2007). SARA has also to be demonstrated to be robust, fast, and more accurate than other functional approaches to provide the knee axis of rotation.

3.3 Soft tissue artefacts

As previously mentioned, the accuracy of any developed technique that estimates the position and movement of skeletal segments from markers attached on the skin surface is subject to soft-tissue artefacts (STAs), with the subject skin, and the attached markers moving relative to each other (Taylor, Ehrig et al. 2005; Cereatti, Della Croce et al. 2006; Kratzenstein, Ehrig et al. 2009). STAs can be separated into two categories: firstly, the movement of an entire marker cluster when the marker set is shifting over the underlying bone structures (combined marker artefact); secondly, the displacement of an individual marker relative to the marker cluster, as a result of non-rigid movement of the marker cluster (single marker artefact). The latter skin marker

error is based on the skin elasticity, soft tissue deformation as well as in inaccuracies of the measurement set-up.

3.3.1 OCST

Recently, several techniques have been introduced to cope with STAs. This group introduced the Optical Common Shape Technique (OCST), a method based on a mathematical technique called “Procrustes Analysis”. The OCST has been shown in a sheep *in vivo* study to efficiently minimize the single marker STAs (Taylor, Ehrig et al. 2005).

3.3.2 wOCST

Although the efficiency of OCST in removing single marker artefacts has been previously demonstrated, the establishment of the SCoRE residual as quality index for SCoRE has presented the opportunity to apply a complex mathematical optimization approach to further improve the minimization of STAs using the OCST. Under this approach, now the weighted OCST (wOCST) weights are assigned to each marker that are optimized until the SCoRE residual is minimized, in order to determine the best possible rigid marker configuration. Markers with the largest single marker artefacts are finally given lower weights, minimizing the impact on the definition of the joint CoR. The wOCST has been *in vivo* shown to minimize the SCoRE residual in less than 5mm (Kratzenstein, Heller et al. 2010) (Fig. 3-5).

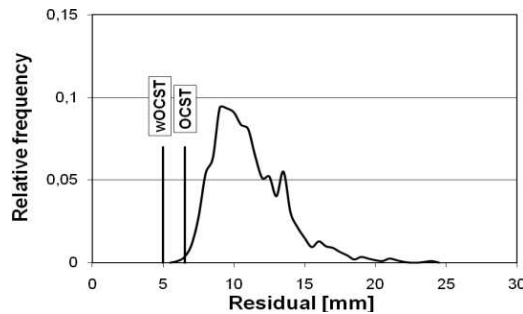


Figure 3-5: Efficacy of wOCST in minimizing the SCoRE residual benchmarked against the normal OCST in 17 subjects ($BMI=28.5\pm2.1$) while performing a StarArc activity (Kratzenstein, Heller et al. 2010).

3.4 OSSCA, a functional approach to analyze the kinematics of the lower extremity

It remains clear from the above mentioned evidence, that these functional approaches offer significant improvement in movement analysis when compared to other solutions. However, it remains unknown whether the combination of these functional methods to identify the joint locations can provide an improvement in reliability, as well as a reduction of user-induced variability over regression methods. We therefore hypothesized that a combination of the OCST, SARA & SCoRE is more reliable (repeatable and reproducible) than a common regression approach (Hunt, Birmingham et al. 2008) for the identification of skeletal structures of the lower limb. The aim of this study was thus to develop the OCST, SARA & SCoRE Combined Approach (OSSCA) to motion analysis and assess its repeatability and reproducibility.

3.4.1 Materials and methods

3.4.1.1 Study protocol and participants

Optical markers were attached to the skin of the right lower limb of six healthy male subjects (age 30.0 ± 4.5 ; BMI 22.8 ± 0.4) on multiple days, followed by motion analysis (12 FX20 cameras, Vicon, Oxford, UK) of standardized movements, as well as a single recording of a static standing posture. All subjects provided written informed consent prior to their participation in the study, and the study was approved by the local ethics committee.

Each entire marker set was attached by 5 independent research assistants, trained to perform gait analysis (referred to as “observers”) on each of 4 different days, according to the marker attachment protocol described below (Figure 1). On each day, movement analysis was performed by each of the observers (totalling five sessions), with each subject recording 5 repetitions consecutively (i.e. 6 subjects * 5 observers * 5 repetitions * 4 days, totalling 600 movement measurements), with a time between measurement of at least two days. While no specific care was taken to remove possible skin impressions, the tape used in normal practice did not leave residue on the skin that could bias inter-observer marker placement.

3.4.1.2 Marker protocol

The marker placement protocol used in this study (Fig. 3-6), which has been described previously (Kornaropoulos, Taylor et al.), consisted of a minimum of 4 reflective markers attached to the skin of each segment (pelvis, thigh, shank and foot) of the lower limb using double sided tape. Additional markers were placed on specific bone landmarks (via palpation); for the pelvis, the Right Anterior Superior Iliac Spine (RASIS), Left Anterior Superior Iliac Spine (LASIS), Right Posterior Superior Iliac Spine (RPSIS) and Left Posterior Superior Iliac Spine (LPSIS); for the knee at the medial and lateral epicondyles; and for the ankle on the medial and lateral malleoli.

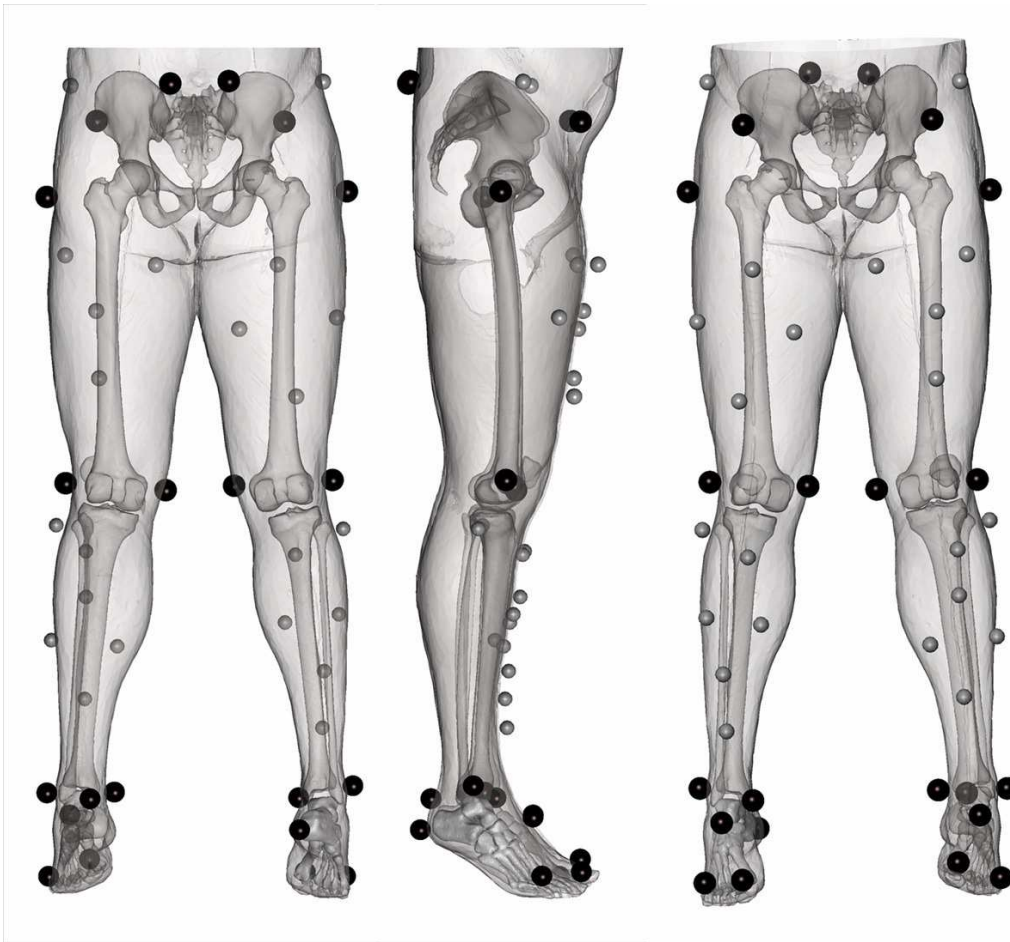


Figure 3-6: General marker placement (from back, side, and front) used for functional determination of skeletal motion. The largest markers (shown in black) represent palpated bony landmarks, while the smaller markers (grey) are placed on the soft tissues of the respective segment. Although the soft tissue markers can be prone to inter- and intra-subject positional variation, the high reproducibility of locating the joint centres using OSSCA demonstrates the robust nature of this functional approach to motion analysis.

3.4.1.3 Standardized motions

For the purpose of functionally identifying the hip and knee joint centres and axes, the participants performed standardized motions to provide the maximum available range of motion for each joint. Starting from a static standing pose, patients performed a “StarArc” motion (Camomilla, Cereatti et al. 2006) to functionally define the hip joint centre. This was immediately followed by two active flexion-extension motions of the knee. These standard motions were performed with support available for the contralateral hand to maintain balance where necessary.

3.4.1.4 Processing of the motion capture data

In an initial step, the skin movement artefact from each motion repetition was minimized using the Optimum Common Shape Technique (OCST) (Taylor, Ehrig et al. 2005). The hip joint centre was then identified using SCoRE (Ehrig, Taylor et al. 2006). Finally, the functional knee axis was identified from the knee flexion-extension motion, using SARA (Ehrig, Taylor et al. 2007). Here, the mid-point of the medial and lateral femoral epicondylar markers at the knee was projected onto the axis in order to centre the knee joint. The ankle centre was defined geometrically as the midpoint of the two reflective markers placed on the two malleoli landmarks.

The generic regression approach included the identification of the hip joint centre based upon the approach described by Hunt and co-workers (Hunt, Birmingham et al. 2008) using the distance between the markers attached on the right and left anterior superior iliac spines as the key parameter. According to their approach, the knee joint centre was defined as the midpoint of the markers placed on the medial and lateral femoral epicondyles, while the ankle joint centre was defined as the midpoint of the markers placed on the malleoli of the shank.

3.4.1.5 The SCoRE residual and assessment of repeatability and reproducibility

The SCoRE residual, r , serves as an indirect measure of the accuracy of the SCoRE’s functionally identified hip joint centre (Kratzenstein, Ehrig et al. 2009). The femur and tibia lengths, representing the distance between the hip-knee joints and the

femur and tibia lengths, representing the distance between the hip-knee joints and the knee-ankle joints respectively, as well as the SCoRE residual, were used to evaluate the repeatability and reproducibility of the 600 standardized movement repetitions for both the OSSCA and regression approach. Femoral and tibial segment lengths were determined using the joint centres identified from the entire motion, on the starting standing pose of the standardized activity. All computational post-processing was performed using in-house algorithms.

3.4.1.7 Statistics

To assess the reliability between different measurements, the 95% confidence interval (CI) of the intra-class correlation coefficient was calculated as a measure of repeatability (inter-day reliability) and reproducibility (inter-observer reliability) (McGraw and Wong 1996). The consistency model ICC(3,4) was chosen, in order to offer the proportion of reliability attributable to inter-day and inter-observer measurements, fitting to our study design. Additionally, to assess inter-measure variance, an analysis of variance (ANOVA) using a mixed linear model was performed for the factors “day” and “observer”, where inter-day variance (low repeatability) and inter-observer variance (low reproducibility) were tested for statistical significance. Statistical analysis was performed using SPSS v 17.0 (SPSS Inc., Champaign IL).

3.4.2 Results

The SCoRE residual measured over all 600 measurements was $7.1 \pm 1.2\text{mm}$ (Fig. 3-7), equivalent to an average error in the hip joint estimation of approximately 3.5 mm.

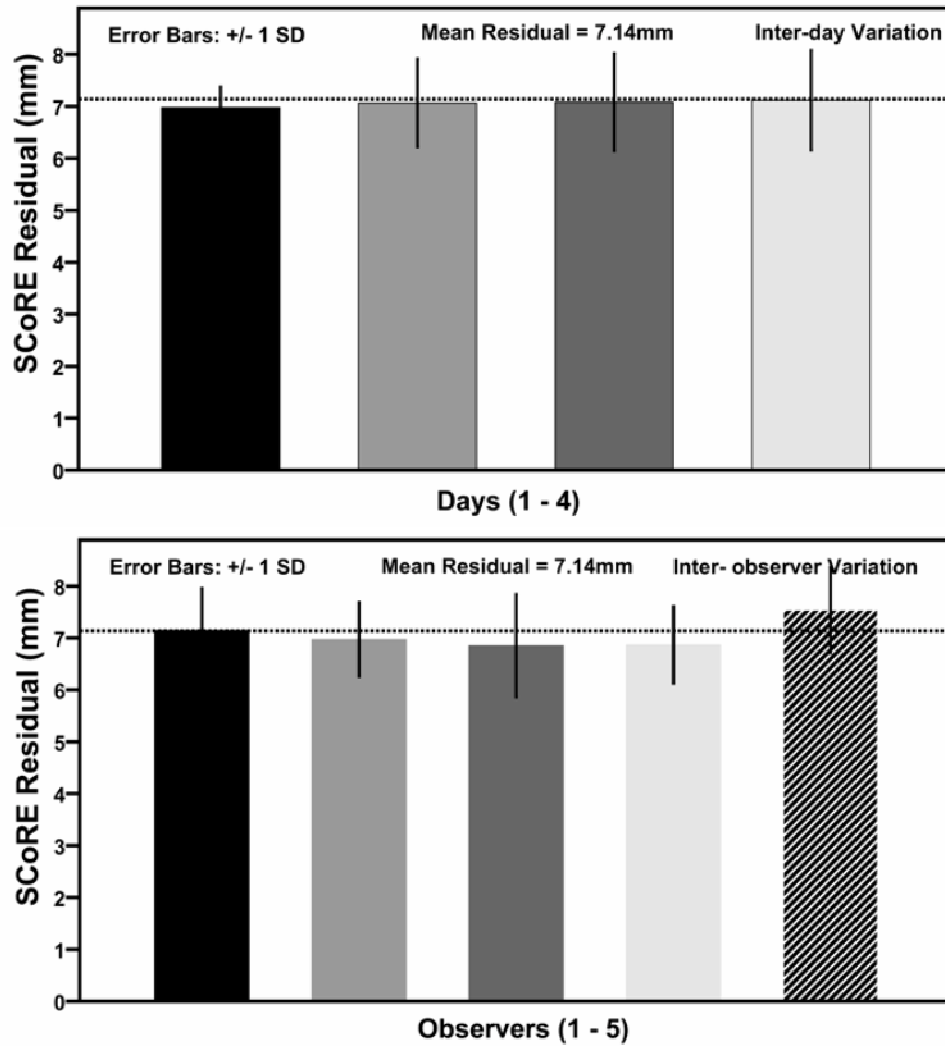


Figure 3-7: SCoRE hip joint centre residual (mm) determined (upper) at different time points and (lower) by different observers. No significant inter-day or inter-observer variation of the residual was determined, demonstrating the repeatable and reproducible identification of the hip joint centre. This was confirmed by a mean SCoRE residual value of $7.1\text{mm} \pm 1.2\text{mm}$, indicating a mean error of the hip joint centre of approximately 3.55mm .

The femoral and tibial segment lengths were determined using the OSCCA and the regression approach. These segment lengths were compared to each other during the repeatability test for the variation in measurements between different days (Fig. 3-8 upper) and measurements between different observers (Fig. 3-8 lower). The ICC for all tests showed that all parameters fall within the high reliability region ($\text{ICC} > 0.8$) (Table 3-1). However, the lower bound of the 95% confidence interval for the femoral length for both the inter-day repeatability (0.793) and the inter-observer

reproducibility (0.695) indicated a lower reliability between consecutive measurements using the regression technique.

To complement these results, the ANOVA revealed no significant variance ($p>0.1$) when using the OSSCA in either the femur or tibia lengths for any of the tested factors of “days” and “observers”. The same tests on the segment lengths calculated using the regression approach, revealed a statistically significant variance for the factor “observers” ($p<0.01$; low-reproducibility) when determining the femur length. Furthermore, a trend approaching significance was observed for the inter-day variance in the regression-based determination of femur length ($p=0.07$), and for the inter-observer variance in determination of tibia length ($p=0.085$). These findings were in agreement with the ICC analysis of femoral length.

Table 3-1: Intra-class correlation (ICC (3,4)) showing repeatability between days (inter-day reliability) and reproducibility between different observers (inter-observer reliability) as well as the upper and lower bounds for the 95% confidence interval (CI).

		Inter-day reliability			Inter-observer reliability		
		ICC	Lower Bound	Upper Bound	ICC	Lower Bound	Upper Bound
Functional	Femur	0.98	0.934	0.997	0.975	0.923	0.996
	Tibia	0.975	0.92	0.996	0.958	0.872	0.993
Regression	Femur	0.934	0.793	0.989	0.888	0.695	0.981
	Tibia	0.978	0.925	0.996	0.966	0.894	0.994

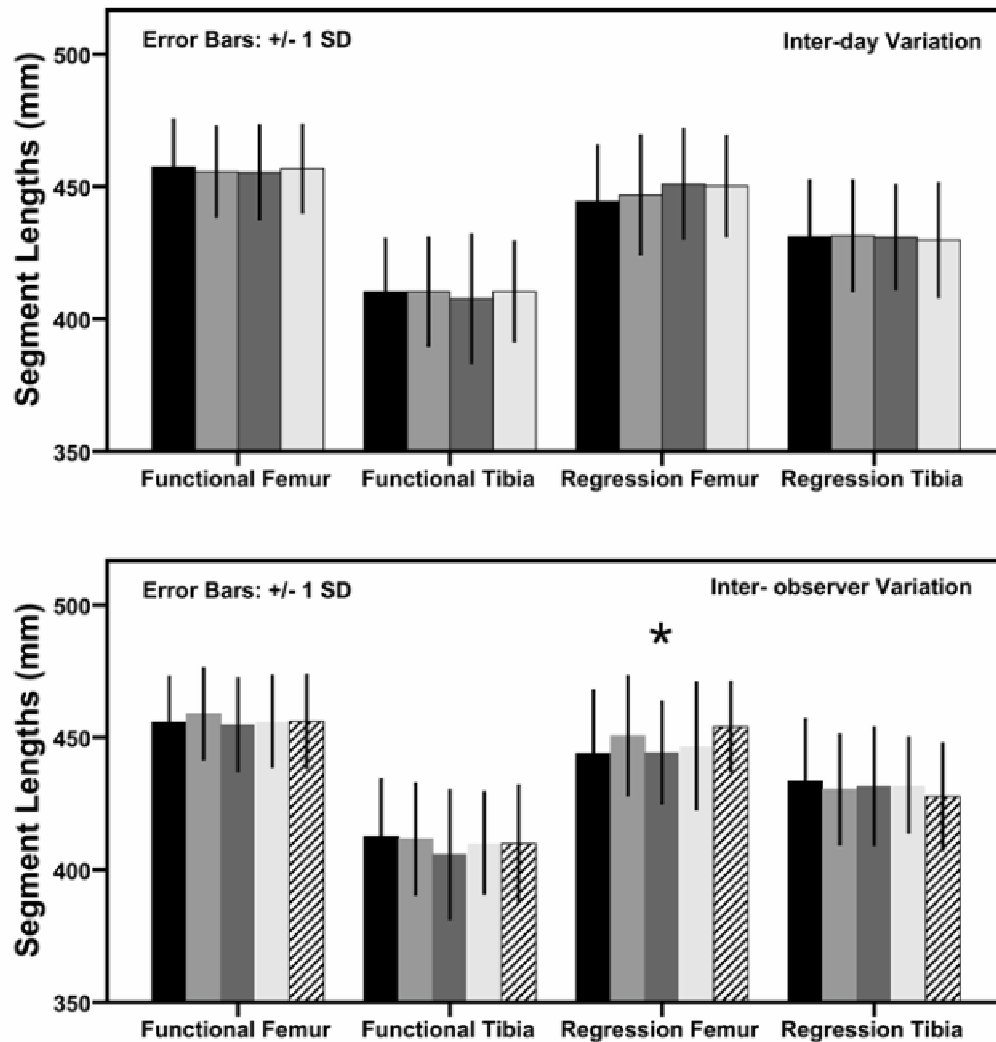


Figure 3-8: Femur and tibia lengths (mm) using the OSSCA and the regression approach, determined (upper) on different days and (lower) by different observers. While OSSCA displayed no significant differences ($p > 0.05$) between days or different observers, the regression approach appears to be heavily influenced by the observer ($p < 0.01$ shown as *), and subsequently by the individual marker placement.

3.4.3 Discussion

The reliable assessment of skeletal motion is important in studies where the ability to detect small differences between groups is essential for the correct interpretation of results. Furthermore longitudinal studies, especially when multiple measurements performed by different observers are required, necessitate methods that can ensure high repeatability and reproducibility. Indeed, the conclusions of a recent

study have indicated that poor reliability in clinical gait analysis is one of the largest error sources and cannot therefore be ignored (Schwartz, Trost et al. 2004; McGinley, Baker et al. 2009), suggesting that alternative approaches with minimal reliance on the observer's skill in marker placement be developed.

In this study, a novel protocol has been documented and characterised for defining a standard for motion analysis of the lower limb based entirely on the functional analysis of dynamic data. Using verified robust and rapid (Rozumalski and Schwartz 2008) methods for the reduction of soft tissue artefact (Taylor, Ehrig et al. 2005), as well as the identification of joint centres (Ehrig, Taylor et al. 2006) and axes (Ehrig, Taylor et al. 2007) of rotation, we have demonstrated a more repeatable and more reproducible approach to motion analysis than a commonly used regression based approach (Hunt, Birmingham et al. 2008). Moreover, despite possible inter-observer variability in marker placement, a high degree of reliability has been demonstrated in both segment lengths and in the quality of joint identification (using the SCoRE residual (Kratzenstein, Ehrig et al. 2009; Kratzenstein, Heller et al. 2010)). Furthermore, this functional approach can also offer access to accurate postural information (lower limb alignment), agreeing better with radiological findings than regression techniques (Kornaropoulos, Taylor et al.).

The SCoRE residual was used as an indirect measure of accuracy for the identification of the hip joint centre. Numerical simulations based on theoretical considerations have demonstrated that in cases where single marker artefacts are not present (i.e. in cases where the OCST is applied to ensure a rigid configuration of the marker set), the SCoRE residual, r , is linearly related to the global error, err , for the estimation of joint centres with the relationship $err \sim 0.5 \cdot r$ (Kratzenstein, Heller et al. 2010). Since the residual was repeatably measured at $7.1 \pm 1.2\text{mm}$ in this study (*Figure 4-2*), the mean error of the hip joint centre estimation is approximately 3.55mm. However, future studies should more directly address the absolute accuracy of the joint identification, as well as compare different functional approaches.

In this study, the largest statistically significant, variations were observed in the length of the femur, when assessed using the regression approach between different observers ($p < 0.01$; lower bound of ICC of 0.695). In agreement with previously published results on the reliability of regression techniques (Schwartz, Trost et al. 2004), we have also found large inter-observer variation when using the regression

approach. Since this was not the case when using OSSCA, this further highlights the robustness of the functional approach. The regression technique investigated (Hunt, Birmingham et al. 2008) in this study used generic equations that parameterized the distance between the two anterior superior iliac spine landmarks to determine the location of the hip joint centre. Even though care was taken by every observer to accurately palpate and place the skin markers over these bone landmarks, the results indicate that regression approaches are prone to inter-observer errors and soft tissue artefacts.

It is known that complex kinematics are a key feature of knee joint motion, but despite its dynamic behaviour, a repeatable and reproducible knee joint centre has been determined in this study using OSSCA, indicating the reliable capture of important aspects of the knee motion. For clinical gait analysis that includes challenging movements or demanding loading conditions (e.g. for assessment of knee joint stability), it might be possible to include a more complex assessment of the knee joint motion. Although a knee joint axis was determined in this study using the SARA neither the reliability of this axis nor the orientation of the associated skeletal segments were evaluated. Since a more complete understanding of knee joint motion is dependent upon the axes at the joint, future studies should focus on examining the reliability of the SARA axis for defining knee joint kinematics.

Whilst all subjects tested in the present study were healthy male adults, with a low BMI, it has been shown previously that the use of the OCST can effectively minimize soft tissue artefacts even in subjects with higher BMI (Kratzenstein, Ehrig et al. 2009). Here, a study cohort with males with a low BMI was specifically selected to ensure a standardized study design, that excluded additional sources of variability e.g. higher BMI, males vs. females. This was important since methods that solely depend upon the placement of and the relative distance between markers attached to the pelvis is prone to errors in cases of large soft tissue coverage (Bell, Pedersen et al. 1990; Cappozzo, Catani et al. 1996; Taylor, Ehrig et al. 2005; Cereatti, Della Croce et al. 2006). Furthermore, no female subjects were recruited in the present study since the pelvic anatomy of males and females is subject to significant variation (Dandachli, Nakhla et al. 2009), and single regression approaches are unable to capture this variability. However, the reliability of the OSSCA in a cohort more diverse, containing patients with higher BMIs, remains to be explored in further studies.

The repeatability and reproducibility of the approach employed to analyse motion in a clinical setting play an important role for both the validity and interpretation of the results (Donati, Camomilla et al. 2008). It is common practice for established gait laboratories to construct databases of previously measured individuals for use as controls in comparative and longitudinal studies. In such cases, where measurements are taken at different time points, or where measurements are performed by different observers, a repeatable and reproducible approach is mandatory since any differences observed between e.g. different time points, can be attributed to altered kinematics, rather than errors that originate from the analysis approach.

3.4.4 Conclusions

In this study, the OSSCA (OCST, SARA & SCoRE Combined Approach), a functional approach for assessing skeletal kinematics from skin marker based motion capture data, has been introduced. Key components in this approach are the minimization of soft-tissue artefact together with accurate, fast and robust methods for the functional identification of joint centres and axes. Our hypothesis that the OSSCA is more repeatable and reproducible than a commonly used regression approach has been confirmed by demonstrating its reliability in 600 motion capture trials. The proven reliability of the OSSCA will allow longitudinal studies in clinical settings to be performed without the uncertainty of systematic errors.

3.5 Use of OSSCA to non-invasively quantify the mechanical femoral-tibial angle

Frontal plane mal-alignment (Paley and Pfeil 2000) has been shown to cause increased adduction moments (Hurwitz, Ryals et al. 2002; Jackson, Teichtahl et al. 2004; Birmingham, Hunt et al. 2007) and knee contact forces (Heller, Taylor et al. 2003), as well as altered medio-lateral distribution of the tibio-femoral contact force (Zhao, Banks et al. 2007). Accurate quantification of frontal plane alignment is therefore important for determining the biomechanical conditions in the knee, particularly in the context of muscular imbalance (Karamanidis and Arampatzis

2009), joint instability (Parratte and Pagnano 2008), or bony deformities (Coventry, Ilstrup et al. 1993; Paley and Pfeil 2000), as well as for monitoring therapeutic interventions at the knee.

Lower limb alignment is commonly characterized by the mechanical femoral-tibial angle (mFTA), the frontal plane angle between the mechanical axes of the femur and tibia (Paley and Pfeil 2000). The standard method for quantifying mFTA in clinical practice uses long standing radiographs of the lower limb. Various studies suggest that although 2D X-ray imaging is the method of choice, this form of measurement is not immune to variability, and can be influenced by numerous factors such as the choice of bony landmarks, the specific X-ray modality (analog vs. digital), or rotation of the foot (Sailer, Scharitzer et al. 2005; Hunt, Fowler et al. 2006; Goker and Block 2007; Specogna, Birmingham et al. 2007). To address many of these issues, a method based on CT data offers an alternative 3D reference to 2D radiographs for the determination of alignment (Kawakami, Sugano et al. 2004), since 3D methods are less susceptible to errors caused by rotational effects. The drawback of both methods, however, is that patients are exposed to ionizing radiation. This factor becomes important in young patients who require multiple follow-up measurements, as well as when following e.g. less invasive treatments that compensate for mal-alignment using in-sole wedges (Kuroyanagi, Nagura et al. 2007) or braces (Gaasbeek, Groen et al. 2007). In such cases, the cumulative radiation dose is an issue (Hinman, May et al. 2006), but could be reduced by using non-invasive techniques. Furthermore, a weight-bearing, non-invasive method to quantify alignment would be critical in cases where radiation exposure may be ethically restricted, especially when young patients or healthy study controls are to be examined.

Motion capture presents an opportunity to assess kinematics non-invasively. Recently, this methodology has been investigated as a means to quantify limb alignment (Hunt, Birmingham et al. 2008; Mundermann, Dyrby et al. 2008; Vanwanseele, Parker et al. 2009). While their results presented a reasonable correlation to radiographic measures, determination of the required skeletal landmarks was limited to geometric regression. As these methods rely upon the accurate placement of skin markers to locate bone landmarks, as well as generic models of skeletal anatomy, the identification of joint centres (Bell, Pedersen et al. 1990), and

therefore the quantification of limb alignment, lacked patient specificity and was possibly subject to error. The authors thus suggested that functional methods be employed to identify landmarks such as the hip joint centre (Hunt, Birmingham et al. 2008).

The goal of this study was therefore to quantify lower limb alignment using non-invasive, functional methodologies, and to evaluate this technique against a 3D CT-based measure of frontal plane lower-limb alignment. We therefore hypothesize that the mechanical femoral-tibial angle can be quantified accurately using a method based on functional determination of the hip and knee joint centres, and that this approach shows better agreement with CT than regression methods.

3.5.1 *Materials and methods*

3.5.1.1 Subject cohorts

A total of 13 patients (15 limbs) were included in this study (Table 3-2). Nine subjects were post-operation total knee arthroplasty (TKA) patients and four were pre-operation total hip arthroplasty (THA) patients suffering from hip osteoarthritis. These subjects' characteristics were selected to demonstrate a diverse cohort, both in demographic characteristics, but also knee joint status (native vs. replaced). All subjects provided written informed consent prior to participation in this study, which was approved by the local ethics committee.

Table 3-2: A considerable variation in patients' characteristics was deliberately selected in this study cohort, including BMI and joint status (native vs. replaced) to demonstrate applicability of the functional methods in clinically relevant situations.

Patient (n=13) and Limb Characteristics (n=15)						
No.	Gender	Age (years)	Height(m)	Weight (kg)	BMI (kg/m ²)	Status
1	Male	64	1.78	134	42.3	TKA
2	Male	70	1.73	92	30.7	TKA
3	Female	65	1.61	61	23.5	TKA
4	Male	77	1.68	78	27.6	TKA
5	Male	84	1.78	80	25.2	TKA
6	Female	59	1.59	90	35.6	TKA
7	Male	61	1.94	100	26.6	TKA
8	Male	64	1.78	103	32.5	TKA
8						Native Joints
9	Male	71	1.80	94	29.0	TKA
9						Native Joints
10	Female	71	1.65	69	25.3	Hip OA
11	Female	71	1.62	80	30.5	Hip OA
12	Male	66	1.78	103	32.5	Hip OA
13	Female	75	1.62	53	20.2	Hip OA
Mean		69.0	1.72	87.5	29.4	
SD		6.9	0.10	21.0	5.7	

3.5.1.2 Quantification of the mFTA

For each patient, the mechanical femoral-tibial angle (mFTA) was quantified using three different methods: a CT based analysis provided the reference against which the functional approach and a regression method were compared. For each method, a frontal plane was defined by three points: the hip centre, and the lateral and medial epicondyles, and all landmarks were projected onto this plane. The mechanical axis of the femur was defined as a vector from the hip centre to the knee centre, while the mechanical axis of the tibia was defined from the knee centre to the ankle centre. The mFTA described the angle between these two vectors.

3.5.1.3 CT evaluation and joint reconstruction

Prior to CT scanning, a limited set of radio-opaque, reflective markers was positioned on each subject's skin to identify a number of bony landmarks. These markers were later captured using motion analysis specifically for the determination of the Regression-mFTA (Hunt, Birmingham et al. 2008). During CT evaluation, patients lay in a supine position with their feet fixed vertically, shoulder width apart, and with their knees fully extended. Each CT scan provided data (Siemens Sensation

64, pixel size 0.39 x 0.39mm, slice thickness: 1mm) sufficient to reconstruct the hip, knee, and ankle joints. Image processing was performed using Amira (Mercury Computer Systems Inc, Chelmsford, MA) and the computational post-processing was executed using in-house algorithms.

A sphere fit process was used to identify the centre of the femoral head from reconstructed CT data. The trans-epicondylar axis was then identified in each knee by identifying the medial and lateral femoral epicondyle. The knee centre was defined as the point that bisected the two epicondylar landmarks. In a similar manner, the ankle centre was defined as the midpoint of the medial and lateral malleoli. The CT-mFTA was then calculated as described previously.

3.5.1.4 Functional assessment of posture

The positions of the complete set of reflective markers attached to the subjects' extremities, were tracked at 100 Hz using a 6-camera infrared optical motion capture system (Vicon, Oxford, UK), while the patients performed a standard dynamic movement. The marker placement protocol involved a minimum of 4 reflective markers on each of the pelvis, thigh, shank, and foot. Using palpation to identify the underlying pelvis bone landmarks, skin markers were attached onto the right anterior superior iliac spine (RASIS), left anterior superior iliac spine (LASIS), right posterior superior iliac spine (RPSIS) and the left posterior superior iliac spine (LPSIS). Additionally, two extra markers were placed on the medial and lateral epicondyles of the knee, and two on the medial and lateral malleoli of the ankle.

3.5.1.5 Quantification of Functional-mFTA

In order to quantify the Functional-mFTA, it was first necessary to functionally identify the hip and the knee joints from the standard dynamic movements, which included a full range of motion (RoM) of each joint; to identify the hip joint centre, patients performed a "Star-arc" motion in a standing position (Camomilla, Cereatti et al. 2006). To identify the knee axis, patients performed active knee flexion-extensions. Finally, a static standing pose with straight legs was recorded, in which the ground reaction force was monitored using a 6 DoF force plate (AMTI, MA, USA).

The skin movement artefact was firstly minimized using the Optimum Common Shape Technique (OCST) (Taylor, Ehrig et al. 2005). This process forms an optimal marker configuration for each segment to minimize the effects of e.g. skin elasticity. The hip joint centre was then identified from the star-arc movements using the Symmetrical Centre of Rotation Estimation (SCORE) (Ehrig, Taylor et al. 2006), an algorithm to determine ball and socket joint centres. The functional knee axis was identified from the knee flexion-extension motion, using the Symmetrical Axis of Rotation Approach (SARA) (Ehrig, Taylor et al. 2007). Since an axis possesses no centre, the functional data was complemented with 3D marker data to ensure a robust definition of the position of the knee centre. Here, the two markers positioned on the femoral epicondyles were projected onto the functional knee axis, with the knee centre defined as their midpoint. The ankle centre was defined geometrically as the midpoint of the two malleoli markers.

The Functional-mFTA was finally quantified by registering the joint centres onto the standing posture, by fitting the rigid OCST marker configuration from the standard dynamic movements, computed as previously described.

3.5.1.6 Quantification of Regression-mFTA

Quantification of the mFTA was also performed using regression methods according to Hunt and co-workers (Hunt, Birmingham et al. 2008), with the hip centre in the standing pose identified based on the distance between the RASIS and LASIS markers. The knee and ankle centres were defined as the midpoint of the two epicondyle and malleoli markers respectively. In a similar manner to the CT- and Functional-mFTA, the Regression-mFTA was defined by projecting the landmarks onto a frontal plane described by the markers.

3.5.1.7 Statistical Analysis

Statistical analysis was performed using SPSS v14.0 (SPSS Inc., Champaign IL). To assess the correlation between the Regression- and the Functional-mFTA to the CT-mFTA, a linear regression model was fitted to the data. The interval of confidence for the tests was set to 0.95. In addition to scatter plots, Bland and Altman (Bland and Altman 1995) plots were used to examine the agreement between the two tested methods and the CT-mFTA as well as to detect any possible bias. Furthermore,

after verification that the errors for each method (compared against CT-mFTA) followed a normal distribution using a one-sample-Kolmogorov-Smirnov test, a Student's T-test test was performed to quantify the accuracy of the Functional-mFTA or the Regression-mFTA against the CT-mFTA.

3.5.2 Results

The CT-mFTA had an absolute range of -1.8° (valgus) to $+5.4^{\circ}$ (varus), which correlated significantly ($R=0.91$; $p<0.0001$) (Fig. 3-9) with the Functional-mFTA that ranged from -1.5° to $+5.4^{\circ}$ (Table 3-3). A significant correlation was also observed ($R=0.76$; $p<0.001$) between the CT-mFTA and the Regression-mFTA.

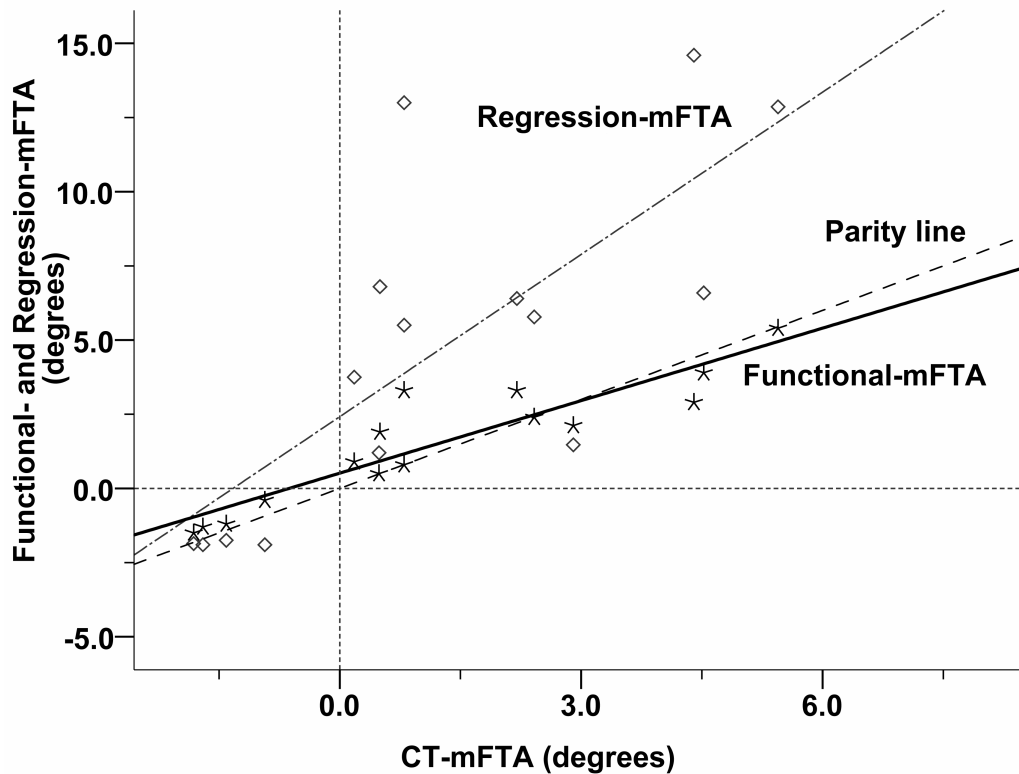


Figure 3-9: Scatter plot depicting the correlation between the mechanical Femoral Tibial Angle (mFTA) measured either functionally (Functional-mFTA), or based on the identification of landmarks and regression analysis (Regression-mFTA), against CT measurements (CT-mFTA). While both the Functional-mFTA ($R=0.91$; $p<0.0001$) and the Regression-mFTA ($R=0.76$; $p<0.001$) correlate significantly with the CT-mFTA, the graph illustrates that the Functional-mFTA adheres to the parity line (dashed) to a much greater degree, suggesting a large bias in the Regression-mFTA results.

The Bland and Altman plots demonstrated a better agreement between the Functional-mFTA (bias of 0.3°) and the CT-mFTA (Fig. 3-10 upper) than between the Regression- mFTA (bias of 3.5°) and the CT-mFTA (Fig. 3-10 lower).

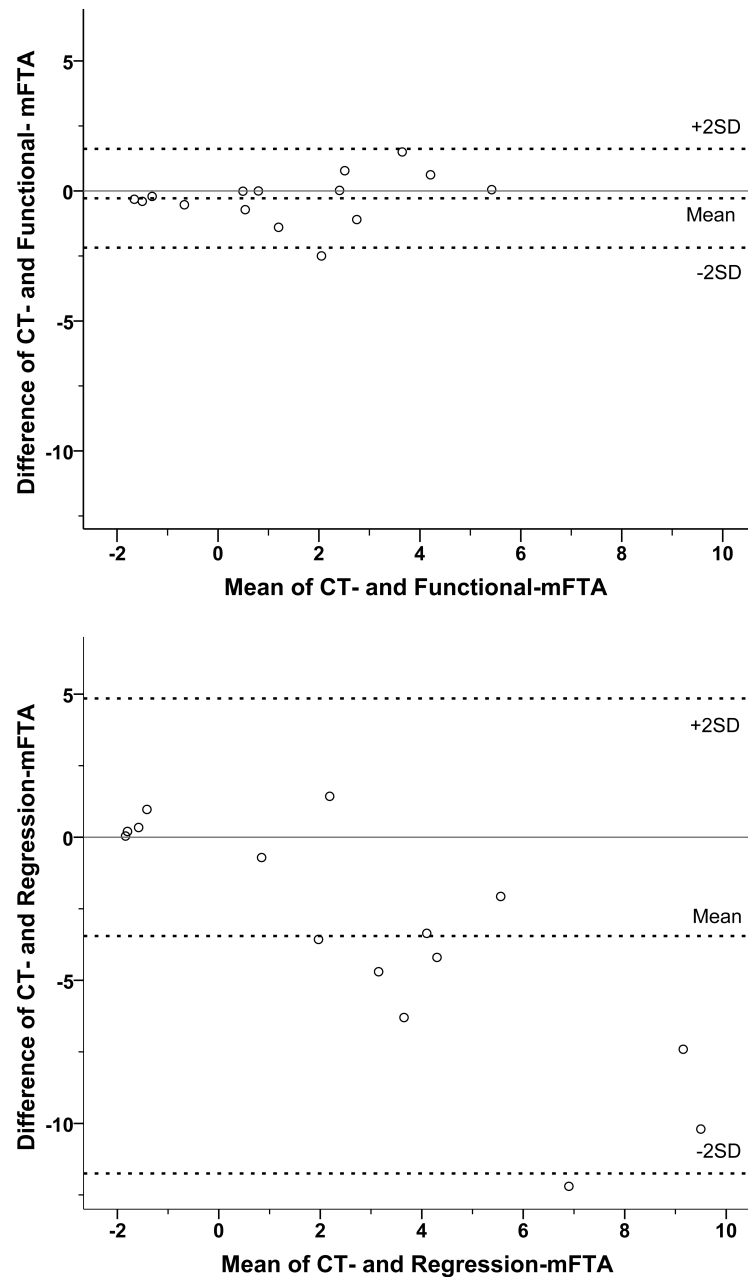


Figure 3-10: Bland and Altman plots of the (upper) Functional-mFTA and (lower) Regression-mFTA against the CT-mFTA. The Functional-mFTA has a small bias (deviation of mean value from zero) and exhibits good agreement (low standard deviations (SD)) with the CT-mFTA. In contrast, a considerable bias is present for the Regression-mFTA, which also shows relatively poor agreement with the CT-mFTA.

The paired t-test for the CT- and Functional-mFTA showed a non-significant ($p>0.25$) difference (Table 3-3). The 95% confidence interval of the difference between CT- and Functional-mFTA ranged from -0.8° to $+0.2^\circ$. The difference between the CT- and Regression-mFTA, however, was significant ($p<0.01$) and ranged from -5.8° to -1.2° , with a tendency to estimate a more varus alignment. Box plots of each mFTA demonstrate that a similar spread, but with a slightly elevated mean value (1.5° , $p=0.27$), is predicted by the Functional-mFTA, while a larger spread, as well as a significantly increased mean (4.7° , $p<0.01$) was predicted by the Regression-mFTA (Fig. 3-11).

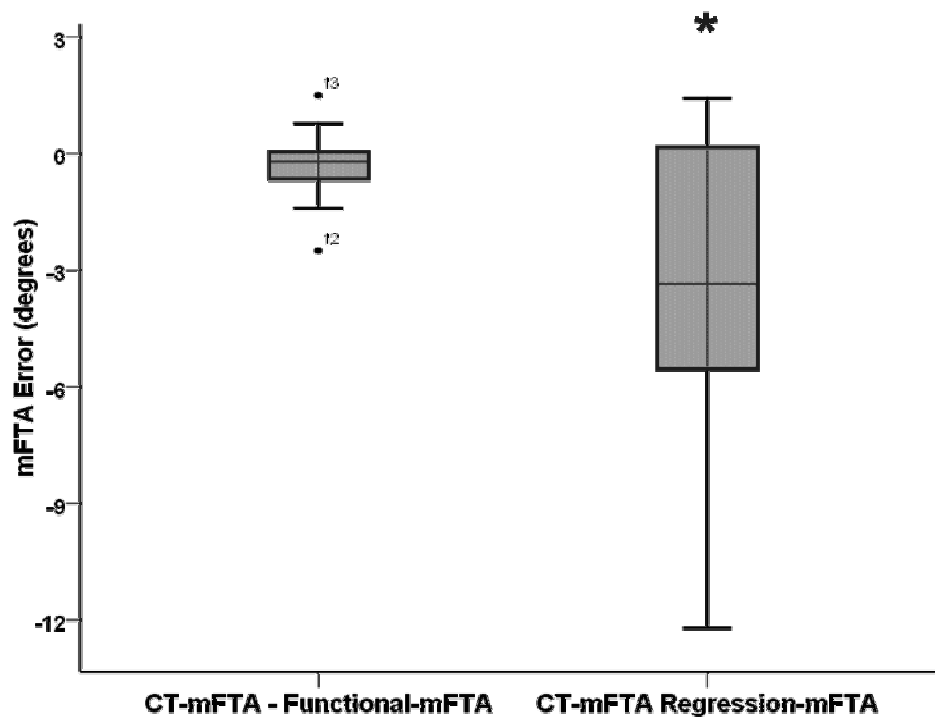


Figure 3-11: Box plots of the differences between CT-mFTA, and the Functional-mFTA and the Regression-mFTA as determined in 15 limbs. The CT-mFTA - Functional-mFTA data, indicates a much better prediction of the mFTA from the functional method if compared to the reference method (CT) ($p=0.27$), than the regression approach, which showed significant ($p=0.006$) errors when compared to the CT-mFTA.

Table 3-3 Lower limb alignment as defined by the mechanical femoral tibial angle (mFTA) determined by the CT-mFTA, the Functional-mFTA, or the Regression-mFTA. Positive mFTAs correspond to varus and negative to valgus knee alignment. Values are reported as mean \pm standard deviation (min, max). For the Functional-mFTA and the Regression-mFTA, the 95% confidence interval of the difference to CT-mFTA [margin of error] is additionally shown. Lower limb alignment as defined by the mechanical femoral tibial angle (mFTA) determined by the CT-mFTA, the Functional-mFTA, or the Regression-mFTA. Positive mFTAs correspond to varus and negative to valgus knee alignment. Values are reported as mean \pm standard deviation (min, max). For the Functional-mFTA and the Regression-mFTA, the 95% confidence interval of the difference to CT-mFTA [margin of error] is additionally shown.

	Method for assessment of lower limb alignment		
	CT-mFTA	Functional-mFTA	Regression-mFTA
Lower limb alignment (°)	1.3 \pm 2.3 (-1.8, 5.4)	1.5 \pm 2.1 (-1.5, 5.4)	4.7 \pm 5.6 (-1.9, 14.6)
Correlation to CT-mFTA ($\alpha=0.05$)	-	R=0.91; p<0.0001	R=0.76; p<0.001
Error [°]	-	[-0.8, 0.2]; p>0.25	[-5.8, -1.2]; p<0.01

3.5.3 Discussion

Lower limb mal-alignment is known to alter the loading conditions at the knee (Heller, Taylor et al. 2003). The accurate assessment of limb alignment therefore plays an important role in clinical monitoring, as well as in studies that aim to elucidate the influence of e.g. muscular imbalance (Karamanidis and Arampatzis 2009) or joint instability (Parratte and Pagnano 2008) on the internal forces in the knee. The use of X-rays as the standard clinical assessment modality is, however, associated with radiation exposure, which should be particularly considered in patients where longitudinal monitoring is required. This study therefore aimed to quantify and thereby demonstrate that an imageless, marker-based method to quantify the frontal plane mFTA, utilizing functional methodologies for the identification of joint centres and axes, is accurate. In this study, the Functional-mFTA has been shown to have a significantly unbiased correlation to the CT-mFTA (R=0.91; p<0.0001), and that there is no significant error between the two methods.

Functional assessment to quantify body posture and motion is safe, non-invasive and easy to acquire. Whilst showing reasonable correlation to radiographic measures of alignment, recent methods (Hunt, Birmingham et al. 2008; Mundermann, Dyrby et al. 2008; Vanwanseele, Parker et al. 2009) employing geometrical regression

techniques and anthropometric data to determine skeletal landmarks have been shown to possess limited patient specificity, suggesting the application of more patient specific methods for possible improvement. Since the mFTA is quantified from the relative positions of the hip, knee and ankle centres, inaccuracies in defining any one of these skeletal reference points could have a critical influence on the predicted alignment. The methodology demonstrated in this study uses established and accurate methods for reducing skin marker motion artefact (Taylor, Ehrig et al. 2005), and for functionally defining the joint centres (Ehrig, Taylor et al. 2006) and axes (Ehrig, Taylor et al. 2007). The results indicate no bias in the determination of the mechanical femoral-tibial angle (Functional-mFTA) compared to 3D imaging data (CT-mFTA) ($R=0.91$, $p<0.0001$) (Fig. 3-9 upper). On the contrary, although determination of the mFTA using regression techniques has shown good correlation to the CT-mFTA ($R=0.76$, $p<0.001$), analysis using methods suggested by Bland and Altman (Bland and Altman 1995) has revealed a considerable bias in the results (Fig. 3-9 upper). Furthermore, while the Functional-mFTA's error is not significant ($p>0.25$) and less than one degree for a 95% confidence interval, the error in the Regression-mFTA is significant ($p<0.01$) and between -5.8 and -1.2 degrees (Table 3-3).

The method used to locate the ankle centre was common to both the functional and the regression methodologies, and its efficacy was confirmed against CT data. The regression methods, however, used geometric relationships to locate the knee centre as the midpoint of the two epicondylar markers. Since this landmark varied by only a few millimetres from the CT knee centre, this small error cannot explain the large bias demonstrated by the Regression-mFTA, which must therefore be attributable to the definition of the hip centre. Here, the Regression-mFTA uses generic relationships to identify the hip joint centre, which are based on the position and distance between the RASIS and LASIS. Whilst care was taken to accurately palpate and exactly place markers on these skeletal landmarks, the pelvis and thigh regions are subject to higher levels of soft tissue, and prediction of the position of the hip centre based on geometric regression equations is limited in accuracy (Bell, Pedersen et al. 1990). The generic approach of the Regression-mFTA therefore seems to be unable to account for the large variation in soft tissue and subject anatomy. The functional methods employed in this study, however, are rapid (Rozumalski A and MH 2008), robust (Taylor, Ehrig et al. 2005; Ehrig, Taylor et al. 2006; Ehrig, Taylor

et al. 2007), independent of marker placement, but also accurate (Schwartz and Rozumalski 2005; Ehrig, Taylor et al. 2006; Ehrig, Taylor et al. 2007), subject specific and do not rely upon generic relationships for the identification of skeletal landmarks.

In this study, the functional methods were capable of predicting the mFTA within 1°, as verified against radiographic measures, and are both safe and non-invasive. Although the cohort presented in this study (15 limbs, 13 subjects) was relatively small, a diverse collection of subjects varying in age, gender, BMI, and joint health were all included (Table 3-2). Although the spread of the mFTA itself was not large, the merits of the proposed functional method have been clearly demonstrated. In this study, only subjects with clinically stable joints and without transverse deformities were included. Joint instability and transverse plane deformities could, however, affect the performance of the proposed functional approach. Future work should elucidate whether the Functional-mFTA can also be accurately determined in subjects with a more diseased limb anatomy than the ones tested in this study. Furthermore, the presented statistical evidence suggests that the cohort size was sufficient to confirm our hypothesis as well as demonstrate differences between regression and functional methods for determining the mFTA. Although additional work is required to establish whether functional methodologies are able to determine dynamic alignment of the lower limb, and whether the same principles can be used to quantify the mFTA in e.g. diseased limbs that function at higher flexion angles only, such as cerebral palsy, these functional methods present an accurate, non-invasive and weight-bearing approach for quantification of lower limb alignment.

It should be noted that long-standing X-rays are the current gold standard for assessing frontal plane alignment and for surgical planning. In this study, CT scanning was chosen to provide a reference limb alignment due to its availability and three-dimensional nature. Although the patients were not weight-bearing, due to the subjects' supine position during CT scanning, differences in limb alignment between weight-bearing and non-weight-bearing for stable knees are generally small (Specogna, Birmingham et al. 2007; Vanwanseele, Parker et al. 2009). Even when deformed knees were assessed using X-rays, the mean error in limb alignment between weight-bearing and non-weight-bearing remained within 1.5° (Specogna,

Birmingham et al. 2007). Furthermore, in subjects with low levels of deformity, alignment can be accurately be predicted using radiographic measures in a supine position (Sabharwal and Zhao 2008). Since the knee joints in this study were stable, there are no reasons to suspect that this error would be larger. Therefore, although supine CTs are not the clinical gold standard, they certainly seem to provide an adequate clinical measure of limb alignment (Matziolis, Kroker et al. 2007). Weight-bearing status, however, might play a role and could possibly explain the small differences between the introduced weight-bearing functional method and the non-weight-bearing supine reference CT values.

The accuracy of the methods presented here suggests that the technique is relevant for both clinical and scientific use. While the aim of this study was not to supersede X-rays as the standard imaging modality for planning surgical interventions, it was intended that an additional means to assess the mFTA non-invasively and under weight-bearing conditions be developed. The presented functional approach therefore targets cases in which radiographic imaging may not be suitable e.g. for longitudinal monitoring where cumulative radiation dosage becomes a problem or where gait analysis is readily available but radiation exposure may be restricted.

3.5.4 Conclusions

An image-free, non-invasive method for quantifying the mechanical femoral tibial angle has been introduced. Key components were procedures to minimise soft-tissue artefact and precise methods for the functional determination of joint centres and axes. Our hypothesis that frontal plane mFTA can be accurately predicted using functional methodologies has been confirmed by demonstrating a significant correlation and no significant error of the approach. This new functional method could help in reducing radiation exposure in scientific, screening, and monitoring applications and therefore become a valuable instrument for quantifying the mFTA.

4

Analysis of the lower limb patho-anatomy in patients with patello-femoral instability

Chapter 4 deals with the analysis of the patho-anatomy of the lower limb related to patello-femoral instability. In what extent mal-alignment of the lower limb, and an imbalance of the quadriceps distribution have effect on patello-femoral instability was not clear in the literature. It is demonstrated in this chapter that patients with patello-femoral instability have a significant valgus knee, and a significantly more internally rotated knee. Additionally, it is demonstrated that whilst the affected leg of the patients seems to be close to normal in terms of the quadriceps anatomy, it is the unaffected side which has a significantly hypotrophic medial quadriceps. The latter suggests both that the patho-anatomy of the quadriceps is a bilateral problem, and that the affected side has been adapted to normal, primarily due to targeted rehabilitation, or functional adaptation to the deficit.

4.1 Magnetic Resonance Imaging for assessing lower limb

anatomy

The function of the knee that is comprised of both the tibio-femoral and patello-femoral joints depends crucially on the interaction of the active and passive structures of the musculoskeletal system, such as bones, muscles, ligaments, and cartilage (Mulford, Wakeley et al. 2007). The interaction of the structures local to the knee is, however, also influenced by the global 3D alignment of the entire lower limb (Heller, Taylor et al. 2003; Cicuttini, Wluka et al. 2004). By changing the mechanical environment at the knee joint, mal-alignment of the lower limb has a direct contribution to overload and instability of the knee (Heller, Taylor et al. 2003; Cicuttini, Wluka et al. 2004). In addition to an examination of the musculoskeletal structures local to the knee measures of frontal plane alignment, femoral and tibial torsion, and knee version, should therefore also be quantified and taken into account when planning therapeutic interventions at the knee joint (Paley and Pfeil 2000).

In standard clinical practice, frontal plane parameters are routinely assessed using 2D X-rays (Paley, Herzenberg et al. 1994) while torsional parameters are typically quantified using CT imaging (Waidelich, Strecker et al. 1992). Both modalities have the drawback of exposing patients to ionizing radiation. MRI on the other hand, a 3D non-invasive modality, is routinely used to capture the local soft tissue anatomy of the knee joint, allowing diagnoses involving the cartilage, the ligaments, or the menisci (Salzmann, Weber et al.; Pfirrmann, Zanetti et al. 2000; Wittstein, Bartlett et al. 2006).

However, whilst MRI as an imaging modality has the additional benefit of being 3D, there are few protocols described using MRI techniques for the determination of the three-dimensional alignment of the lower extremities (Tomczak, Guenther et al. 1997; Hinterwimmer, Graichen et al. 2008). It is when planning for therapeutic intervention at the knee joint, where soft tissue reconstruction is often

indicated and MRI examination is routinely performed (Pfirrmann, Zanetti et al. 2000; Wittstein, Bartlett et al. 2006) that an MRI protocol to also determine 3D limb alignment becomes even more appealing. An additional examination with a dedicated protocol designed to be fast is unlikely to significantly increase either the cost, or introduce discomfort to the patient. However, during MR imaging patient motion might considerably affect the determination of limb alignment, necessitating the use of careful patient positioning but also fast imaging protocols.

4.2 Characterization of a dedicated MRI protocol to capture the entire lower limb 3D alignment

It becomes evident, that the development of a dedicated MR imaging protocol for the analysis of the 3D lower limb skeletal anatomy is highly relevant. Within the context of this project, a study is presented, including the development, and validation of the reliability of a fast MRI protocol for the 3D evaluation of the 3D skeletal anatomy of the entire lower limb. We hypothesized that such a protocol would be reliable (reproducible and repeatable) when used in a clinical setting to measure the femur and tibia lengths, the femoral and tibial torsion, the knee version, and the frontal plane mechanical femoral-tibial angle (Hypothesis T1 - Chapter 2).

4.2.1 Methods

4.2.1.1 Study protocol and participants

Fifteen healthy adults (8 male and 7 female) were recruited after approval of this study from the local ethics committee. The study cohort involved young (age 27.5 ± 4.2 years) individuals with no history of injuries at the lower limb joints, joint pain, or indications of osteoarthritis. The subjects were invited to be measured in the radiology department on two separate occasions. All participants provided informed consent prior to their participation in the study.

4.2.1.2 MRI protocol

All MR imaging was performed using one of two 1.5-T scanners (either Avanto or Symphony; both Siemens Medical Systems, Erlangen, Germany). Subjects underwent imaging using a dedicated peripheral angiography coil, lying in a supine position, with the knee positioned in full extension and the foot in 0° of plantar-flexion. The following sequence was used in all subjects (Table 4-1): Half fourier Acquisition Single shot Turbo spin Echo (HASTE) (repetition time msec/echo time msec, 600/65; flip angle, 150°), with a field of view of 372.7mm, a matrix size of 384 x 512, a slice thickness of 5mm, and slice spacing of 6mm. The scan extended from the anterior superior iliac spines to the tip of the toes, and both legs were included in the FoV. Body scouts were used to locate the specific areas of interest at the hip, knee, and ankle joint. By using incremental and automated table repositioning, three scanning blocks were acquired containing 43 slices each. The scan time for each block was 34 sec, with the entire protocol lasting approximately 3 min.

Table 4-1: MRI protocol for the assessment of the 3D skeletal anatomy of the lower limb.

Sequence	T2 HASTE (Half-Fourier single-shot turbo spin-echo)
Coil	Angiography RF lower limb coil
Slice Thickness	5mm
Resolution	0.74 x 0.74 mm
TR/TE	600 / 65 ms
Matrix	384 x 512 pixels
Field of View	372.7 mm

4.2.1.3 Data analysis

In order to analyze the imaging data, the MRI scans were imported in Amira (Visage Imaging GmbH, Berlin, Germany) for the 3D reconstruction of the hip, knee, and ankle joints. A series of skeletal landmarks were then identified for all three joints of the right leg of each subject (Brunner and Baumann 1998):

- (1) Femoral Head Center: The FHC, representing the center of the hip joint, was identified as the center point of the largest possible sphere fitting into the femoral head in all three planes.

- (2) Mid of Femoral Neck: The MFN was defined as the center point of the femoral neck in the transversal plane. The line connecting FHC and MFN defines the femoral neck axis.
- (3) Dorsal border of Medial and Lateral Femoral and Tibial condyles: DMFC, DLFC, DMTC and DLTC were identified as the most dorsal points of the respecting condyle. Between those points lines were defined to determine the dorsal tangents of the femoral and tibial condyles (DTFC and DTTC).
- (4) Medial and Lateral Epicondyles: The ME and LE were defined as the center of the largest circle fitting in the cylindrical shape that the condyles form in the sagittal plane. The midpoint of ME and LE determines the Knee Center (KC).
- (5) Medial and Lateral Malleoli: The MM and LM are represented by landmarks at the most medial respectively lateral point of the malleoli. The midpoint of the MM and LM determines the ankle centre (AC).
- (6) Medial and Lateral Torsional Malleoli: In addition the MTM and LTM were defined as the center points of the largest circles fitting in the malleoli in the transversal plane in a slice, where both malleoli can be assessed well. The line connecting MTM and LTM represents the malleoli axis.

With the coordinates of these landmarks, key parameters of length, torsion and frontal plane alignment were calculated (Table 4-2). The anatomical transversal plane was defined as the plane of the transverse MRI slices, while the same plane rotated by 90° around a mediolateral axis defined by the ME and LE was the frontal plane. The mechanical axes of the lower limb were projected on the frontal anatomical plane, while all of the transverse axes were projected on the transverse anatomical plane (Paley and Pfeil 2000). Positive values for the torsion angles were defined as follows: for the femoral anteversion as an internal rotation of the distal femur; for the knee version as an internal rotation of the proximal tibia; for the tibial torsion as an external rotation of the distal tibia. For the mechanical femoral tibial angle (mFTA) positive values were defined as genu varum.

Table 4-2: Definition of the parameters (lengths, frontal plane, and rotational alignment) characterizing 3D skeletal anatomy of the lower extremity. FHC, KC, and AC represent the hip, knee, and ankle centre respectively. FNA is the femoral neck axis. DTFC and DTTC are the dorsal tangents of the femoral and tibial condyles respectively, while MA represents the torsional malleoli axis.

	Measure	Definition
Femur Length	3D distance	FHC-KC
Tibia Length	3D distance	KC-AC
Femoral Torsion	2D angle (transversal plane)	FNA / DTFC
Tibial Torsion	2D angle (transversal plane)	DTTC / MA
Knee Version	2D angle (transversal plane)	DTFC / DTTC
mFTA	2D angle (frontal plane)	FHC-KC-AC

4.2.1.4 Statistics

In order to assess the inter-observer reproducibility, and the user-induced variability, each of the calculations of lengths and angles were performed by two independent investigators. To evaluate the inter-day repeatability, the MRI examination and the measurements were performed twice on two different occasions for each subject, in a test-retest design. To reduce a “memory effect” the results were compared not before the calculations were separately completed by each investigator. The data was analyzed by calculating the intra-class correlation coefficient (ICC(3,4)), and the 95% confidence interval (95% CI), for the repeatability, and the reproducibility tests. As an additional measure, the mean difference (MD) between measurements, representing a possible bias, was calculated. All statistical analysis was performed using PASW v18.0 (SPSS Inc., Champaign IL).

4.2.2 Results

The scanning time was approximately three minutes. The subsequent, offline image analysis, including the definition of the anatomical landmarks and the quantification of the relevant parameters was approximately 5-10 minutes per subject. The segmentation of the muscle borders to calculate muscle CSA took considerably longer, with approximately 30-40 minutes per subject.

The ICC for all evaluated parameters that provides a measure of the repeatability of this protocol (inter-day reliability) (Table 4-3) was greater than 0.99, with the 95% CI greater than 0.97 for every parameter. The possible bias, as indicated by the mean difference between measurements was less than 1mm for the segment lengths, and less than 1° for the angular relationships.

Table 4-3: Intra-class correlation coefficients (ICC (3,4)) including the upper and lower bounds for the ICCs 95% confidence interval (CI) showing repeatability at different time points (inter-day reliability). In addition, the mean differences (MD) between the two measurements are provided (and standard deviation (SD)), with the AD indicating a possible bias in the measurements.

Inter-day reliability			
	ICC	95% CI	MD \pm SD
Femur Length	1.000	[0.999, 1.000]	-0.1 \pm 0.9 (mm)
Tibia Length	1.000	[0.999, 1.000]	-0.3 \pm 0.9 (mm)
Femoral Torsion	0.998	[0.994, 0.999]	-0.3 \pm 0.5 (°)
Tibial Torsion	0.998	[0.993, 0.999]	0.0 \pm 0.7 (°)
Knee Version	0.995	[0.985, 0.998]	0.1 \pm 0.4 (°)
mFTA	0.992	[0.974, 0.998]	0.2 \pm 0.4 (°)

The analysis of the inter-observer variation (Table 4-4) representing the reproducibility of the protocol (inter-observer reliability), revealed an ICC of larger than 0.898 in all cases. While the lower bound of the 95% CI for the mFTA was moderate (0.697), the bias (represented by the MD) between the two observers for this particular measure was only 0.3°.

Table 4-4: Intra-class correlation coefficients (ICC (3,4)) including the upper and lower bounds for the ICCs 95% confidence interval (CI) showing reproducibility between different evaluators (inter-observer reliability). In addition, the mean differences (MD) between the two measurements are provided (and standard deviation (SD)), with the AD indicating a possible bias in the measurements.

Inter-observer reliability			
	ICC	95% CI	MD \pm SD
Femur Length	0.998	[0.995, 0.999]	2.1 \pm 1.6 (mm)
Tibia Length	0.997	[0.992, 0.999]	-0.6 \pm 2.7 (mm)
Femoral Torsion	0.982	[0.946, 0.994]	1.4 \pm 1.8 (°)
Tibial Torsion	0.985	[0.954, 0.995]	-0.3 \pm 1.8 (°)
Knee Version	0.948	[0.846, 0.983]	-0.2 \pm 1.2 (°)
mFTA	0.898	[0.697, 0.966]	0.3 \pm 1.3 (°)

The ICC for the evaluation of all quadriceps CSAs that provides a measure of the reproducibility of this protocol (intra-observer reliability) (Table 4-5) was greater than 0.95. The possible bias, in percent of the absolute size of the segmented areas, as indicated by the %err was under 2% in all but one case: vastus intermedius - left leg (2.3% error).

Table 4-5: Table 5: Intra-class correlation coefficients (ICC (3,4)) including the upper and lower bounds for the ICCs 95% confidence interval (CI) showing reproducibility between different measurements by the same evaluator (intra-observer reliability).

Intra-observer reliability			
		ICC	95% CI
Right leg	Vastus Medialis	0.962	[0.888, 0.987]
	Vastus Lateralis	0.987	[0.962, 0.996]
	Vastus Intermedius	0.998	[0.995, 0.999]
	Rectus Femoris	0.997	[0.992, 0.999]
	Total area	0.996	[0.989, 0.999]
Left leg	Vastus Medialis	0.982	[0.946, 0.994]
	Vastus Lateralis	0.991	[0.972, 0.997]
	Vastus Intermedius	0.998	[0.995, 0.999]
	Rectus Femoris	0.987	[0.962, 0.996]
	Total area	0.998	[0.996, 0.999]

Table 4-6: The mean differences (MD) between the two measurements of the quadriceps of 15 healthy adults are provided (and standard deviation (SD)), with the AD indicating a possible bias in the measurements. As a measure of comparison, the mean values of each measurement (MV) are presented, as well as the % error of the MD as a percent of the MV. All area values are in mm².

		MD \pm SD	MV	%err
Right leg	Vastus Medialis	-24.6 \pm 144.3	2008.2	-1.2
	Vastus Lateralis	21.9 \pm 117.3	2220.4	1.0
	Vastus Intermedius	-21.8 \pm 66.2	3131.4	-0.7
	Rectus Femoris	-5.8 \pm 22.7	661.3	-0.9
	Total area	93.4 \pm 120.9	6746.3	1.4
Left leg	Vastus Medialis	24.6 \pm 121.6	1988.2	1.2
	Vastus Lateralis	37.7 \pm 104	2166.6	1.7
	Vastus Intermedius	75.6 \pm 73.4	3320.3	2.3
	Rectus Femoris	-2 \pm 50.3	708.3	-0.3
	Total area	-24.7 \pm 181.8	6854.5	-0.4

4.2.3 Discussion

Aim of this study was the development and evaluation of a dedicated MRI protocol to quantify the 3D lower limb alignment. The protocol presented describes not only the data acquisition but also the image analysis process. The analysis of the inter-observer variance of the overall process with ICCs larger than 0.898 indicates a

similar reproducibility of this MRI protocol to the one described by Hinterwimmer et al. (Hinterwimmer, Graichen et al. 2008). Additionally we examined the inter-day repeatability and found the procedure to be highly repeatable as demonstrated by ICCs larger than 0.99.

It has been reported that mal-alignment of the lower limb, both rotational and frontal plane, can contribute worsen a patient's functional deficit, by severely altering the biomechanical environment of the knee, in which the various structures actively or passively interact. For example a varus mechanical axis measured in the frontal plane has been shown to correlate with an increased tibio-femoral contact force (Heller, Taylor et al. 2003) and with the shift of the tibio-femoral loading to the medial side (Hurwitz, Ryals et al. 2002; Kanamiya, Naito et al. 2002; Cicuttini, Wluka et al. 2004; Zhao, Banks et al. 2007), and has also been categorized as a risk factor for the early onset of knee osteoarthritis (Sharma, Song et al. in press). Similarly, increased valgus alignment and increased femoral anteversion both lead to an increased Q-Angle, thereby lateralizing the force acting on the patella, and the pressure distribution on the patello-femoral joint (Maenpaa and Lehto 1997; Ramappa, Apreleva et al. 2006; Mulford, Wakeley et al. 2007). The presented MRI protocol can now be used for the reliable determination of frontal and coronal plane limb alignment and thereby facilitates clinical diagnosis, as well as the planning and monitoring of surgical interventions at the knee.

Clinically, frontal plane alignment is typically assessed using 2D radiographs (Paley, Herzenberg et al. 1994), while CTs are used to determine torsional alignment of the lower limb (Waidelich, Strecker et al. 1992). X-rays and CTs, however, use ionizing radiation and are hence invasive. Certain patient populations with knee problems, such as those with patello-femoral instability, are typically young and the radiation dose becomes particularly relevant (Hinman, May et al. 2006). For those subjects MRI is routinely used for assessing the musculoskeletal structures local to the knee, and under such conditions, an MRI protocol for the assessment of the entire 3D lower limb skeletal anatomy would be most useful. An additional benefit of MRI to assess alignment against X-rays is the 3D nature of MRI. It has been reported that X-rays are prone to rotational errors, due to their 2D nature (Kawakami, Sugano et al. 2004; Hunt, Fowler et al. 2006). Furthermore studies have shown that long radiographs are not reliable with a patellar rotation of more than 10° off the frontal plane (Wright, Treble et al. 1991). This becomes increasingly significant with subjects

having severe deviations in the lower limb alignment, often present in patients with inherent anatomical deformities in the knee joint.

Recently, methods based on movement analysis, have been also proposed as a non-invasive alternative, for determining the lower limb frontal plane alignment (Kornaropoulos, Taylor et al.; Hunt, Birmingham et al. 2008; Mundermann, Dyrby et al. 2008). These approaches are either using generic anatomical relationships, or functional movement analysis to identify skeletal landmarks such as the joint centres and axes. Whilst the efficacy of such approaches has been shown to be comparable to that of radiographic data, it seems unlikely to employ a movement analysis approach to obtain reliable measures of axial alignment such as the femoral anteversion or the tibial torsion, parameters that can be easily quantified using MRI.

The results presented in this manuscript show negligible differences in inter-day measurements. With the 95% CI of the ICC above 0.97, it can be safely assumed that the protocol presented here is highly repeatable, and that it can be routinely applied in clinical practice without the uncertainty of measurement errors originating either by the measurement technique, or the image analysis procedure. The inter-observer variance results additionally reveal a highly reproducible protocol. A small deviation in the average difference in segment lengths ($MD \pm SD$: 2.1 ± 1.6 mm for the femur 0.6 ± 2.7 mm for the tibia) is observed. This could be attributed to a bias in the strategy for the axial positioning the malleoli and the epicondyle landmarks. These numbers, however, represent an error of less than 1% in the total segment lengths, and with the 95% CI being greater than 0.99 it seems safe to assume that these deviations are negligible. Finally, based on the 95% CI of the mFTA determination between the two observers (0.697, 0.966) there seems to be an inter-observer bias for the measurements in the frontal plane, but with a value of 0.3 ± 1.3 (°), this bias is too small to influence clinical decisions.

In conclusion, this study presents a dedicated MRI protocol for the non-invasive evaluation of the 3D skeletal anatomy of the lower limb, including the determination of the rotational and frontal plane alignment. This protocol was shown to be fast, with an entire scanning session typically lasting less than 5 minutes. Additionally, both the scanning sequence and the data analysis process have been proven to be highly repeatable, and highly reproducible, confirming the original hypothesis T1. Based on the merits of speed and high reliability, this protocol can be

applied on everyday clinical practice for the non-invasive determination of the 3D angular relationships of the lower limb, especially in cases where MRI is readily available.

4.3 Frontal and rotational malalignment of the femur: key factors of the patho-anatomy in patellofemoral instability

Patellofemoral (PF) instability, as demonstrated in the Introduction of this work, is a multifactorial problem (Colvin and West 2008), but it seems well accepted that the anatomical configuration of the lower limb plays a key role. Torsional deformities of the femur or the tibia, as well as genu valgum can all increase the quadriceps angle (Q angle) (Walsh 2003), thereby lateralize the force vector acting on the patella and possibly increase the risk of lateral dislocation. Surgical procedures for dealing with PF instability often target the tibia for correction of the Q angle and e.g. medialize the tibial tubercle (Ramappa, Apreleva et al. 2006), but there is no strong evidence suggesting that the patho-anatomy is restricted to the tibia only. If indeed the patho-anatomy was on the femur, a surgical intervention that targets the tibia may not efficiently restore normal patellar mechanics, and might rather prolong the mechanical deficit rather than eliminating it.

A careful evaluation of the lower limbs to identify the location and degree of a possible underlying patho-anatomy is therefore an essential step in the diagnosis and treatment of PF instability. Whilst reliable and fast, clinically applicable protocols that allow leveraging this potential of MR imaging for a non-ionizing assessment of 3D limb alignment, are not widely available, we have already demonstrated the validity of an MR imaging protocol that allows the rapid assessment of the frontal and rotational lower limb alignment.

Goal of this study was therefore to employ the aforementioned protocol to detect abnormalities predisposing to PF instability. The hypothesis was that patients with PF instability possess both significantly increased knee valgus and an internally rotated knee (Hypothesis C1, Chapter 2), and further, that the main patho-anatomy lies on the femur and not with the tibia (Hypothesis C2, Chapter 2).

4.3.1 Methods

4.3.1.1 Study protocol and participants

Fifteen patients with recurrent patello-femoral instability were measured in the local radiology department (Age = 24.8 ± 7.7). MR imaging was used to assess the severity of the local knee patho-anatomy, and the global lower limb mal-alignment. Control group for this study was used the healthy cohort of subjects without knee pathology mentioned in 3.2 (age 27.5 ± 4.2 years). The study was approved by the local ethics committee.

4.3.1.1.1 MRI protocol

All MR imaging was performed using one of two 1.5-T scanners (either Avanto or Symphony; both Siemens Medical Systems, Erlangen, Germany). The MR scanning protocol is in detail described in paragraph 3.2, with the details of it summarized in table 3.1.

4.3.1.2 Data analysis

In order to analyze the imaging data, the MRI scans were imported in Amira (Visage Imaging GmbH, Berlin, Germany) for the 3D reconstruction of the hip, knee, and ankle joints. A series of skeletal landmarks were then identified for all three joints of the injured leg of the patient cohort, and the right leg of the control cohort, as described in 3.2.1.2.

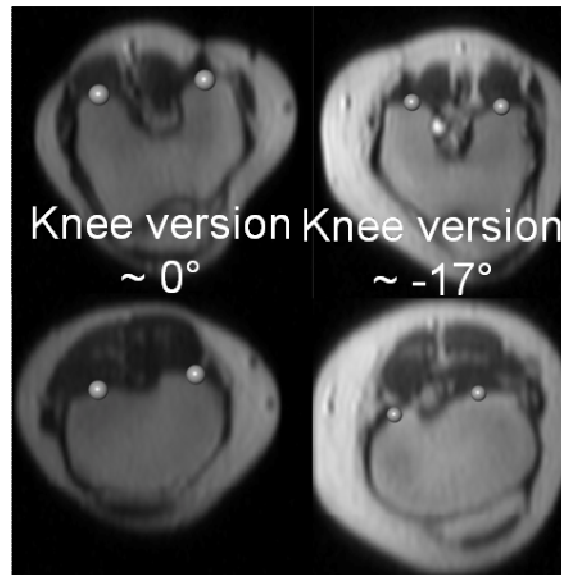


Figure 4-1: Example of landmarks defined on posterior femoral condyles (up) and posterior tibial condyles (down) for a healthy adult (left) with almost no relative rotation of the femur and the tibia, and a patient with PF instability (right) with a relative internal rotation of the femu.

4.3.1.3 Statistics

A Students' t-test was used to detect differences ($p < 0.05$) between the control and the patient cohorts. Additionally to detect the origin of the knee version angle, a simple Pearson's Correlation test was performed in pairs between the femoral torsion and the knee version, and the tibial torsion and the knee version. All statistical analysis was performed using PASW v18.0 (SPSS Inc., Champaign IL).

4.3.2 Results

After confirming a normal distribution for each read-out parameter using a Kolmogorov-Smyrnov goodness of fit test, it was observed that patients with PF instability had significantly more valgus knees ($p < 0.01$) than the control subjects. Additionally, significantly ($p < 0.01$) higher femoral torsion and knee version angles were observed in the patient cohort in comparison to the controls, while no significant differences were observed for the tibial torsion between the two groups. Results are summarized in table 4-7 and figure 4-2.

Table 4-7: Mean and standard deviation of rotational and frontal (mFTA) alignment parameters in both healthy subjects (n=15) and patients with PF instability (n=15). P-values are presented in bold for parameters when significant differences are observed.

Angle (°)	Healthy	Patients	p-value
Femoral Torsion	10.2 ± 7.0	18.2 ± 7.7	0.006
Tibial Torsion	29.2 ± 7.1	25.2 ± 8.0	0.155
Knee Version	-2.5 ± 2.9	-8.2 ± 6.3	0.003
mFTA	0.6 ± 2.1	-1.7 ± 1.6	0.002

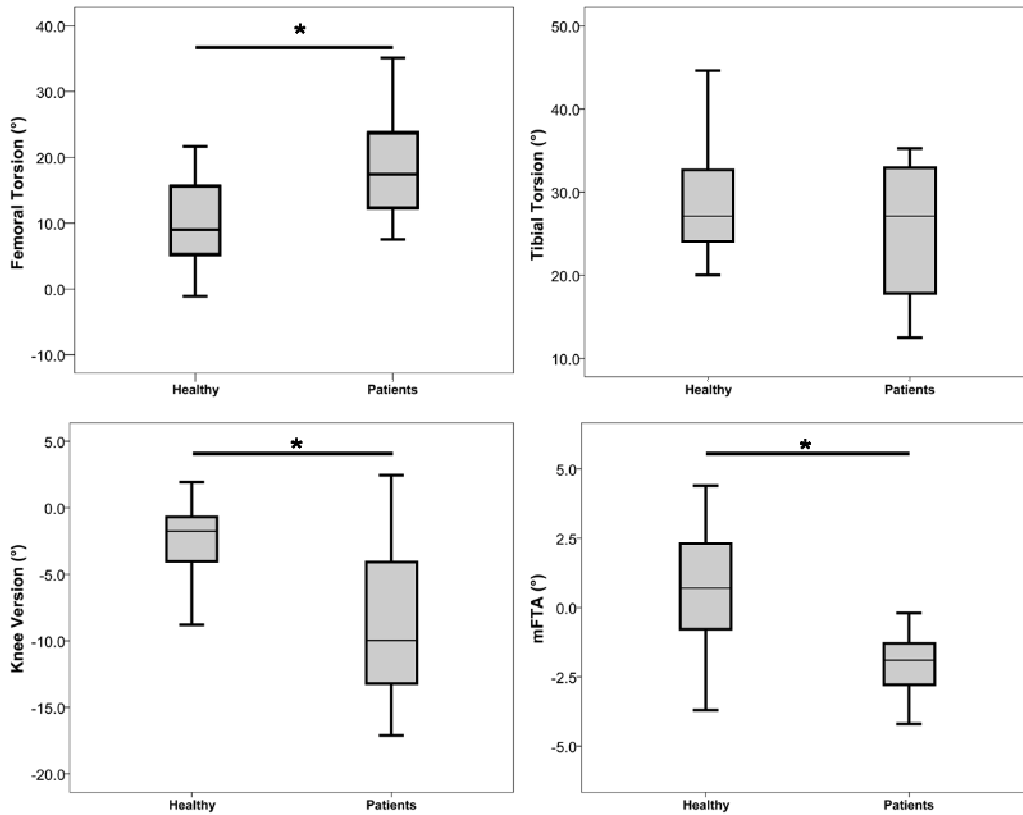


Figure 4-2: Rotational and frontal plane alignment differences between healthy (n=15) adults, and patients (n=15) with patello-femoral instability. Significant differences ($p < 0.01$) are indicated with a *. Negative knee version means either internal rotation of the distal femur or external rotation of the proximal tibia. Negative values for the mFTA indicate genu valgum.

Furthermore, the knee version measured in the patients correlated significantly ($R = -0.555$; $p < 0.01$) with femoral torsion, but did not correlate with tibial torsion when examined using the Pearson's correlation coefficient, indicating a closer relationship

between the knee version and a femur-based deformity, and no connection between the knee version and a tibia-based deformity (Fig 4-3).

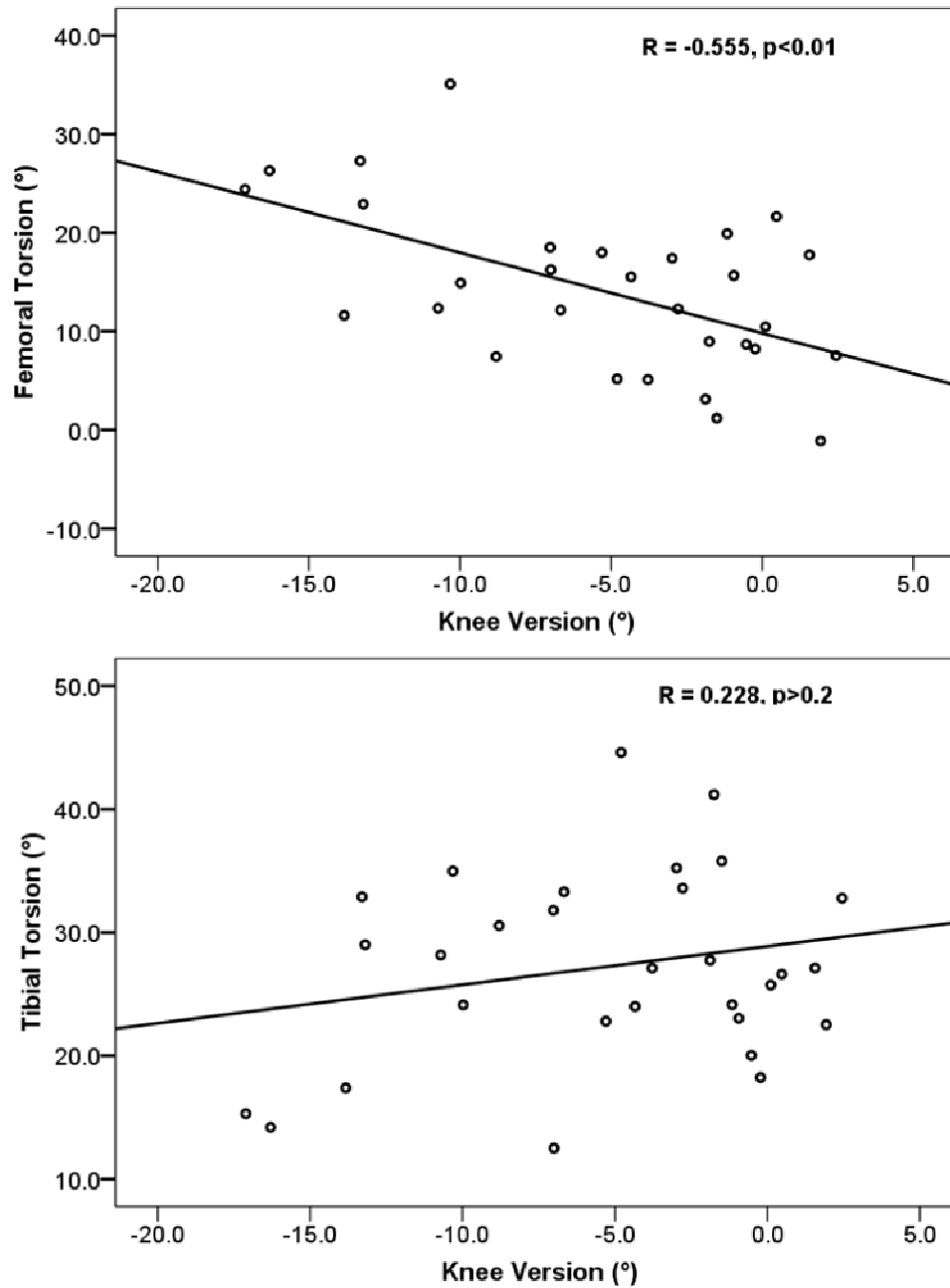


Figure 4-3: Relationship between knee version and femoral torsion (up) and knee version and tibial torsion (down). There is a mild, significant correlation between femoral torsion and knee version ($R = -0.555$), and no correlation between tibial torsion and knee version. This indicates that the torsional deformity local to the knee, is more likely to originate from a femoral deformity than from a tibial deformity.

4.3.3 Discussion

Using a novel MR imaging protocol (Chapter 3.2) we demonstrated that the patients with PF instability exhibited a significantly more valgus knee, and also possessed significantly increased knee version, when compared to healthy adults, confirming the original hypothesis. The finding of the increased knee version resulting mainly from an internally rotated distal femur is further corroborated by evidence presented suggesting that knee version in these patients correlates significantly with femoral, but not with tibial torsion. Together these findings suggest that in our patients the relative rotation of the tibiofemoral joint (knee version) originates from the femur, confirming the original hypothesis.

Both frontal plane as well as rotational malalignment observed in the patient cohort increase the Q-angle and can therefore increase the lateral forces acting on the patella (Rünow A 1983). The multi-planar patho-anatomy observed in those subjects might predispose to PF instability and suggests that surgical interventions targeting the tibia might not efficiently restore normal patellar mechanics in patients in which the rotational malalignment mainly originates from the femur. Whilst future studies should aim to identify whether increased knee version is an independent risk factor for PF instability, our results confirm that at least a subgroup of patients with PF instability might particularly benefit from treatment options that focus on the femur rather than the tibia. Additionally, if left untreated, in the long term, this lateral shift of forces acting on the patella, increases the lateral patello-femoral pressure, and could be one of the factors leading to long term effects such as patello-femoral OA, and patello-femoral pain syndrome.

In conclusion, this study identified increased knee version as a new patho-anatomic feature linked to PF instability. Furthermore, the measurement protocol presented here allows for the reliable and fast, non-invasive determination of the 3D lower limb alignment. It thereby enables a detailed, quantitative assessment of the anatomy that could help to better target the underlying patho-mechanisms and restore normal PF joint mechanics in interventions for the treatment of PF instability in the future.

4.4 Effect of patello-femoral instability on the quadriceps

anatomy

The quadriceps muscles act as the extensor mechanism of the knee. Having this role thus, this group is a major factor influencing the biomechanical environment of the knee, and especially the patello-femoral joint. Whilst the rectus femoris (RF) and the vastus intermedius obliquus (VI) are generally placed along the long axis of the bone, the vastus medialis obliquus (VM) and vastus lateralis obliquus (VL) are approaching the patella from directions deviating from the anatomical axis of the femur, thus pulling the patella medially or laterally (Wittstein, Bartlett et al. 2006; Colvin and West 2008).

Literature suggests that in normal cases, if the muscle vectors of the VM and VL are added together, the resultant force should follow the anatomical axis of the femur (Wittstein, Bartlett et al. 2006). It is suggested though throughout the literature, that an imbalance between the two muscles, more specifically, a bias towards a weaker VM can result into increased lateral force acting on the patella, hence increasing the risk for lateral patellar dislocation, and subsequent patello-femoral (PF) instability (Wittstein, Bartlett et al. 2006).

The physiological cross-sectional area (CSA) of the quadriceps muscles is indicative of the muscle power. Whilst some studies have focussed on the influence of limb mal-alignment to the distribution of the quadriceps CSA (Specogna, Birmingham et al. 2007; Tsakoniti, Stoupis et al. 2008), not very much is known as to the physiological range of these values, or the normal differences that can be observed between the right and the left leg of healthy adults. These studies only suggest that difference in the mediolateral distribution of the quadriceps is influenced by the Q angle or by the varus-valgus angle.

To add to this, family history has been proposed as a risk factor for recurrent PF instability to both limbs of a patient, meaning that inherent anatomical deficits, such a muscle imbalance, can be bilaterally observed in such patients. Whilst approximately half of the subjects suffering from PF instability seem to have a bilateral problem, little to no indications are given to whether there are risk factors influencing both sides, and whether a unilateral problem is only observed because of chance.

Goal of this MRI study was to shed some light on the patho-anatomy of the quadriceps muscles in respect to patello-femoral instability. Specifically, this study wished to explore the normal variation of the quadriceps CSA between two legs of the same subject in healthy adults, and to confirm that affected limbs of patients with PF instability were different than normal. Moreover, major goal of this study was to establish a possible link between patho-anatomic features of the quadriceps, and the risk for bilateral PF instability associated with non-traumatic patellar dislocation.

4.4.1 Methods

4.4.1.1 Study protocol and participants

Fifteen healthy adults (8 male and 7 female) were recruited after approval of this study from the local ethics committee. The study cohort involved young (age 27.5 ± 4.2 years) individuals with no history of injuries at the lower limb joints, joint pain, or indications of osteoarthritis. Thirteen patients with recurrent patello-femoral instability (age 24.1 ± 8.2 years) were additionally recruited to the study. Selection criteria for the subjects included: at least one episode of patellar dislocation; mild trochlear dysplasia; no known incidence of patellar dislocation to the contralateral limb. All subjects were invited to be measured in the local MR scanner. All participants provided informed consent prior to their participation in the study.

4.4.1.2 MRI protocol & data analysis

Using one of two 1.5-T scanners (either Avanto or Symphony; both Siemens Medical Systems, Erlangen, Germany), the subjects underwent imaging using a dedicated peripheral angiography coil, lying in a supine position. A HASTE sequence was used (repetition time msec/echo time msec, 600/65; flip angle, 150°), with a field of view of allowing the imaging of both legs of the subjects. The scan extended from the anterior superior iliac spines to the tibia tuberosity, and included scans with a slice thickness of 5mm, and slice spacing of 6mm.

In order to post-process the imaging data, the MRI scans were imported in Amira (Visage Imaging GmbH, Berlin, Germany) for the 3D reconstruction of the hip and knee joints, as well as the middle, and distal third of the femur. Firstly, the centre of the hip and knee joint were identified. Based on the distance between the two joint centres, two single MRI slices were identified according to the following: The first

MRI slice was located in the middle of the femur, the closest slice to the 50% of the distance between the hip and the knee joint centre; the second MRI slice was located on the distal femur, at the 30% of the distance between the two joint centres.

The CSA of the quadriceps muscles was quantified by manually segmenting the borders of the different muscles, and measuring the area within the borders. In accordance with previous studies, the vastus medialis (VM) CSA was quantified on the 30% slice, while the vastus lateralis (VL), vastus intermedius (VI), and rectus femoris (RF), were quantified on the 50% slice. The ratios of each muscle in respect to the total quadriceps CSA (TA) was taken by dividing each muscles measured value to the entire quadriceps CSA measured at the slice in the middle of the femur. Additionally to examine the relative relation of the VM and the VL, the ratios VL/VM was also calculated.

4.4.1.3 Statistics

In order to assess the variability between right and left leg of the healthy, as well as affected and contralateral limb of the patients, in terms of quadriceps CSA, a paired student's t-test was employed. A Pearson's correlation test was also performed to identify the correlation between measurements from the right and left leg of healthy subjects, as well as from injured and contralateral limb of patients. To identify differences between controls and patients, independent t-tests were used. All statistical analysis was performed using PASW v18.0 (SPSS Inc., Champaign IL).

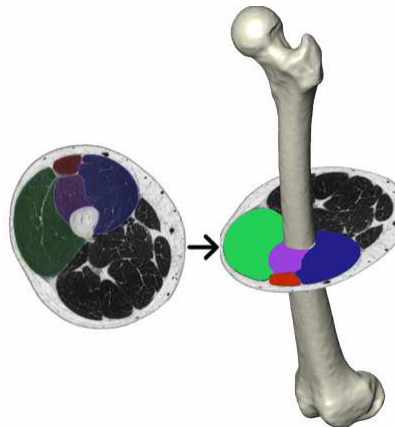


Figure 4-4: Example of segmentation and extraction of the quadriceps muscles from an MRI scan of the femur, using Amira(Visage Imaging GmbH, Berlin, Germany).

4.4.2 Results

Initially, a normal distribution was confirmed for all the measured parameters using a Kolmogorov-Smirnov goodness-of-fit test. The values of the different muscles of the quadriceps group (Table 4-8) for the healthy indicated that there is no significant bias between the right and the left leg. Significant ($p=0.027$), although small, difference was found for the RF (664.2 ± 199.3 vs. 709.3 ± 203.0 mm²) (Fig. 4-5). The muscle CSAs from the two legs also demonstrated strong significant correlations ($R^2 > 0.8$ for all muscle groups) (Table 4-8).

Table 4-8: Average area of the four quadriceps muscle groups (VM at 30%, the rest at 50% of the distance between hip and knee joint centre) for 15 healthy adults. P-values of the differences are also indicated (* $p<0.05$), as well as the correlation coefficients between the absolute values.

Muscle	Side	Area (mm ²)	p-value	R ²
VM	Right	2020.5 \pm 395.4	0.228	0.925
	Left	1975.8 \pm 449.1		
VL	Right	2209.4 \pm 449.0	0.306	0.819
	Left	2147.7 \pm 495.5		
RF	Right	664.2 \pm 199.3	0.029	0.893
	Left	709.3 \pm 203.0		
VI	Right	3142.3 \pm 739.1	0.070	0.925
	Left	3282.5 \pm 874.5		
TA	Right	6758.7 \pm 1349.5	0.566	0.956
	Left	6807.8 \pm 1433.4		

On the other hand, the differences between muscle measurements from the affected and contralateral side of the patients indicated a consistent trend towards a hypotrophic contralateral limb (Fig. 4-6). The VM had a significantly ($p=0.05$) larger CSA at the affected side than the non-affected (1859.8 ± 489.0 vs. 1627.9 ± 364.4 mm²) (Table 4-9). Additionally, in contrast to the control group, the correlation coefficients for the muscles' CSA between the affected and unaffected side of the patients were low ($R^2 < 0.4$ for the VM and VL and $R^2 < 0.6$ for the VI) (Table 4-9).

Table 4-9: Average area of the four quadriceps muscle groups (VM at 30%, the rest at 50% of the distance between hip and knee joint centre) for 13 subjects with PF instability. P-values of the differences are indicated ($p < 0.05$), as well as the correlation coefficients between the absolute values.

Muscle	Side	Area (mm ²)	p-value	R ²
VM	Injured	1859.8 ± 489.0	0.050	0.394
	Contralateral	1627.9 ± 364.4		
VL	Injured	2109.4 ± 631.5	0.992	0.376
	Contralateral	2110.9 ± 630.6		
RF	Injured	662.8 ± 223.0	0.124	0.937
	Contralateral	696.5 ± 263.8		
VI	Injured	3038.8 ± 762.0	0.053	0.543
	Contralateral	2723.5 ± 688.9		
TA	Injured	6453.7 ± 1712.0	0.21	0.728
	Contralateral	6121.9 ± 1330.3		

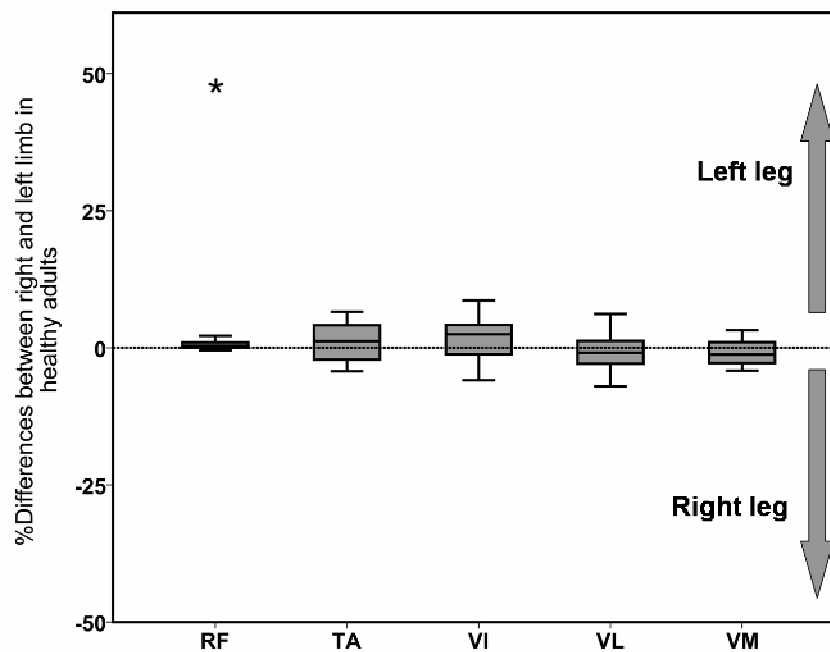


Figure 4-5 Differences between right and left leg of 15 healthy adults in distribution of the quadriceps muscles (VM, VL, VI, RF) and the total quadriceps area in the 50% distance between hip centre and knee centre (* $p < 0.05$).

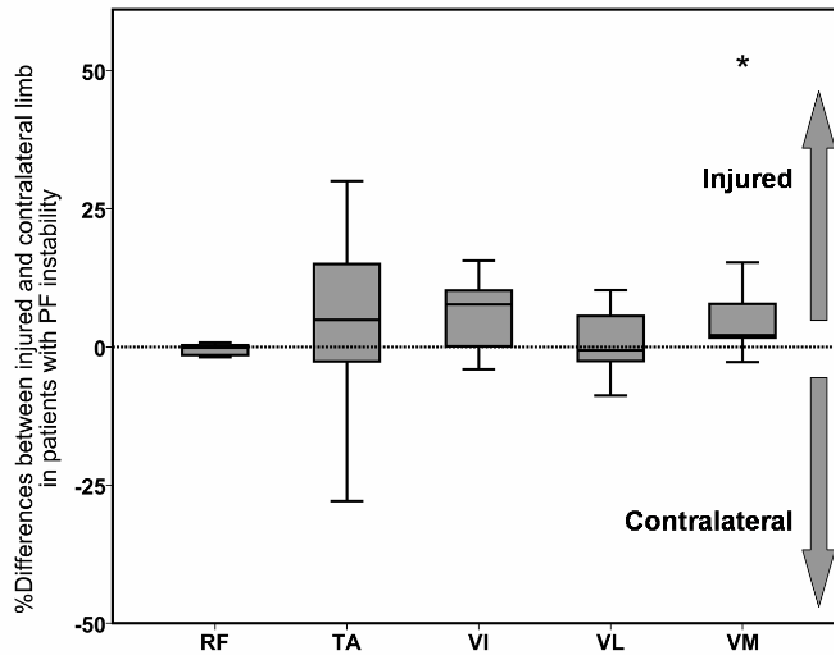


Figure 4-6: Differences between injured and contralateral limb of 13 subjects PF instability in distribution of the quadriceps muscles (VM, VL, VI, RF) and the total quadriceps area in the 50% distance between hip centre and knee centre (* $p < 0.05$).

The comparison between patients and healthy group revealed no significant difference between the control (healthy right leg) and the affected side of the patients. On the other hand significant differences were observed between the contralateral side of the patients and the control group. A significantly smaller VM CSA was observed for the patients ($p=0.024$) against the healthy (Fig. 4-7). An additional small but significant difference ($p=0.030$) was observed when the contralateral limb of the patients was compared to the right leg of the healthy (Fig. 4-7), but not when compared to the left.

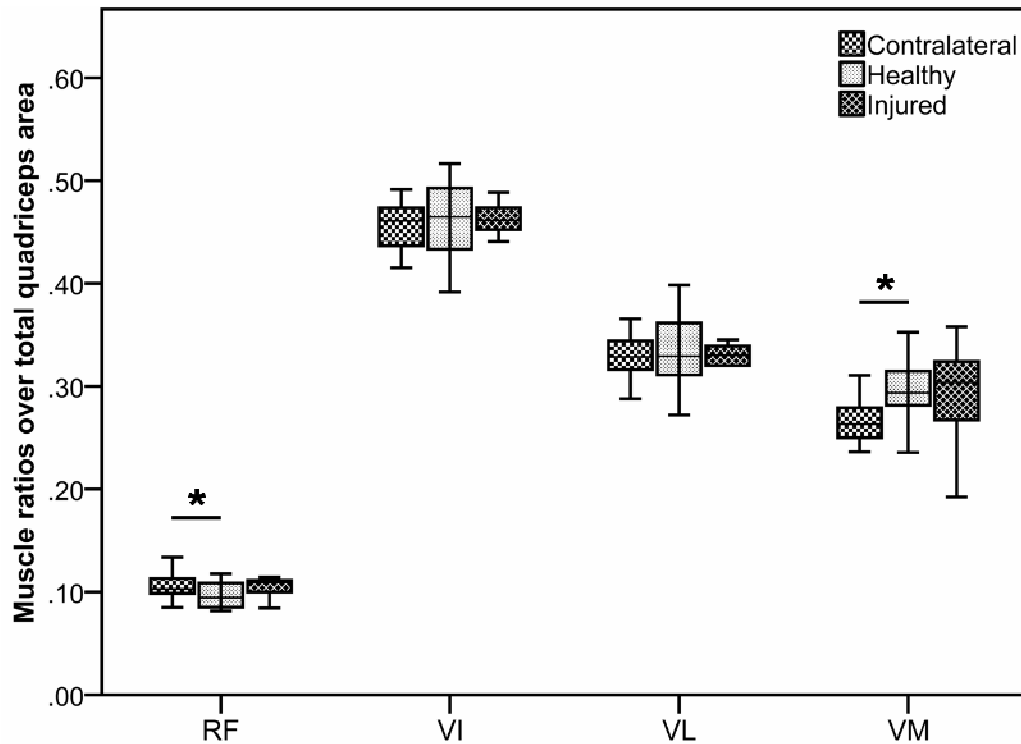


Figure 4-7: Differences in the ratios of the four muscles of the quadriceps group over the entire quadriceps area between healthy adults, and the injured and contralateral limb of patients with PF instability (* $p < 0.05$).

Finally, when examining the relative ratios of the VL and the VM in the healthy and the patients, whilst no significant differences were actually observed, a rather clear trend to significance was found for the difference between healthy (1.13 ± 0.22) and contralateral limb (1.31 ± 0.27) of the patients ($p = 0.065$) and between the contralateral limb and the affected limb (1.15 ± 0.25) of the patients ($p = 0.058$) (Fig. 4-8).

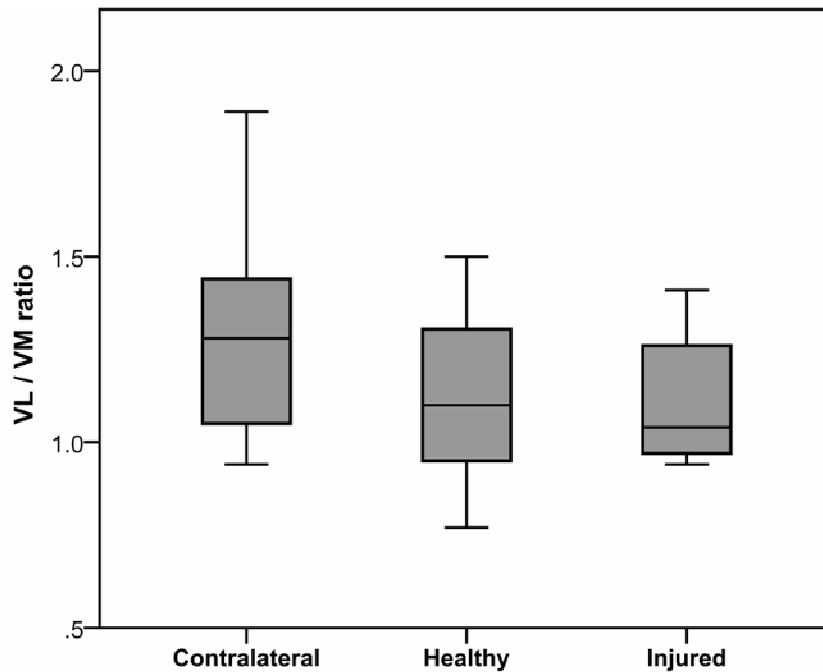


Figure 4-8: Ratios of the VL over VM in the injured and contralateral limb of patients with patello-femoral instability, as well as control of healthy adults. Whilst no significant differences were found between the different groups, a very clear trend approaching significance ($p=0.065$) was observed as a difference between contralateral and healthy, with the VM being less strong than the VL, as well as between injured and contralateral ($p=0.058$).

4.4.3 Discussion

The anatomy and function of the quadriceps muscle group has been linked to various knee pathologies, especially ones associated with the patello-femoral joint, such as PF instability and PF pain syndrome (PFPS). Of special interest is a pathologic relation of the VM and the VL. A weak VM leads to an increased lateral force acting on the patella, thereby increasing the risk for lateral patellar dislocation, and the risk for lateral joint overload leading to PFPS or osteoarthritis.

By measuring the physiological CSA of healthy adults with no history of knee problems in both the right and the left leg, it was established that there is no bias present in the mediolateral distribution of the quadriceps CSA. A significant difference was observed for the RF, but this difference was both small in absolute and relative numbers (approximately 6% of the smaller of the four quadriceps muscles), and since according to the literature, the centroid line of the RF creates an acting force

along the femoral anatomical axis, such an imbalance does not lead to a mediolateral imbalance of the quadriceps vector.

The analysis of the quadriceps CSA of the thirteen subjects with PF instability led to two somewhat surprising results. Firstly, no significant difference, not even a trend, was observed between the affected limb of the patients and the control group. As indicated in both Table 4-8 and 9 and Fig. 4-7, the affected side of the patients displays the same results with the control.

On the other hand, the analysis of the contralateral limb of the patients with PF instability revealed a significantly weaker VM against both the affected side, and the control group. These differences were observed both in absolute surface area of the VM CSA if compared to the affected side, and as ratios of the total quadriceps CSA when compared against the controls.

In addition to this finding, we found a clear trend to significant differences when we compared the relative size of the VL and VM (VL/VM) of the affected and the unaffected limb of the patients ($p=0.058$) and the unaffected limb and the healthy ($p=0.065$). No difference was observed when comparing the affected limb of the patients and the controls. The lack of significance in these comparisons, although the differences are quite large, can be explained by the relatively high standard deviation of the ratios, accounting for approximately 20% of the mean values. Nevertheless, the differences are pronounced, indicating a much more medially weaker (biased) side on the patients' unaffected limb.

Moreover, a Pearson's correlation test suggested that the quadriceps CSA variation of the one side can with a very high success probability ($R^2 > 0.8$ for all muscles) explain the variation observed on the other side (Table 4-8). This was not by any means the case for the patient group, with R^2 for particularly the two muscles of special interest (VM and VL) of less than 0.4. This means that whilst a prominent risk factor for patellar dislocation was identified for the unaffected side of the patient group, this factor was not present on the side that has suffered multiple dislocations.

If the aforementioned findings are put under the scope of the goals of this study there is certainly some room for interesting interpretation. First of all, it was established that in healthy adults there is no significant differences between the quadriceps muscle group (apart from small differences in the RF). It was intended to show a pathologically weaker medial side on the unaffected side of the patients. This has been succeeded, offering some explanation of why approximately half of patients

suffering from PF instabilities, according to some studies demonstrate bilateral symptoms. A weaker VM results into a laterally biased force vector acting on the patella, increasing the risk for lateral dislocation. Hence it can be ascertained, that a unilateral primary dislocation in patients who have a bilateral risk can be a product of “bad momentum”, with the patients involved in an activity where the stability of the patella dynamically is compromised only on one side, but the risk for a contralateral dislocation remains.

Room for a more speculative interpretation exists for the finding suggesting that the affected side of the patients is not different than the control in terms of the quadriceps CSA. Taken into account the contralateral deficit, and the fact that these subjects suffer indeed from PF instability, one can deduct that an original deficiency in the quadriceps existed, but is no longer present after the injury.

All the patients included in the study were patients with recurrent PF dislocations, candidates for surgical treatment. Whilst the exact rehabilitation protocol followed prior to the recruitment of the subjects is unknown, it is quit common for patients with PF instability to receive extensive rehabilitation as an attempt to non-operative treatment initially. This rehabilitation is often targeted to strengthen the medial side of the quadriceps, in order to offer medial support to the patella, thus decreasing the risk for redislocation. An additional explanation for this study’s finding is that by functional adaptation processes initiated by the feeling of instability, the VM of the affected side of the patients got stronger over the course of time.

The importance of these findings lies within the exposure of the medial weakness of the contralateral side. If a patient experiences a primary unilateral dislocation, an MRI examination of this subject’s quadriceps can reveal whether a pathologic mediolateral distribution of the quadriceps muscles is to be accounted in either of the two limbs. If a bilateral imbalance is in deed observed, this patient might benefit significantly from targeted rehabilitation to strengthen not only the VM of the affected side, but also the contralateral, hence decreasing the chances that this subject suffers in the future a contralateral dislocation episode.

4.4.4 Conclusion

In conclusion, this study has demonstrated three major findings in terms of the anatomy of the quadriceps muscles in respect to PF instability: no bias between the right and the left leg is observed for healthy adults; the affected side of the patients

examined in this group was not different than the control, possibly as a result of targeted rehabilitation; there was a significantly weaker VM in the contralateral side of the patients, when compared both against the affected side, and against the healthy controls.

5

The influence of patello-femoral instability on lower limb function

Chapter 5 deals with characterizing the influence of recurrent patello-femoral instability on the lower limb kinematics during activities of daily living. By performing gait analysis on patients with patello-femoral instability and healthy adults, it was possible to demonstrate that patients with patello-femoral instability do not perform activities of the daily living with normal lower limb kinematics. More specifically, it was observed that patients demonstrated increased dynamic valgus and internal rotation of the femur, a configuration promoting lateral patella-femoral and tibio-femoral overload.

5.1 wOSSCA and registration of identified joint centres and axes with ordinary procrustes analysis

Based on the results presented in Chapter 4, one can safely deduct that the OCST SARA SCoRE Combined Approach (OSSCA) provides the efficacy and accuracy for reliable movement analysis of adults. This entire process has been already demonstrated. In order to maximize efficacy of the approach, the next advancement, which is applied on the analysis of patients with patello-femoral instability, presented in this chapter, includes the combination of wOCST in the OSSCA approach, hence the “weighted-OSSCA or wOSSCA”.

The exact process used through wOSSCA to analyze lower limb kinematics is summarized in the following flow diagram (Fig 5-1). This process is described here as following: the wOCST, SARA, SCoRE are used once, in order to identify the optimal marker clusters, the joint centres and joint axes, during analyzing the standardized activities (“calibration” activities); a secondary registration of the produced functional dataset (wOCST marker cluster, joint centres and axes) is applied onto the raw data marker set of the targeted activities (second calibration) using a best fit ordinary Procrustes analysis. The subsequent analysis of the joint kinematics is based on an Euler rotation sequence (Cardan angle decomposition) (Ramakrishnan and Kadaba 1991) using the registered marker set and joint centres and axes to produced the appropriate segment coordinate systems.

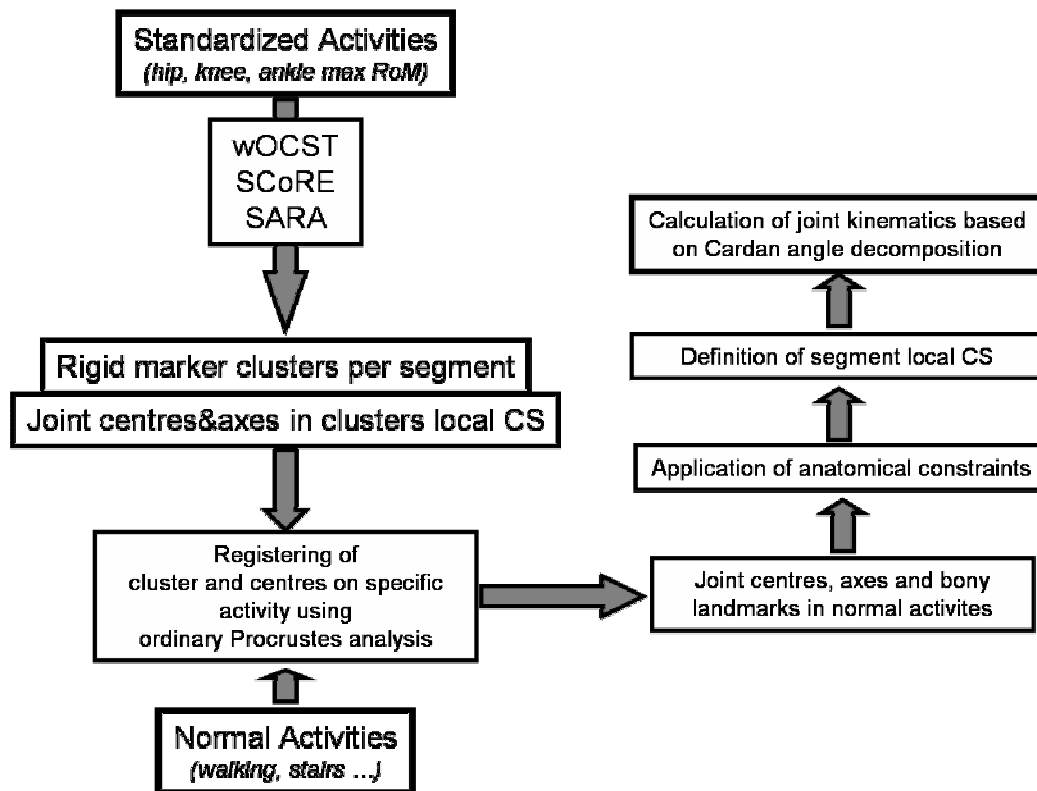


Figure 5-1: wOSSCA using as input both standardized activities which provide greater RoM for the joints of the lower extremity and the targeted for analysis activities.

5.2 Analysis of lower limb function in patients with patella-femoral instability

It has been established that PF instability is a multifactorial problem. More than 9 out of 10 subjects that suffer from a patellar dislocation have some degree of dysplasia of the lateral facet of the trochlear groove (Dejour H 1994; Murray TF 1999). Nevertheless, a secondary anatomical deficit is quit often present. In this project, focus has been given of the role of dynamic mal-alignment of the lower extremity. It has been previously reported that a static valgus mal-alignment, or a relative internal rotation of the distal femur in respect to the proximal tibia would increase the Q-angle, thereby lateralizing the quadriceps force vector (Amis, Firer et al. 2003). This would result in a direct increase of the lateral force applied on the patella, thereby increasing the immediate risk of patellar dislocation.

In addition to the contribution of mal-alignment of the lower extremity to the increase of the risk for patellar dislocation, it is previously documented that frontal plane mal-alignment leads to an increase on the loading of the knee joint (Heller, Taylor et al. 2003; Zhao, Banks et al. 2007). More specifically, a genu valgum would directly increase the loading of the lateral part of the knee joint, and hence the pressure applied on the lateral part of both the tibio-femoral, and patello-femoral cartilage (Hinterwimmer, Gotthardt et al. 2005). This increase of applied pressure has been linked with degenerative conditions such as OA, or PFPS (patello-femoral pain syndrome) (Connolly, Ronsky et al. 2009; Draper, Besier et al. 2009).

It has been elaborately demonstrated in this study, that patients with PF instability have a significant valgus knee, and a significantly increased knee version, when compared to a healthy control group. To which extent this static anatomical deficits influence the function of the patients is not documented. Such anatomical deficits could lead to functional, dynamic deficits, such as joint laxity, or excessive rotational or varus-valgus RoM at the knee joint, something which would only magnify the negative effects of an increased Q angle.

To our knowledge there is only one study that has examined the function of subjects with patello-femoral instability and additionally commented on the efficacy of the technique employed in improving patient function (Paulos, Swanson et al. 2009). Despite the promising results presented in this study, a proper control group was not used and the patients were rather compared to their contralateral limb. It has been already suggested that a great percentage of patients with PF instability have the propensity to suffer bilaterally. This translates into a virtually untouched field, with the evidence concerning the function of patients with patello-femoral instability limited to *in vitro* or *in silico* studies (Goudakos, König et al.; Yamada, Toritsuka et al. 2007; Yamada, Toritsuka et al. 2007; Goudakos, König et al. 2008; Draper, Besier et al. 2009; Goudakos, König et al. 2009).

A vast majority of subjects suffering from PF instability get surgical treatment which is not targeted to correct these underlying patho-anatomic features, but merely reinstate the initial patellar stability by repairing damaged passive structures such as the medial patello-femoral ligament. MPFL reconstruction has been shown to be successful in reinstating patellar stability, but as an approach suffers from longitudinal joint degeneration, and patient discomfort and dissatisfaction. It has not been previously documented whether the MPFL reconstruction is somehow successful into

normalizing patient function. If this is the case, the negative effects of joint instability could be held accountable for future joint degeneration.

In this study the aim was to identify whether patients with PF instability do have an altered lower limb function in terms of secondary knee motion. We have therefore hypothesized that subjects with PF instability will demonstrate significant RoM of internal-external rotation, and ab-adduction of the knee during normal everyday activities such as walking, stair ascending, and stair descending.

5.2.1 Methods

5.2.1.1 Study protocol and participants

Twelve patients with recurrent patello-femoral instability were measured in the local gait laboratory (Table 5-1). All subjects have undergone reconstruction of the medial patella-femoral ligament (MPFL). The assumption was that any changes in function originating from either the instability, or the patho-anatomical features leading to instability would have been preserved after this MPFL reconstruction. This is expectable since an MPFL reconstruction as intervention does not target into correcting underlying pathologies.

Fifteen healthy adults (Table 5-1) were also invited to the local gait laboratory to undergo movement analysis, in order to be used as an aged matched, control group against the patient cohort. All subjects provided written informed consent prior to their participation in the study, and the study was approved by the local ethics committee.

Table 5-1: Demographic characteristics of healthy controls and patients with patello-femoral instability.

Angle (°)	Healthy	Patients
Age	27.8±3.7	22.9±3.8
Height	175.0±8.2	177.5±25.2
Weight	66.8±8.4	79.1±20.5
BMI	21.8±1.6	25.7±8

5.2.1.2 Marker protocol & gait analysis

The process for the gait analysis involves the standardized procedure followed in the Julius Wolff Institut gait laboratory. The marker protocol has been extensively described in Chapter 3, consisted of a minimum of 4 reflective markers attached to the skin of each segment (pelvis, thigh, shank and foot) of the lower limb using double sided tape. Additional markers were placed on specific bone landmarks (via palpation); for the pelvis, the Right Anterior Superior Iliac Spine (RASIS), Left Anterior Superior Iliac Spine (LASIS), Right Posterior Superior Iliac Spine (RPSIS) and Left Posterior Superior Iliac Spine (LPSIS); for the knee at the medial and lateral epicondyles; and for the ankle on the medial and lateral maleoli.

The applied marker set was visible from the 12 infrared cameras (Vicon, Oxford, UK). For the purpose of functionally identifying the hip and knee joint centres and axes, the participants performed a “StarArc” followed by two active flexion-extension motions of the knee. After the performance of these standardized activities, the subjects completed multiple repetitions of walking, stair ascending and stair descending. The height of the steps was standardized, and did not vary according to subject body height.

5.2.1.3 Data analysis

The data analysis process to provide the lower limb joint angles during the performance of the aforementioned activities by the patients is extensively described in Chapter 5.1. In order to apply Cardan angle decomposition as mentioned in the start of this chapter, appropriate, anatomically-relevant coordinate systems for every segment of the lower limb (pelvis, femur, tibia, and ankle) needed to be identified. The general rule for all four segments was that on a local coordinate system with unit vectors $\hat{i}, \hat{j}, \hat{k}$ the following rule would apply:

- \hat{i} follows a medial-lateral direction, always pointing laterally
- \hat{j} follows an anterior-posterior direction, always pointing anteriorly
- \hat{k} follows a cranial-caudal direction, pointing upwards

At the end of this procedure, the orientation angles for the hip, knee and ankle joint were calculated and exported for further analysis (Fig. 5-2). To provide a measure of comparison across subjects, and cohorts, the activities were broken down

into cycles, and for each cycle, the min and the max values for each of the angles was calculated. The achieved dynamic range of motion (RoM) was then calculated as the distance between the min and the max values. The measured joint angles can be explained as follows:

- Positive flexion-extension: Flexion
- Positive internal-external rotation: Internal rotation of the proximal segment in respect to the distal
- Positive ab-adduction: Functional valgus

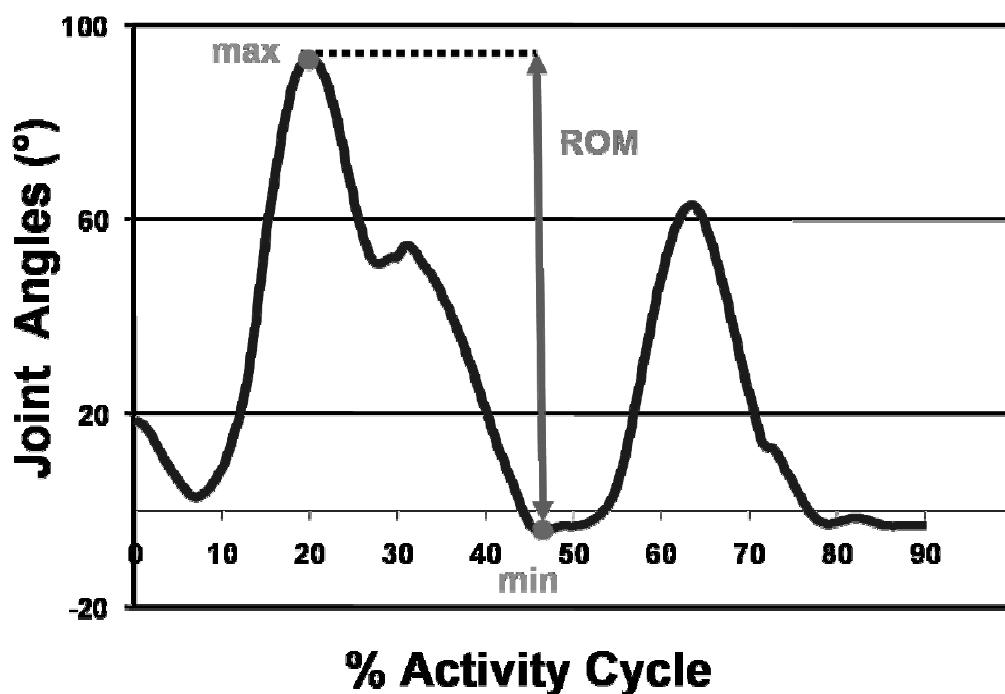


Figure 5-2: Sample of knee joint flexion calculated during a stair ascending activity. The figure shows how the max, min, and RoM values are being identified.

5.2.1.4 Statistics

A Students' t-test was used to detect differences ($p < 0.05$) between the control and the patient cohorts. All statistical analysis was performed using PASW v18.0 (SPSS Inc., Champaign IL).

5.2.2 Results

Multiple significant differences were detected between the patients and the control group (Table 5-3, Fig. 5-3, 5-4, 5-5, 5-6, 5-7). Of specific interest were the “knee instability” angles, these are the secondary motion angles of the knee (internal-external rotation, ab-adduction). The patient cohort showed a significantly more functional valgus knee ($p < 0.01$) in both the min and the max values for all activities (Fig. 5-3). On the other hand, whilst the RoM in that direction was significantly larger for the stair descending ($13.3 \pm 5.7^\circ$ vs. $7.7 \pm 2.6^\circ$) activity, this was not the case for the walking ($10.3 \pm 3.3^\circ$ vs. $10.2 \pm 4.0^\circ$) and stair ascending activity ($12.5 \pm 3.5^\circ$ vs. $11.6 \pm 6.0^\circ$) (Fig. 5-5).

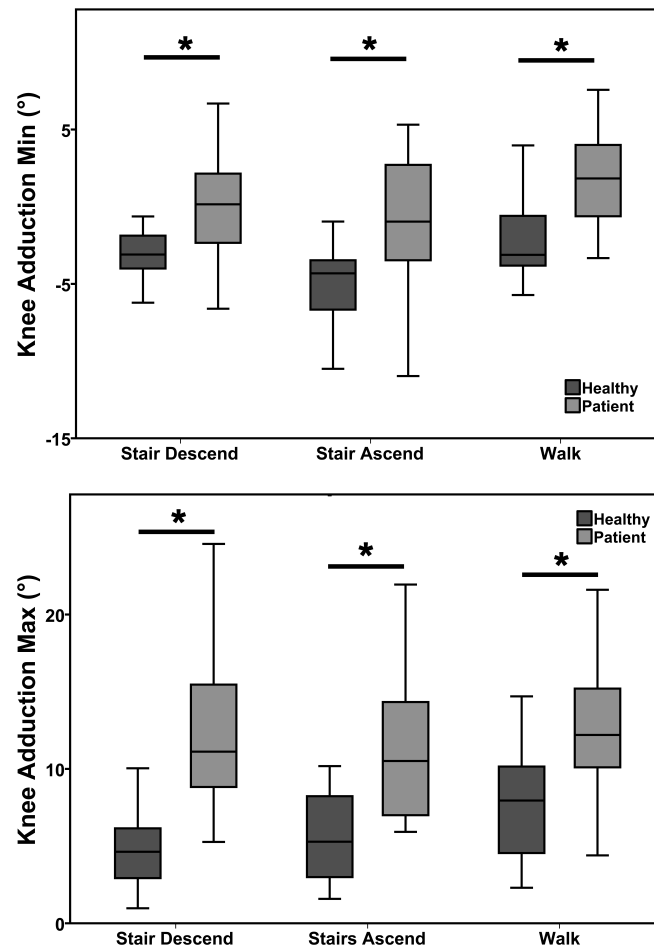


Figure 5-3: Knee ab-adduction angles for three different activities in a comparison between healthy controls (blue) and patients with patella-femoral instability (green). The minimum values during an activity cycle are displayed on top, while the maximum are displayed on the lower graph (*: $p < 0.01$).

For the knee internal-external rotation the findings were as following. No differences between either groups or activities were observed on the min findings of the knee internal-external rotation. On the other hand, significant differences between patients and controls were observed for the max values (Fig. 5-4). The RoM of internal-external rotation was also significantly larger for the patients during walking ($19.5\pm 8.1^\circ$ vs. $14.3\pm 4.5^\circ$), stair ascending ($17.9\pm 5.8^\circ$ vs. $13.7\pm 3.9^\circ$), and stair descending ($20.2\pm 8.6^\circ$ vs. $15.0\pm 3.6^\circ$) (Fig. 5-5).

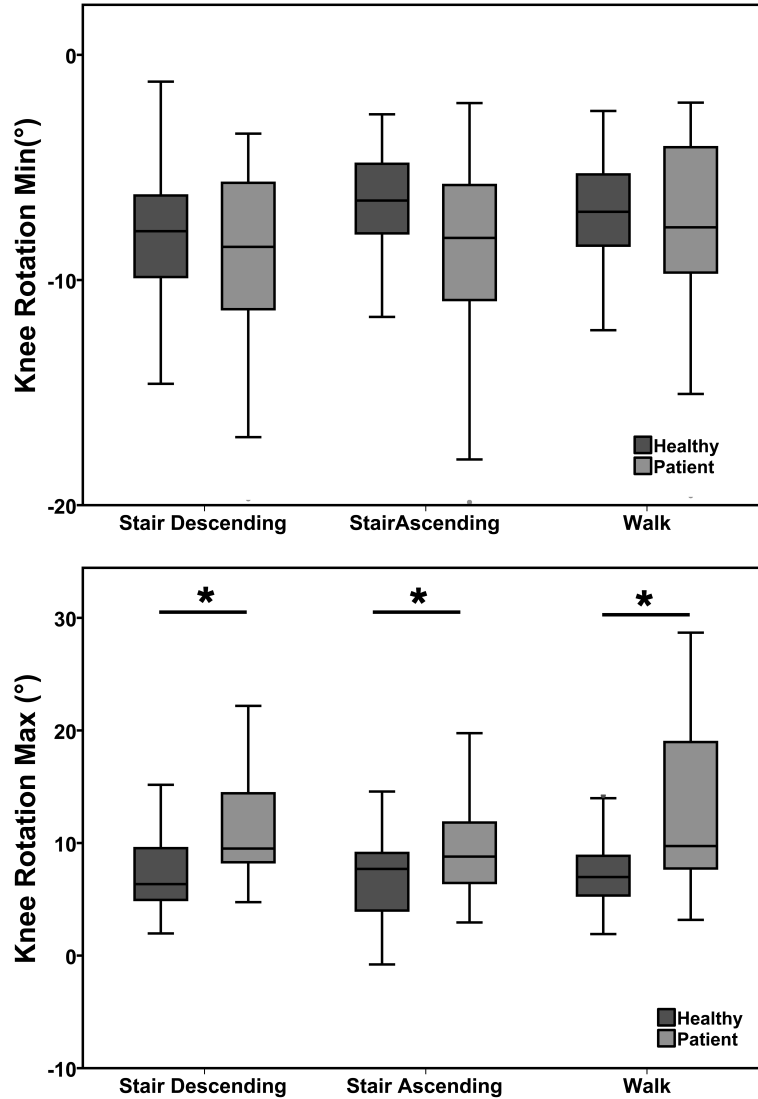


Figure 5-4: Knee internal-external rotation angles for three different activities in a comparison between healthy controls (blue) and patients with patella-femoral instability (green). The minimum values during an activity cycle are displayed on top, while the maximum are displayed on the lower graph (*: $p < 0.01$).

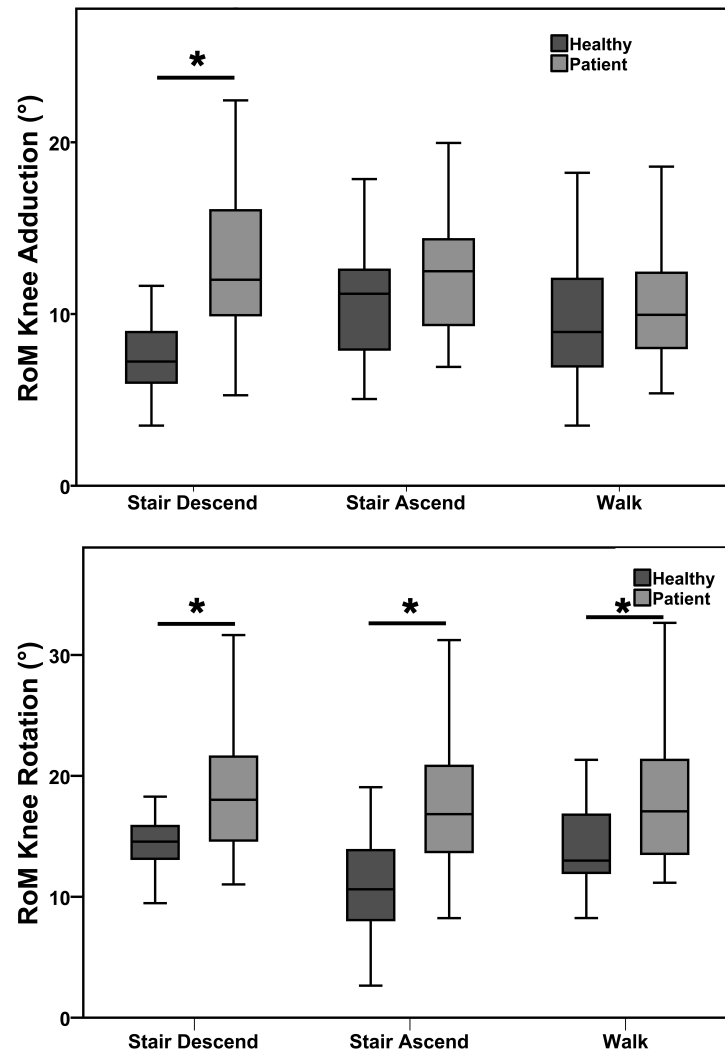


Figure 5-5: RoM in degrees for knee ab-adduction (top) and internal-external rotation (bottom) during three different activities between healthy adults (blue) and patients with patella-femoral instability (green) (*: $p < 0.01$).

The primary rotational angles for all three joints during these activities are the flexion angles. The patients seem to employ a different strategy for descending stairs by flexing the hip and the knee joint significantly more (Fig. 5-6). Some of the other differences observed during stair ascending can be very well attributed to the differences of height in respect to a standardized step height.

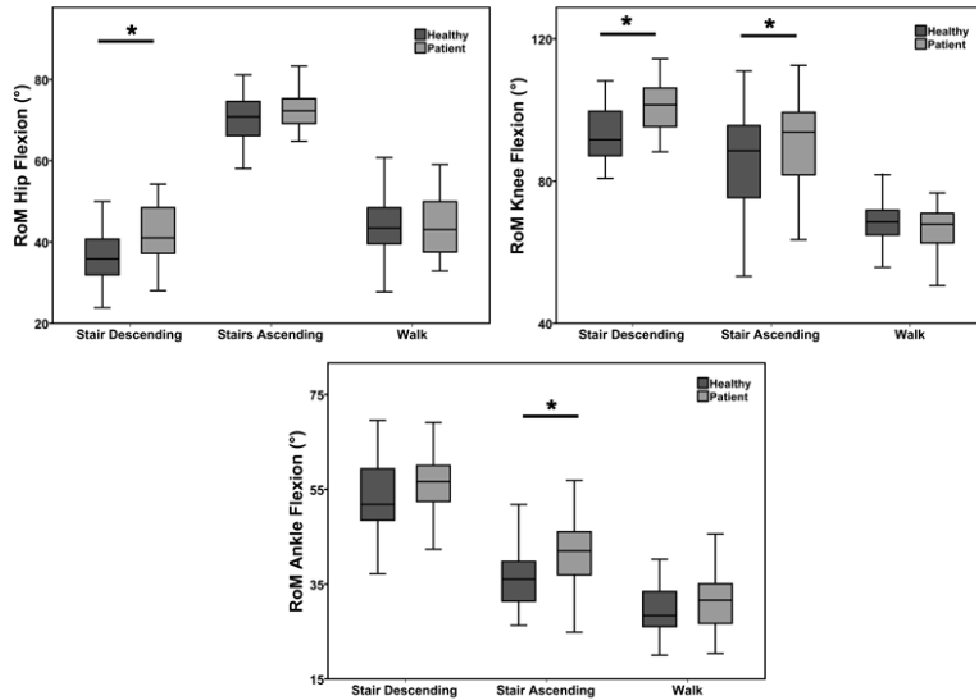


Figure 5-6: RoM in degrees for hip, knee and ankle flexion RoM between healthy adults (blue) and patients with patella-femoral instability (green) during walking, stair ascending and stair descending.

The secondary movement of the hip and the ankle joint was also increased for the patients, as indicated by the significantly higher ab-adduction and internal-external rotation RoM observed during all three activities for these two different joints. Particularly consistent was to observe an increased RoM for the ankle rotation (Fig. 5-7).

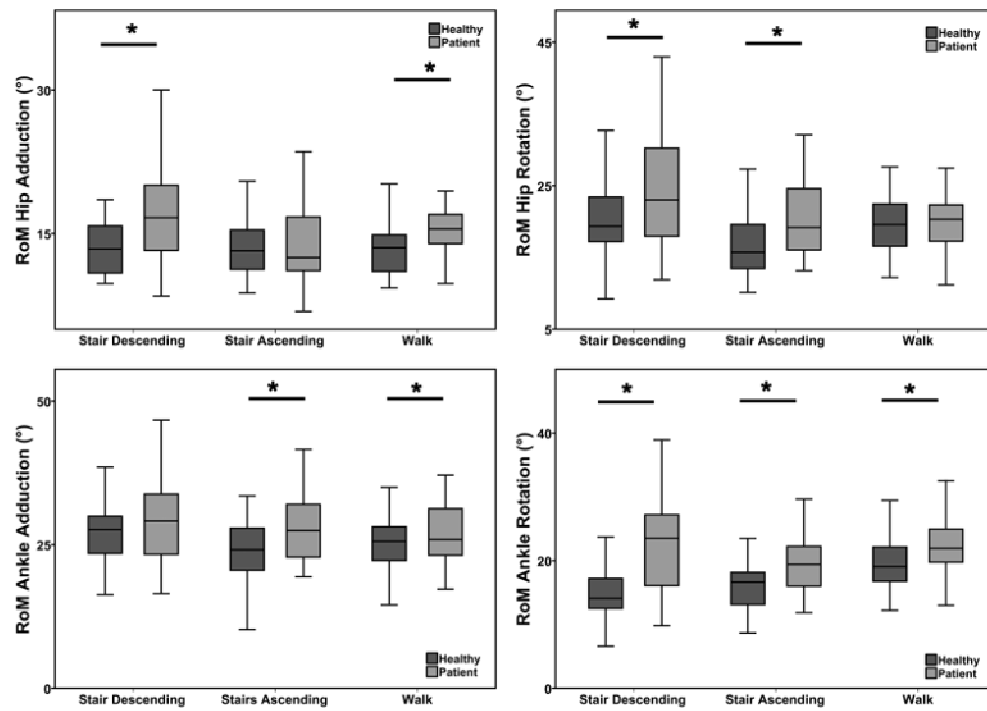


Figure 5-7: Secondary motion RoM (rotation and ab-adduction) in degrees for hip and ankle joints between healthy adults (blue) and patients with patella-femoral instability (green) during walking, stair ascending and stair descending.

Table 5-2: Summary of all measured values for the RoM of flexion, ab-adduction, and internal-external rotation, for the three lower limb joints (hip, knee and ankle), and during three different activities (walking, stair ascending, stair descending). Significance of the differences is also provided, with the significance levels being set on $p < 0.05$.

	Angle	Group	Stair Descending		Stair Ascending		Walk	
			Angle (°)	P Value	Angle (°)	P Value	Angle (°)	P Value
Hip	Flexion	Healthy	37.9 ± 9.7	0.008	70.0 ± 6.0	0.287	44.8 ± 7.9	0.534
		Patients	42.8 ± 8.5		71.3 ± 7.2		43.8 ± 7.2	
	Ab-adduction	Healthy	13.7 ± 3.1	0.000	13.7 ± 3.8	0.518	13.2 ± 2.4	0.000
		Patients	17.4 ± 5.2		14.2 ± 4.3		16.2 ± 4.2	
	Rotation	Healthy	21.0 ± 6.6	0.018	16.7 ± 4.4	0.000	19.6 ± 3.7	0.602
		Patients	24.5 ± 8.4		20.3 ± 5.1		19.9 ± 3.5	
Knee	Flexion	Healthy	92.6 ± 7.5	0.000	85.5 ± 13.5	0.018	68.9 ± 6.7	0.018
		Patients	100.9 ± 7.2		91.4 ± 11.5		66.8 ± 5.3	
	Ab-adduction	Healthy	7.7 ± 5.7	0.000	11.6 ± 6.1	0.400	10.2 ± 4.0	0.601
		Patients	13.3 ± 7.4		12.5 ± 3.5		10.3 ± 3.3	
	Rotation	Healthy	15.0 ± 3.6	0.000	13.7 ± 3.8	0.000	14.3 ± 4.5	0.000
		Patients	20.2 ± 8.6		17.9 ± 5.8		19.5 ± 8.1	
Ankle	Flexion	Healthy	53.7 ± 7.5	0.291	36.5 ± 6.3	0.001	29.7 ± 5.3	0.024
		Patients	55.3 ± 7.7		41.2 ± 7.6		31.6 ± 6.3	
	Ab-adduction	Healthy	26.6 ± 5.9	0.083	24.1 ± 6.6	0.001	25.6 ± 5.9	0.018
		Patients	28.8 ± 6.6		28.2 ± 6.2		27.2 ± 5.4	
	Rotation	Healthy	15.1 ± 4.4	0.000	16.1 ± 3.1	0.000	20.4 ± 4.7	0.001
		Patients	22.5 ± 7.4		19.8 ± 4.3		22.8 ± 5.1	

5.2.2.1 Relationship between static frontal plane alignment and dynamic valgus

Whilst the RoM for the internal-external rotation of the knee is significantly larger for all three activities for the patients, this was not the case as previously mentioned for the dynamic varus-valgus. In fact, the RoM was significantly different only in the stair descending activity, something that seems to comply with clinical observations characterizing this activity as the most challenging with patients. Nevertheless, significant differences were in fact observed for the patients in both the min and max cases for all three activities. The absence of differences found in the RoM can be comprehended as a possible anatomical offset, observed in the min and max cases, which fades out in the RoM.

To investigate into this matter further we used the Functional-mFTA, a functional approach to quantify the frontal plane varus-valgus angle, described thoroughly on Chapter 3 of this work to access both the patients and the healthy controls' static frontal plane alignment. These 5-7° of differences observed in the dynamic varus-valgus seem to be in deed originating from the static alignment of the patients; we were able to show that the patients had a significantly more valgus knee when standing with their too legs on shoulder width (Fig. 5-8).

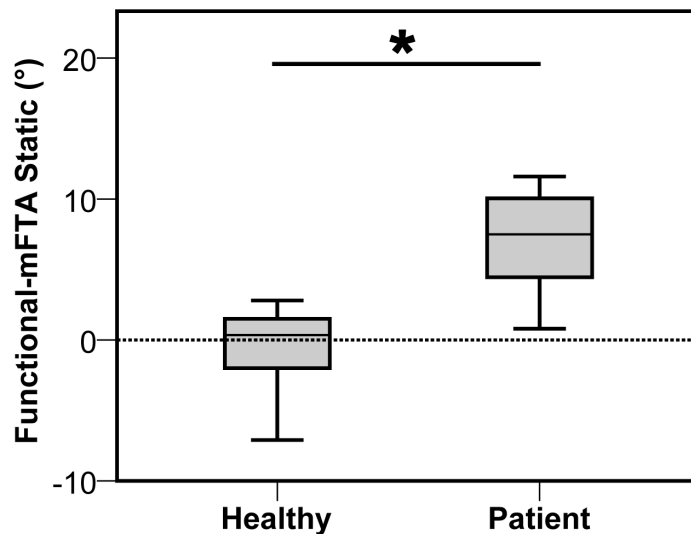


Figure 5-8: Frontal plane mechanical femoral-tibial angle for patients with patello-femoral instability and healthy controls using the Functional-mFTA. Positive values in this figure indicate valgus alignment (*: $p < 0.000$)

Based on these findings it is believed that the increased max dynamic valgus angles observed for the patients can be explained by the patients' static alignment. To corroborate this claim we performed a Pearson's correlation test to correlate the Functional-mFTA of the patients with the max valgus angle measured. With a strong significant correlation ($R^2=0.795$; $p<0.01$) it can be confirmed that the previously stated relationship is at least for this patient sub-group correct (Fig. 5-9).

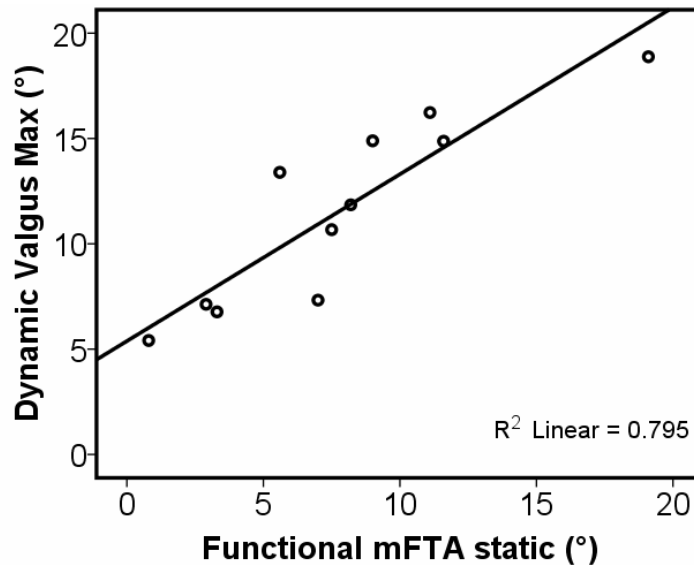


Figure 5-9: Correlation between frontal plane anatomical alignment (Functional-mFTA) and dynamic valgus alignment in patients with patello-femoral instability.

This observed relation between static and dynamic frontal-plane alignment could offer an at least preliminary explanation concerning the origins of dynamic functional deficits in patients with patello-femoral instability. A conclusion of the mentioned data, can be that in order to correct the dynamic valgus deficit in patients with patello-femoral instability and effectively unload the lateral facet of the patello-femoral and tibio-femoral joint, avoiding future complication such as pain and joint degeneration, one needs to consider correcting the anatomical frontal plane alignment. With no image data for this patient group, same claims cannot be made for the internal-external rotation dynamic deficit, and hence future work should focus more on correlating anatomy and function in order to create a solid link between dynamic and static deficits.

5.2.3 Discussion

To the author's knowledge this is the first study where patients with patello-femoral instability were compared with healthy adults in terms of their joint kinematics during activities of daily living. It has been demonstrated that the patients' joints' dynamic function differs significantly from that of the healthy controls in all three of the examined activities (walking, stair ascending and descending).

Of particular interest was the kinematics of the knee. The dynamic function of the knee is of major importance to patients with patello-femoral instability because there is a direct link between the function and the mechanics of the joint. We have found that there are significant differences in the secondary motion of the knee joint (internal-external rotation, ab-adduction).

More specifically, whilst the min values that were observed for the femoral-tibial internal-external rotation were not different between healthy and patient cohorts, significant differences in the order of $\sim 5^\circ$ were measured in the max values (Fig. 5-3). Subsequently, the rotational RoM was also significantly increased for the patients. This finding indicates that the knee joint of the patients demonstrates rotational laxity.

Whilst significant differences in both the min and the max values for the functional knee valgus (ab-adduction) were found during the analysis of the walking, stair ascending and descending, that was not the case for the frontal plane knee RoM, significant differences were observed only for the stair descending activity (Fig. 5-5). These results verify clinical observations which characterize the stair descending activity one of the most challenging for patients with patello-femoral instability. This activity seems the one where most of the knee joint laxity is being demonstrated.

In addition to the major findings supporting the hypothesis that patients with patello-femoral instability have a significantly different knee function, we did find a different functional strategy in the primary and secondary angles of the hip and ankle joints as well. Of particular interest are the increased rotation observed for the hip and ankle rotation. These differences can be explained as an approach of the patients to compensate the increased secondary knee motion on the other two joints.

The aforementioned findings correlate very well with the findings observed in Chapter 4. It has been shown that patients with patello-femoral instability have a

significant valgus knee, and a significantly internally rotated distal femur. These findings are supported here by the max dynamic values observed for the patient group. However, what is now added is the observation that there is not only a static anatomical deficit in those patients, but a dynamic instability expressed by the increased secondary knee RoM measured.

The Q-angle, the angle between the quadriceps and the patellar tendon expresses the direction of the force vector applied on the patella. This measure is directly associated with the knee rotation and the varus-valgus knee alignment. The increased secondary knee motion observed in patients with patello-femoral instability dynamically increases the Q-angle during patient function, thereby further lateralizing the quadriceps force vector, increasing the risk for lateral patellar dislocation or lateral patellar overload (Amis, Firer et al. 2003).

A possible link between the static anatomy of the patients and the functional outcome has been established here. It is proposed that the dynamic valgus observed during the functional activities, is at least partially, if not entirely attributable to the static anatomical valgus measured with OSSCA (see Chapter 3) during stance (Fig. 5-9). Whilst this link is not definitive, and does not offer explanation about the increased internal rotation of the knee in these patients, is to our knowledge the very first step in establishing and understanding a link between anatomy and function in patients with patello-femoral instability. It remains to be investigated in the future whether a static valgus can be indeed be used as predictive for a functional deficit in these patients, and to what extent a patient would functionally benefit from an anatomical correction of the frontal plane alignment.

The patients measured in this study have undergone reconstruction of the medial patello-femoral ligament. Whilst this procedure does not treat the underlying anatomical patho-anatomic characteristics that originally led to a primary patellar dislocation, it has been shown to be successful in terms of treating recurrent instability (Fisher, Nyland et al.; Colvin and West 2008). Nevertheless, it has been shown that on the long term, patients who undergo treatment are complaining of pain (patello-femoral pain syndrome), joint degeneration, and OA (Rünow A 1983; Maenpaa and Lehto 1997; Grelsamer, Dejour et al. 2008). Here, evidence suggests that the MPFL reconstruction together with post-operative rehabilitation in no means can be designated as appropriate to reinstate normal patient function. Based on these

findings, it might be deemed appropriate for additional treatment to prevent future complications.

The increased dynamic valgus observed here is directly associated with an increased knee adduction moment, a lateralize of the pressure applied on the joint, and an overall increase of the resultant joint force (Hurwitz, Ryals et al. 2002; Heller, Taylor et al. 2003; Zhao, Banks et al. 2007). Additionally, knee laxity in terms of increased internal-external rotation RoM can cause wear of the soft tissues surrounding the knee, which have been already damaged from the chronic patellar instability. Both these conditions can very well lead to a dynamic, chronic overloading condition that could be part-responsible for the joint degeneration observed in those patients.

5.2.4 Conclusion

This study demonstrates that the pathology associated with patients with patello-femoral instability cannot only be attributed to anatomical deficits. There are significant functional deficits found when those patients were compared to healthy adults. In particular, the increased secondary motion found for the knee joint can be directly associated with a dynamic increase of the Q-angle. The latter leads to a lateralization of the resultant quadriceps force vector, thereby increasing the risk for lateral patellar dislocation and lateral patellar overload, conditions which can very well be responsible for long term joint degeneration.

6

Conclusions - Future work

Chapter 6 serves as conclusions section for this work. The results presented throughout are summarized and put under context here. The clinical impact of these results is highlighted.

6.1 *Clinical context*

This study has focused on the area of patello-femoral instability. It had been already established that patello-femoral instability is a multi-factorial problem. A laterally dysplastic trochlear groove is most often the primary anatomical deficit. According to previous studies however, a number of other anatomical deficits including pathologies associated with bony structures, passive soft tissues and active soft tissues have been associated with PF instability.

There are two major issues faced currently when treating patello-femoral instability. The primary reason is associated with the decision about the intervention treatment that would be employed. Due to the wide spectrum of underlying anatomical deficits responsible for instability, the palette of offered surgical treatments is rich. Yet, a clear algorithm with which a surgeon would select the best possible treatment for a patient does not exist due to the complexity of the problem.

Hence, many surgeons decide against an invasive corrective operative approach and prefer a minimally invasive repair of the MPFL. By doing so, it is shown that the stability of the patello-femoral joint is successfully reinstated, but the underlying risk factors remain unchanged. Consequently, and this is the second major issue concerning PF instability, it seems that in the long term some of those patients develop secondary problems leading to disability, including patello-femoral or tibio-femoral OA, or patello-femoral pain syndrome.

This study has much focused on the role of frontal plane and rotational malalignment within the context of PF instability. There is a clear biomechanical link between these two parameters and both clinical issues mentioned. An increased valgus knee, and/or an internally rotated distal femur in respect to the tibia will increase the Q-angle, thereby lateralizing the resultant force vector acting on the patella. The latter increases the risk for lateral dislocation, but also leads to lateral overload which could explain future complications if left untreated. Furthermore, the dynamic function of the knee joint in patients with PF instability is not well documented. Increased secondary movement of the knee (ab-adduction, internal-external rotation) would result into a scenario where the Q-angle dynamically increases during normal everyday activities. The role of frontal plane and rotational malalignment can be summarized in Fig. 6-1.

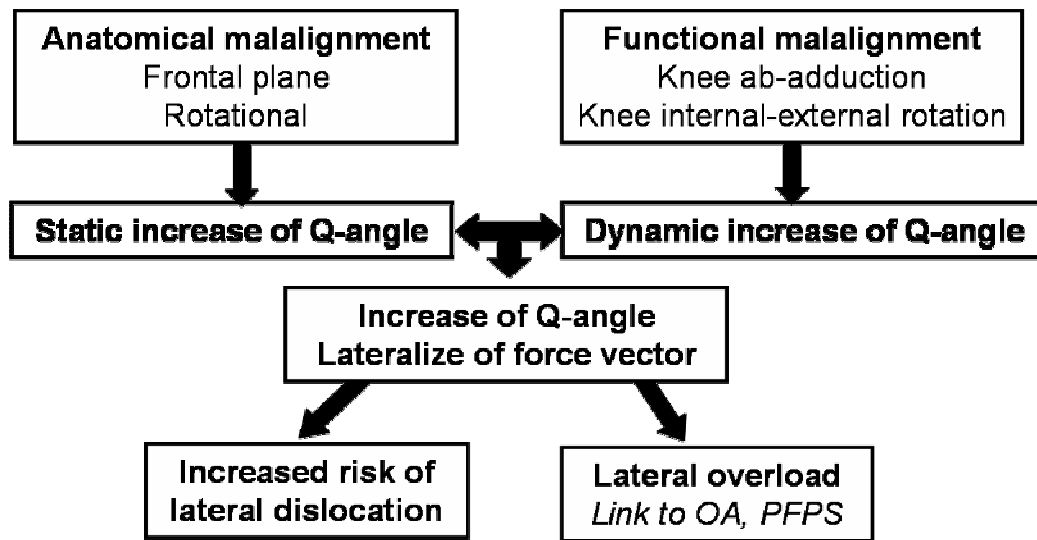


Figure 6-1: How frontal plane and rotational mal-alignment can influence both the stability of the PF joint and future joint degeneration by increasing the Q-angle.

Major goals of this study was to measure, understand and highlight the patho-anatomical features of frontal plane and rotational malalignment in the context of patello-femoral instability, and further explore whether functional deficits exist and in what degree.

6.2 Major findings

In order for the clinical practitioner to evaluate in what degree malalignment is associated with PF instability, one needs to be able to measure it reliably. In this study we have introduced a novel MRI scanning protocol and analysis approach that allows the non-invasive and reliable quantification of parameters of the 3D lower limb anatomy such as the mechanical femoral tibial angle, the femoral and tibial torsion, and the knee version. We later applied this protocol and demonstrated that patients with patello-femoral instability have a significant valgus knee, and a significantly internally rotated distal femur when compared to healthy adults. It was additionally demonstrated that this rotational deformity most probably originates from the femur.

It was additionally demonstrated that in patients with patello-femoral instability that have undergone a standard rehabilitation protocol which includes strengthening of the vastus medialis to increase medial stability to the patella, whilst the affected limb does not differ significantly from healthy adults, the contralateral

limb shows a weaker vastus medialis in respect to the vastus lateralis if compared to both the healthy adults and the injured leg of the patients, indicating a risk for lateral dislocation on the unaffected link of the patients.

To further explore a possible functional deficit, in the context of this study, a novel functional approach to movement analysis has been developed. This functional approach, OSSCA, has been demonstrated to accurately, repeatably and reproducibly identify key skeletal landmarks of the lower limb from motion data.

Using OSSCA, a group of patients with patello-femoral instability has been analyzed post-operatively after an MPFL reconstruction. The results revealed a significantly increased dynamic secondary motion of the knee (internal rotation, functional valgus) during all daily activities measured (walking, stair ascending, stair descending). Additionally, it was observed that a strong link exists in the patients between the static anatomical frontal plane alignment, and the dynamic functional valgus, a link that encourages the explanation suggesting that anatomical deformities, even of minor scale can lead to more severe functional deficits.

6.3 Impact and future work

The results presented in this study confirm the original hypothesis placed during the design of this study. It seems that patients with patello-femoral instability, at least a part of them, suffer from an anatomical frontal plane and rotational mal-alignment that increases the Q-angle. The evidence for a weaker medial than lateral side of the quadriceps, although not definitive, lead to a further increase of the lateral part of the force applied on the patella. Finally, the increased functional valgus and internal rotation of the knee, further burden the biomechanical environment of the knee joint by dynamically increasing the Q-angle. It appears to be that three different mechanisms exist in place that lead to a challenging biomechanical environment for the knee which promotes lateral patella instability and lateral patello-femoral and tibio-femoral overload. The latter deduction can be confidently made.

It remains partially unclear whether a specific link exists among all of these three mechanisms. Whilst it was demonstrated that the anatomical frontal plane alignment at least partially explains the increased max values of functional valgus, the same link was not established between the anatomy and the RoM of neither varus-valgus nor internal-external rotation of the knee. This increased RoM indicates joint

laxity which could be traced in the soft tissue damage sustained by the knee during the multiple patellar dislocations. Furthermore no specific link has been found between static bony alignment and quadriceps adaptation. Future studies on this area should focus on investigating a common link among these pathologies, and whether a single treatment strategy can be employed to compensate for these deficits.

Additionally, whilst the link between anatomical valgus and dynamic valgus was strongly demonstrated it remains unclear and should be examined in the future whether the static anatomical alignment can be used in this case as predictive parameter for functional deficits. It is also suggested that studies should investigate whether anatomical correction of frontal plane alignment leads to improvement of patient function.

Furthermore, future studies should focus on establishing a link between such deficits and future joint degeneration. Based on the short lifespan of a PhD project, a longitudinal patient follow-up to establish whether certain patients with certain characteristics would develop secondary pathologies was not possible.

A direct outcome of this study apart from the understanding gained about the importance and the range on the aforementioned characteristics is the link established between the increased knee version and the femur. To date, increased Q-angle is treated by medializing the patellar tendon on the side of the tibia. If the source though of the increased Q-angle is on the femur, such an approach may not resolve this issue.

An additional direct impact is the observation that the contralateral limb of patients who have undergone rehabilitation protocols to strengthen the vastus medialis seems to have a weaker medial than lateral quadriceps CSA, thereby exposing a possible risk factor for patellar dislocation on the contralateral, unaffected limb. It would therefore be meaningful the same rehabilitation protocol to be employed for the unaffected limb to decrease the risk for future dislocation.

Furthermore, the MPFL reconstruction, although a popular approach to correct patellar stability, lacks the efficacy into reinstating normal knee specific, and lower limb in general, function. If no other surgical approach is to be used, it is advised that patients post-operatively are somehow retrained into a more “normal” movement. This could be achieved with methods such as gait retraining, or knee bracing to avoid dynamic valgus, or extreme rotational movement, and preserve the integrity of the joint.

6.4 Epilogue

Whilst patello-femoral instability is not a mass affecting orthopedic disease, the impact it has on patient quality of life is severe. In this study we succeeded in investigating and highlighting areas which have not been closely followed by the literature, and yet have a significant impact on affecting the biomechanical environment of the patella influencing both directly patellar stability, but also predispose the knee for future degeneration. By confirming the stated hypothesis this study has fulfilled the original aims.

7

References

- Adouni, M. and A. Shirazi-Adl (2009). "Knee joint biomechanics in closed-kinetic-chain exercises." Comput Methods Biomech Biomed Engin **12**(6): 661-70.
- Alexander, E. J. and T. P. Andriacchi (2001). "Correcting for deformation in skin-based marker systems." J Biomech **34**(3): 355-61.
- Amis, A. A., P. Firer, J. Mountney, W. Senavongse and N. P. Thomas (2003). "Anatomy and biomechanics of the medial patellofemoral ligament." Knee **10**(3): 215-20.
- Amis, A. A., C. Oguz, A. M. Bull, W. Senavongse and D. Dejour (2008). "The effect of trochleoplasty on patellar stability and kinematics: a biomechanical study in vitro." J Bone Joint Surg Br **90**(7): 864-9.
- Balcarek, P., J. Ammon, S. Frosch, T. A. Walde, J. P. Schüttrumpf, K. G. Ferlemann, H. Lill, K. M. Stürmer and K.-H. Frosch "Magnetic Resonance Imaging Characteristics of the Medial Patellofemoral Ligament Lesion in Acute Lateral Patellar Dislocations Considering Trochlear Dysplasia, Patella Alta, and Tibial Tuberosity-Trochlear Groove Distance." Arthroscopy: The Journal of Arthroscopic & Related Surgery **26**(7): 926.
- Bell, A. L., D. R. Pedersen and R. A. Brand (1990). "A comparison of the accuracy of several hip center location prediction methods." J Biomech **23**(6): 617-21.
- Birmingham, T. B., M. A. Hunt, I. C. Jones, T. R. Jenkyn and J. R. Giffin (2007). "Test-retest reliability of the peak knee adduction moment during walking in patients with medial compartment knee osteoarthritis." Arthritis Care Research **57**(6): 1012-7.
- Bland, J. M. and D. G. Altman (1995). "Comparing methods of measurement: why plotting difference against standard method is misleading." Lancet **346**(8982): 1085-7.
- Brunner, R. and J. U. Baumann (1998). "Three-dimensional analysis of the skeleton of the lower extremities with 3D-precision radiography." Arch Orthop Trauma Surg **117**(6-7): 351-6.
- Camomilla, V., A. Cereatti, G. Vannozzi and A. Cappozzo (2006). "An optimized protocol for hip joint centre determination using the functional method." J Biomech **39**(6): 1096-106.
- Cappozzo, A., F. Catani, A. Leardini, M. G. Benedetti and U. D. Croce (1996). "Position and orientation in space of bones during movement: experimental artefacts." Clin Biomech (Bristol, Avon) **11**(2): 90-100.
- Carson, W. G., Jr., S. L. James, R. L. Larson, K. M. Singer and W. W. Winternitz (1984). "Patellofemoral disorders: physical and radiographic evaluation. Part II: Radiographic examination." Clin Orthop Relat Res (185): 178-86.
- Cereatti, A., U. Della Croce and A. Cappozzo (2006). "Reconstruction of skeletal movement using skin markers: comparative assessment of bone pose estimators." J Neuroeng Rehabil **3**: 7.
- Cicuttini, F., A. Wluka, J. Hankin and Y. Wang (2004). "Longitudinal study of the relationship between knee angle and tibiofemoral cartilage volume in subjects with knee osteoarthritis." Rheumatology (Oxford) **43**(3): 321-4.
- Colvin, A. C. and R. V. West (2008). "Patellar instability." J Bone Joint Surg Am **90**(12): 2751-62.
- Connolly, K. D., J. L. Ronsky, L. M. Westover, J. C. Küpper and R. Frayne (2009). "Differences in patellofemoral contact mechanics associated with patellofemoral pain syndrome." Journal of Biomechanics **42**(16): 2802.
- Coventry, M. B., D. M. Ilstrup and S. L. Wallrichs (1993). "Proximal tibial osteotomy. A critical long-term study of eighty-seven cases." J Bone Joint Surg Am **75**(2): 196-201.
- Dandachli, W., A. Nakhla, F. Iranpour, V. Kannan and J. P. Cobb (2009). "Can the acetabular position be derived from a pelvic frame of reference?" Clin Orthop Relat Res **467**(4): 886-93.
- Davis, R. B., S. Ounpuu, D. Tyburski and J. R. Gage (1991). "A gait analysis data collection and reduction technique." Human Movement Science **10**: 575-587.
- Dejour, D. and B. Le Coultre (2007). "Osteotomies in patello-femoral instabilities." Sports Med Arthrosc **15**(1): 39-46.

- Dejour H, W. G., Nove-Josserand L, Guier C (1994). "Factors of patellar instability: an anatomic radiographic study." Knee Surg Sports Traumatol Arthrosc **2**(1): 19-26.
- Diederichs, G., A. S. Issever and S. Scheffler "MR imaging of patellar instability: injury patterns and assessment of risk factors." Radiographics **30**(4): 961-81.
- Donati, M., V. Camomilla, G. Vannozzi and A. Cappozzo (2008). "Anatomical frame identification and reconstruction for repeatable lower limb joint kinematics estimates." J Biomech **41**(10): 2219-26.
- Draper, C. E., T. F. Besier, J. M. Santos, F. Jennings, M. Fredericson, G. E. Gold, G. S. Beaupre and S. L. Delp (2009). "Using real-time MRI to quantify altered joint kinematics in subjects with patellofemoral pain and to evaluate the effects of a patellar brace or sleeve on joint motion." J Orthop Res **27**(5): 571-7.
- Dryden, I. L. and K. V. Mardia (2002). Statistical Shape Analysis. Chichester, Wiley.
- Ehrig, R. M., W. R. Taylor, G. N. Duda and M. O. Heller (2006). "A survey of formal methods for determining the centre of rotation of ball joints." J Biomech **39**(15): 2798-809.
- Ehrig, R. M., W. R. Taylor, G. N. Duda and M. O. Heller (2007). "A survey of formal methods for determining functional joint axes." J Biomech **40**(10): 2150-7.
- Farahmand, F., W. Senavongse and A. A. Amis (1998). "Quantitative study of the quadriceps muscles and trochlear groove geometry related to instability of the patellofemoral joint." J Orthop Res **16**(1): 136-43.
- Fisher, B., J. Nyland, E. Brand and B. Curtin "Medial Patellofemoral Ligament Reconstruction for Recurrent Patellar Dislocation: A Systematic Review Including Rehabilitation and Return-to-Sports Efficacy." Arthroscopy: The Journal of Arthroscopic & Related Surgery **26**(10): 1384.
- Fithian, D. C., E. W. Paxton, M. L. Stone, P. Silva, D. K. Davis, D. A. Elias and L. M. White (2004). "Epidemiology and natural history of acute patellar dislocation." Am J Sports Med **32**(5): 1114-21.
- Fucetese, S. F., A. von Roll, P. P. Koch, D. R. Epari, B. Fuchs and P. B. Schottle (2006). "The patella morphology in trochlear dysplasia--a comparative MRI study." Knee **13**(2): 145-50.
- Gaasbeek, R. D. A., B. E. Groen, B. Hampsink, R. J. van Heerwaarden and J. Duysens (2007). "Valgus bracing in patients with medial compartment osteoarthritis of the knee: A gait analysis study of a new brace." Gait Posture **26**(1): 3-10.
- Goker, B. and J. A. Block (2007). "Improved Precision in Quantifying Knee Alignment Angle." Clin Orthop Relat Res **458**: 145-9.
- Goodfellow, J., D. S. Hungerford and M. Zindel (1976). "Patello-femoral joint mechanics and pathology. 1. Functional anatomy of the patello-femoral joint." J Bone Joint Surg Br **58**(3): 287-90.
- Goudakos, I., C. König, P. Schöttle, W. R. Taylor, G. N. Duda and M. Heller (2008). "Impact of muscle load level on patello-femoral contact mechanics and kinematics." Journal of biomechanics **41**: S209.
- Goudakos, I. G., C. König, P. B. Schottle, W. R. Taylor, J. E. Hoffmann, B. M. Popplau, N. B. Singh, G. N. Duda and M. O. Heller "Regulation of the patellofemoral contact area: An essential mechanism in patellofemoral joint mechanics?" J Biomech.
- Goudakos, I. G., C. König, P. B. Schottle, W. R. Taylor, N. B. Singh, I. Roberts, F. Streitharth, G. N. Duda and M. O. Heller (2009). "Stair climbing results in more challenging patellofemoral contact mechanics and kinematics than walking at early knee flexion under physiological-like quadriceps loading." J Biomech **42**(15): 2590-6.
- Grelsamer, R. P., D. Dejour and J. Gould (2008). "The pathophysiology of patellofemoral arthritis." Orthop Clin North Am **39**(3): 269-74, v.
- Hawkins RJ, B. R., Anisette G (1986). "Acute patellar dislocations. The natureal history." Am J Sports Med **14**: 117-20.
- Heller, M. O., G. Bergmann, G. Deuretzbacher, L. Durselen, M. Pohl, L. Claes, N. P. Haas and G. N. Duda (2001). "Musculo-skeletal loading conditions at the hip during walking and stair climbing." J Biomech **34**(7): 883-93.

- Heller, M. O., W. R. Taylor, C. Perka and G. N. Duda (2003). "The influence of alignment on the musculo-skeletal loading conditions at the knee." Langenbecks Arch Surg(388): 291-7.
- Hewett, T. E., G. D. Myer, K. R. Ford, R. S. Heidt, Jr., A. J. Colosimo, S. G. McLean, A. J. van den Bogert, M. V. Paterno and P. Succop (2005). "Biomechanical measures of neuromuscular control and valgus loading of the knee predict anterior cruciate ligament injury risk in female athletes: a prospective study." Am J Sports Med **33**(4): 492-501.
- Hinman, R. S., R. L. May and K. M. Crossley (2006). "Is there an alternative to the full-leg radiograph for determining knee joint alignment in osteoarthritis?" Arthritis Rheum **55**(2): 306-13.
- Hinterwimmer, S., M. Gotthardt, R. von Eisenhart-Rothe, S. Sauerland, M. Siebert, T. Vogl, F. Eckstein and H. Graichen (2005). "In vivo contact areas of the knee in patients with patellar subluxation." J Biomech **38**(10): 2095-101.
- Hinterwimmer, S., H. Graichen, T. J. Vogl and N. Abolmaali (2008). "An MRI-based technique for assessment of lower extremity deformities-reproducibility, accuracy, and clinical application." Eur Radiol **18**(7): 1497-505.
- Hunt, M. A., T. B. Birmingham, T. R. Jenkyn, J. R. Giffin and I. C. Jones (2008). "Measures of frontal plane lower limb alignment obtained from static radiographs and dynamic gait analysis." Gait Posture **27**(4): 635-40.
- Hunt, M. A., P. J. Fowler, T. B. Birmingham, T. R. Jenkyn and J. R. Giffin (2006). "Foot rotational effects on radiographic measures of lower limb alignment." Can J Surg **49**(6): 401-6.
- Hurwitz, D. E., A. B. Ryals, J. P. Case, J. A. Block and T. P. Andriacchi (2002). "The knee adduction moment during gait in subjects with knee osteoarthritis is more closely correlated with static alignment than radiographic disease severity, toe out angle and pain." J Orthop Res **20**(1): 101-7.
- Insall, J., V. Goldberg and E. Salvati (1972). "Recurrent dislocation and the high-riding patella." Clin Orthop Relat Res **88**: 67-9.
- Jackson, B. D., A. J. Teichtahl, M. E. Morris, A. E. Wluka, S. R. Davis and F. M. Cicuttini (2004). "The effect of the knee adduction moment on tibial cartilage volume and bone size in healthy women." Rheumatology (Oxford) **43**(3): 311-4.
- Kadaba, M. P., H. K. Ramakrishnan and M. E. Wootten (1990). "Measurement of lower extremity kinematics during level walking." J Orthop Res **8**(3): 383-92.
- Kanamiya, T., M. Naito, M. Hara and I. Yoshimura (2002). "The influences of biomechanical factors on cartilage regeneration after high tibial osteotomy for knees with medial compartment osteoarthritis: clinical and arthroscopic observations." Arthroscopy **18**(7): 725-9.
- Karamanidis, K. and A. Arampatzis (2009). "Evidence of mechanical load redistribution at the knee joint in the elderly when ascending stairs and ramps." Ann Biomed Eng **37**(3): 467-76.
- Kawakami, H., N. Sugano, K. Yonenobu, H. Yoshikawa, T. Ochi, A. Hattori and N. Suzuki (2004). "Effects of rotation on measurement of lower limb alignment for knee osteotomy." J Orthop Res **22**(6): 1248-53.
- Kornaropoulos, E. I., W. R. Taylor, G. N. Duda, R. M. Ehrig, G. Matziolis, M. Muller, G. Wassilew, P. Asbach, C. Perka and M. O. Heller (2010). "Frontal plane alignment: an imageless method to predict the mechanical femoral-tibial angle (mFTA) based on functional determination of joint centres and axes." Gait Posture **31**(2): 204-8.
- Kratzenstein, S., R. M. Ehrig, E. Heller and W. R. Taylor (2009). "Reduction of the influence of skin marker artefact using the optimal common shape technique." Gait & Posture **30**: S31.
- Kratzenstein, S., M. O. Heller, R. M. Ehrig, G. N. Duda and W. R. Taylor (2010). The residual: a reliable measure of accuracy in the determination of joint centres. ORS.

- Kratzenstein, S., M. O. Heller, R. M. Ehrig, G. Wassilew, G. N. Duda and W. R. Taylor (2010). A new approach for optimally reducing skin marker artifact allows determination of the hip joint center within 3mm. *ORS*.
- Kuroyanagi, Y., T. Nagura, H. Matsumoto, T. Otani, Y. Suda, T. Nakamura and Y. Toyama (2007). "The lateral wedged insole with subtalar strapping significantly reduces dynamic knee load in the medial compartment gait analysis on patients with medial knee osteoarthritis." *Osteoarthritis Cartilage* **15**(8): 932-6.
- Leardini, A., L. Chiari, U. Della Croce and A. Cappozzo (2005). "Human movement analysis using stereophotogrammetry. Part 3. Soft tissue artifact assessment and compensation." *Gait Posture* **21**(2): 212-25.
- Maenpaa, H. and M. U. Lehto (1997). "Patellofemoral osteoarthritis after patellar dislocation." *Clin Orthop Relat Res*(339): 156-62.
- Matziolis, G., D. Kroker, U. Weiss, S. Tohtz and C. Perka (2007). "A prospective, randomized study of computer-assisted and conventional total knee arthroplasty. Three-dimensional evaluation of implant alignment and rotation." *J Bone Joint Surg Am* **89**(2): 236-43.
- McGinley, J. L., R. Baker, R. Wolfe and M. E. Morris (2009). "The reliability of three-dimensional kinematic gait measurements: a systematic review." *Gait Posture* **29**(3): 360-9.
- McGraw, K. O. and S. P. Wong (1996). "Forming Inferences About Some Intraclass Correlation Coefficients." *Psychological Methods* **1**(1): 30.
- Mesfar, W. and A. Shirazi-Adl (2008). "Knee joint biomechanics in open-kinetic-chain flexion exercises." *Clin Biomech (Bristol, Avon)* **23**(4): 477-82.
- Mulford, J. S., C. J. Wakeley and J. D. Eldridge (2007). "Assessment and management of chronic patellofemoral instability." *J Bone Joint Surg Br* **89**(6): 709-16.
- Mundermann, A., C. O. Dyrby and T. P. Andriacchi (2008). "A comparison of measuring mechanical axis alignment using three-dimensional position capture with skin markers and radiographic measurements in patients with bilateral medial compartment knee osteoarthritis." *Knee* **15**(6): 480-5.
- Murray TF, D. J., Fulkerson JP (1999). "Axial and lateral radiographs in evaluating patellofemoral malalignment." *Am J Sports Med* **27**(5): 580-4.
- Paley, D., J. E. Herzenberg, K. Tetsworth, J. McKie and A. Bhav (1994). "Deformity planning for frontal and sagittal plane corrective osteotomies." *Orthop Clin North Am* **25**(3): 425-65.
- Paley, D. and J. Pfeil (2000). "Principles of deformity correction around the knee." *Orthopäde* **29**(1): 18-38.
- Parratte, S. and M. W. Pagnano (2008). "Instability after total knee arthroplasty." *J Bone Joint Surg Am* **90**(1): 184-94.
- Paulos, L., S. C. Swanson, G. J. Stoddard and S. Barber-Westin (2009). "Surgical correction of limb malalignment for instability of the patella: a comparison of 2 techniques." *Am J Sports Med* **37**(7): 1288-300.
- Pfirrmann, C. W., M. Zanetti, J. Romero and J. Hodler (2000). "Femoral trochlear dysplasia: MR findings." *Radiology* **216**(3): 858-64.
- Ramakrishnan, H. K. and M. P. Kadaba (1991). "On the estimation of joint kinematics during gait." *J Biomech* **24**(10): 969-77.
- Ramappa, A. J., M. Apreleva, F. R. Harrold, P. G. Fitzgibbons, D. R. Wilson and T. J. Gill (2006). "The effects of medialization and anteromedialization of the tibial tubercle on patellofemoral mechanics and kinematics." *Am J Sports Med* **34**(5): 749-56.
- Rose, S. A., P. A. DeLuca, R. B. Davis, 3rd, S. Ounpuu and J. R. Gage (1993). "Kinematic and kinetic evaluation of the ankle after lengthening of the gastrocnemius fascia in children with cerebral palsy." *J Pediatr Orthop* **13**(6): 727-32.
- Rozumalski, A. and M. H. Schwartz (2008). "P041 A comparison of two functional methods for calculating joint centers and axes in a clinical setting." *Gait & posture* **28**: S74.

- Rünow A (1983). "The dislocating patella. Etiology and prognosis in relation to generalized joint laxity and anatomy of the patellar articulation." Acta Orthop Scand Suppl **201**: 1-53.
- Sabharwal, S. and C. Zhao (2008). "Assessment of Lower Limb Alignment: Supine Fluoroscopy Compared with a Standing Full-Length Radiograph." J Bone Joint Surg Am **90**: 43-51.
- Sailer, J., M. Scharitzer, P. Peloschek, A. Giurea, H. Imhof and S. Grampp (2005). "Quantification of axial alignment of the lower extremity on conventional and digital total leg radiographs." Eur Radiol **15**(1): 170-3.
- Salzmann, G. M., T. S. Weber, J. T. Spang, A. B. Imhoff and P. B. Schottle "Comparison of native axial radiographs with axial MR imaging for determination of the trochlear morphology in patients with trochlear dysplasia." Arch Orthop Trauma Surg **130**(3): 335-40.
- Schottle, P., I. Goudakos, N. Rosenstiel, J. E. Hoffmann, W. R. Taylor, G. N. Duda and M. O. Heller (2009). "A comparison of techniques for fixation of the quadriceps muscle-tendon complex for in vitro biomechanical testing of the knee joint in sheep." Med Eng Phys **31**(1): 69-75.
- Schwartz, M. H. and A. Rozumalski (2005). "A new method for estimating joint parameters from motion data." J Biomech **38**(1): 107-16.
- Schwartz, M. H., J. P. Trost and R. A. Wurvey (2004). "Measurement and management of errors in quantitative gait data." Gait Posture **20**(2): 196-203.
- Sharma, L., J. Song, D. Dunlop, D. Felson, C. E. Lewis, N. Segal, J. Torner, T. D. Cooke, J. Hietpas, J. Lynch and M. Nevitt (in press). "Varus and valgus alignment and incident and progressive knee osteoarthritis." Ann Rheum Dis.
- Shultz, S. J., A. D. Nguyen and R. J. Schmitz (2008). "Differences in lower extremity anatomical and postural characteristics in males and females between maturation groups." J Orthop Sports Phys Ther **38**(3): 137-49.
- Specogna, A. V., T. B. Birmingham, M. A. Hunt, I. C. Jones, T. R. Jenkyn, P. J. Fowler and J. R. Giffin (2007). "Radiographic Measures of Knee Alignment in Patients With Varus Gonarthrosis: Effect of Weightbearing Status and Associations With Dynamic Joint Load." Am J Sports Med **35**(1): 65-70.
- Stout, J. L., J. R. Gage, M. H. Schwartz and T. F. Novacheck (2008). "Distal femoral extension osteotomy and patellar tendon advancement to treat persistent crouch gait in cerebral palsy." J Bone Joint Surg Am **90**(11): 2470-84.
- Taylor, W. R., R. M. Ehrig, G. N. Duda, H. Schell, P. Klein and M. O. Heller (2005). "On the influence of soft tissue coverage in the determination of bone kinematics using skin markers." J Orthop Res **23**(4): 726-34.
- Taylor, W. R., M. O. Heller, G. Bergmann and G. N. Duda (2004). "Tibio-femoral loading during human gait and stair climbing." J Orthop Res **22**(3): 625-32.
- Tomczak, R. J., K. P. Guenther, A. Rieber, P. Mergo, P. R. Ros and H. J. Brambs (1997). "MR imaging measurement of the femoral antetorsional angle as a new technique: comparison with CT in children and adults." AJR Am J Roentgenol **168**(3): 791-4.
- Trepczynski, A., I. Kutzner, E. I. Kornaropoulos, W. R. Taylor, G. N. Duda, G. Bergmann and M. O. Heller (2010). Patello-Femoral Forces during Functionally Demanding Activities Predicted by a Validated Musculoskeletal Model. 56th Annual Meeting of the Orthopaedic Research Society, New Orleans, LA, USA.
- Tsakoniti, A. E., C. A. Stoupis and S. I. Athanasopoulos (2008). "Quadriceps cross-sectional area changes in young healthy men with different magnitude of Q angle." J Appl Physiol **105**(3): 800-4.
- Vanwanseele, B., D. Parker and M. Coolican (2009). "Frontal knee alignment: three-dimensional marker positions and clinical assessment." Clin Orthop Relat Res **467**(2): 504-9.
- von Knoch, F., T. Bohm, M. L. Burgi, M. von Knoch and H. Bereiter (2006). "Trochleaplasty for recurrent patellar dislocation in association with trochlear dysplasia. A 4- to 14-year follow-up study." J Bone Joint Surg Br **88**(10): 1331-5.

- Waidelich, H. A., W. Strecker and E. Schneider (1992). "[Computed tomographic torsion-angle and length measurement of the lower extremity. The methods, normal values and radiation load]." Rofo **157**(3): 245-51.
- Walsh, W. (2003). Recurrent Dislocation of the Knee in the Adult. Philadelphia, USA, Saunders.
- White, B. J. and O. H. Sherman (2009). "Patellofemoral instability." Bull NYU Hosp Jt Dis **67**(1): 22-9.
- Wittstein, J. R., E. C. Bartlett, J. Easterbrook and J. C. Byrd (2006). "Magnetic resonance imaging evaluation of patellofemoral malalignment." Arthroscopy **22**(6): 643-9.
- Wright, J. G., N. Treble and A. R. Feinstein (1991). "Measurement of lower limb alignment using long radiographs." J Bone Joint Surg Br **73**(5): 721-3.
- Yamada, Y., Y. Toritsuka, S. Horibe, K. Sugamoto, H. Yoshikawa and K. Shino (2007). "In vivo movement analysis of the patella using a three-dimensional computer model." J Bone Joint Surg Br **89**(6): 752-60.
- Yamada, Y., Y. Toritsuka, H. Yoshikawa, K. Sugamoto, S. Horibe and K. Shino (2007). "Morphological analysis of the femoral trochlea in patients with recurrent dislocation of the patella using three-dimensional computer models." J Bone Joint Surg Br **89**(6): 746-51.
- Zhao, D., S. A. Banks, K. H. Mitchell, D. D. D'Lima, C. W. C. Jr and B. J. Fregly (2007). "Correlation between the knee adduction torque and medial contact force for a variety of gait patterns." J Orthop Res **25**(6): 789-797.

8

Appendix

List of most frequent abbreviations

–	ACL	: Anterior cruciate ligament
–	ANOVA	: Analysis of variance
–	ASIS	: Anterior posterior iliac spine
–	BMI	: Body mass index
–	BW	: Body weight
–	CI	: Confidence interval
–	CSA	: Cross-sectional area
–	ICC	: Intraclass correlation coefficient
–	mFTA	: Mechanical femoral-tibial angle
–	MPFL	: Medial patello-femoral ligament
–	MRI	: Magnetic resonance imaging
–	OA	: Osteoarthritis
–	OCST	: Optimal common shape technique
–	OSSCA	: OCST SARA SCoRE combined approach
–	PF	: Patello-femoral
–	PFPS	: Patello-femoral pain syndrome
–	PSIS	: Posterior superior iliac spine
–	Q-Angle	: Quadriceps angle
–	RF	: Rectus femoris
–	RoM	: Range of motion
–	SARA	: Symmetrical axis of rotation approach
–	SCoRE	: Symmetrical centre of rotation estimation
–	SD	: Standard deviation
–	STA	: Soft tissue artefact
–	THA	: Total hip arthroplasty
–	TKA	: Total knee arthroplasty
–	TTTG	: Tibia tubercle to trochlear groove
–	VI	: Vastus intermedius
–	VL	: Vastus lateralis
–	VM	: Vastus medialis
–	wOCST	: Weighted OCST

List of peer-reviewed publications associated with this work

Published in scientific journals

- Kornaropoulos, E. I., W. R. Taylor, G. N. Duda, R. M. Ehrig, G. Matziolis, M. Muller, G. Wassilew, P. Asbach, C. Perka and M. O. Heller (2010). "Frontal plane alignment: an imageless method to predict the mechanical femoral-tibial angle (mFTA) based on functional determination of joint centres and axes." Gait Posture **31**(2): 204-8.
- Taylor, W. R., E. I. Kornaropoulos, G. N. Duda, S. Kratzstein, R. M. Ehrig, A. Arampatzis and M. O. Heller (2010). "Repeatability and reproducibility of OSSCA, a functional approach for assessing the kinematics of the lower limb." Gait Posture **32**(2): 231-6.

In preparation for submission in scientific journals

- Kornaropoulos, E. I., G. Diederichs, S. Scheffler, J. Kreye, W. R. Taylor, G. N. Duda, H. C. Hege, and M. O. Heller (2011). "Towards establishing a standardized MRI protocol and reference data of the frontal plane and rotational alignment, as well as the anatomy of the quadriceps muscles in healthy adults." J Orthop Res **planned submission**.
- *Diederichs G., *E. I. Kornaropoulos, S. Scheffler, M. O. Heller, G. N. Duda, W. R. Taylor, and S. Scheffler (2011). "Knee version as a key factor of the patho-anatomy in patients with patello-femoral instability" Am J Sports Med **planned submission** (*: shared first authorship).
- Kornaropoulos, E. I., W. R. Taylor, G. Diederichs, S. Scheffler, J. Kreye, G. N. Duda, H. C. Hege, and M. O. Heller (2011). "The pathology of the vastus medialis and the vastus lateralis in patients with patello-femoral instability" Am J Sports Med **planned submission**.
- Kornaropoulos, E. I., W. R. Taylor, A. Trepczynski, S. Scheffler, M. Kraft, G. N. Duda, M. O. Heller (2011). "The MPFL does not restore normal knee function in patients with patello-femoral instability" Am J Sports Med **planned submission**.

International Congresses

- Kornaropoulos EI, Taylor WR, Duda GN, Ehrig RM, Heller MO. "An imageless method to quantify the Mechanical Femoral-Tibial Angle (MFTA) using functionally defined joint centers and axes". Annual meeting of the German Society for Biomechanics - Münster 2009 (Oral presentation)/
- Kornaropoulos EI, Taylor WR, Duda GN, Ehrig RM, Heller MO. "An imageless method to quantify the mechanical femoral-tibial angle based on the functional determination of joint centers and axes". Annual meeting of the ESMAC- London 2009 (oral presentation).
- Taylor WR, Kornaropoulos EI, Ehrig RM, Heller MO, Duda GN. "Reproducibility of a functional approach to movement analysis". Annual meeting of the ESB- Edinburgh 2010 (oral presentation).
- Kornaropoulos EI, Scheffler S, Diederichs G, Taylor WR, Duda GN, Heller MO. "Rotational malalignment of the femur: knee version as key factor of the patho-anatomy in patellofemoral instability". Annual meeting of the ORS- Long Beach 2011 (poster and oral presentation).

Curriculum Vitae

Evgenios I. Kornaropoulos

1983 born in Athens, Greece

Education

- | | |
|-------------|---|
| 1998 – 2001 | 3 rd Lyceum of Rhodes (Apolitirio)
graduated with <i>honours</i> |
| 2001 – 2006 | National Technical University of Athens
School of Electrical & Computer Engineering
Diploma of engineering, graduated with <i>very good</i> |
| 2006 - 2007 | University of Oxford, UK
MSc. in Biomedical Engineering, graduated with <i>distinction</i> |

Education

- | | |
|-------------|--|
| 2006 - 2011 | Julius Wolff Institute
Charité – Universitätsmedizin Berlin, Germany
Research Fellow in Musculoskeletal Biomechanics |
|-------------|--|